

THE ROLE OF FORMIN CYTOSKELETAL EFFECTOR PROTEINS IN T CELL
MIGRATION AND AUTOIMMUNE DISEASE

by

SCOTT BECKETT THOMPSON

B.S., Haverford College, 2008

A thesis submitted to the
Faculty of the Graduate School of the
University of Colorado in partial fulfillment
of the requirements for the degree of
Doctor of Philosophy
Program in Immunology
2019

This thesis for the Doctor of Philosophy degree by

Scott Beckett Thompson

has been approved for the

Immunology Program

by

Raul Torres, Chair

Eric Clambey

Peter Henson

Ross Kedl

David Wagner

Jordan Jacobelli, Advisor

Date: May 17, 2019

Thompson, Scott Beckett (Ph.D., Immunology)

The Role of Formin Cytoskeletal Effector Proteins in T cell Migration and Autoimmune Disease

Thesis directed by Associate Professor Jordan Jacobelli

ABSTRACT

T cells must traffic through the bloodstream to sites of inflammation to execute their effector function. To enter tissues, T cells extravasate through the vascular endothelial cell wall by a process known as transendothelial migration (TEM). While many of the adhesion molecules and chemokine signaling pathways required for TEM have been previously characterized, little is known about how downstream cytoskeletal effectors mediate the mechanical forces and shape changes needed for T cell TEM. Formins are terminal cytoskeletal effectors directly involved in actin network remodeling. Formin-like 1 (FMNL1) and Diaphanous-related formin 1 (mDia1) are the two main formins expressed by T cells. While mDia1 is expressed ubiquitously, it is upregulated by activated T cells and has been previously implicated in T cell trafficking. FMNL1 expression is restricted to hematopoietic cells and is upregulated in autoreactive T cells that enter immune privileged sites. However, the function of FMNL1 in T cell trafficking is unknown. In this work we examined the role of these formins in activated T cell extravasation and induction of autoimmune disease.

To investigate the function of FMNL1 in T cells, we developed and characterized a novel FMNL1-deficient mouse. *In vivo*, we found that FMNL1 was dispensable for lymphocyte development and homeostatic trafficking. Instead, FMNL1 regulated the ability of effector T cells to extravasate into inflamed tissues and induce autoimmune disease in mouse models of type 1 diabetes and multiple sclerosis (Experimental Autoimmune Encephalomyelitis, EAE). Mechanistic *in vitro* studies revealed that FMNL1 promotes transmigration of the rigid T cell

nucleus through the vascular endothelium during the completion of TEM. Further experiments demonstrated that T cell chemotaxis through restrictive barriers is FMNL1 dependent.

To investigate the role of mDia1 in T cell extravasation and autoimmune disease, we used previously developed mDia1-deficient mice. Similar to FMNL1-deficient T cells, mDia1-deficient T cells were impaired in their ability to induce EAE. Additionally, mDia1-deficient T cells were also impaired in their ability to complete TEM. Collectively, our data suggest that formins are key regulators of T cell TEM and may be promising therapeutic targets for regulating T cell-mediated autoimmune disease.

The form and content of this abstract are approved. I recommend its publication.

Approved: Jordan Jacobelli

DEDICATION

I dedicate this thesis to my mentors past and present who have helped me develop as a scientist and a person: John Thompson, Catherine Thompson, Sue Maroney, Dave Lewinsohn, Marielle Gold, Phil Meneely, Karen Mahan, Paul Lieberman, and Jordan Jacobelli.

ACKNOWLEDGEMENTS

This work would not have been possible without the contributions of a great many people. First and foremost I would like to acknowledge my Ph.D. mentor Jordan Jacobelli for his outstanding guidance, support, patience, and enthusiasm, in addition to excellent scientific training during my time in graduate school.

Secondly, I would like to acknowledge those who made direct experimental contributions to this work: Jennifer Matsuda and the National Jewish Mouse Genetics Core for generating the FMNL1 KO mice, Adam Sandor and Victor Lui for performing the islet trafficking experiments, Jeffrey Chung and Rob Long for their assistance with the CNS trafficking experiments, Monique Waldman for assistance with the naive T cell trafficking experiments, and Jordan Jacobelli for precisely timed addition of reagents during the actin polymerization experiments. I would also like to thank Rachel Friedman for her input on the diabetes and islet trafficking experiments and Mira Estin for her input on the CNS trafficking and EAE induction experiments. Thank you to Kristen Dew, Katie Morgan, Jessica Olivas, Dayna Tracy, Matt Gebert, Seth Yannacone, Orlando Castro-Villasano, Jerimiah Phares, Erika Rodriguez, Briana Traxinger and Eric Wigton for technical help with mouse genotyping and colony maintenance. Thank you to Matt Rosenbaum, Ruth Franceschi and Mary Keuttel and the Biological Resources Center for looking after the health and wellbeing of the mouse colony. Thank you to Josh Loomis Shirley Sobus for maintenance of and technical assistance with the microscopes and flow cytometers. Additionally, I would like to acknowledge those who helped edit the text of this work: Kelsey Haist, Jordan Jacobelli, and Elizabeth Thompson.

I would also like to acknowledge my thesis advisory committee, Raul Torres, Eric Clambey, Peter Henson, Ross Kedl, and David Wagner. Thank you for your guidance and the productive discussions that shaped the course of this work and my growth as a scientist.

Thank you to all the members of the Jacobelli-Friedman lab past and present who have made the lab such a wonderful place to work and learn. Thank you all for putting up with my Tier 73 jokes for 5 years. Thank you to the lab PIs, Jordan Jacobelli and Rachel Friedman for creating an excellent work environment where everyone supports each other and talks about science at least 10% of the time. Thank you to the lab managers past and present: Matt Gebert, Rob Long, and Kristen Dew for keeping the lab exceptionally well run as well as going above and beyond when I needed reagents at the last minute. I would also like to acknowledge my current and past graduate student labmates: Robin Lindsay for teaching me everything I know about mice and for enforcing scientific integrity with panache; Mira Estin for always having a word of encouragement and for teaching me many of the techniques for this paper; Adam Sandor for being a loyal friend, my science song co-author, and for rigorous scientific debates; Jeffrey Chung for being an exceptional team player, for monitoring my timer when I'm not there, and for providing ursine gelatin glucose amalgams (Sprouts); Jen Whitesell for being a peerless lab citizen and for your scientific curiosity; Monique Waldman for your excitement, efficient problem solving, and friendliness. As mentioned above, thank you to all the technicians past and present for your hard work in making the lab run smoothly.

I would also like to thank my fellow graduate students who have been great mentors, friends, and colleagues. Thank you for building and maintaining a fantastic community. In particular I'd like to acknowledge Cisco Ramirez, Nathan Pennock, Kjersten Anderson, Seth Welsh, Jingjing Zhang, Katie Tuttle, Katie Waugh, Nick Bishop, Eric Cross, Jason White, Kristin Shotts, Shannon Miller, Divij Mathew, Sandy Larson, Sarah Greaves, Elizabeth Franks, Kelly Higa, Joe Westrich, Nikki Bortell, and Isabel Fernandez. Whether it was scientific advice, life advice, a good argument or just a couple beers, you all gave lent me tremendous support during graduate school.

I would not have even made it to graduate school or through this process without my family. I would like to thank my parents John and Catherine Thompson for their love, support and encouragement from D0 until now. I would also like to acknowledge my sisters Elizabeth and Leah Thompson, for always being willing to listen, whether when I was talking about science or about my life and for making me laugh when I needed to.

Lastly, but certainly not least, I would like to acknowledge Kelsey Haist for being my constant companion and partner throughout graduate school. Thank you for all your love and patience, especially when my experiments ran significantly longer than expected ($p < 0.0001$ $n = 300$). Thank you for your scientific input, your emotional support and for always having my back. Thank you for knowing when I needed a break from the lab, and encouraging me when experiments were frustrating.

This work was supported in part by NIAID R56AI105111 and R21AI119932-01 and JDRF #5-2013-200. I was supported in part by NIH Training Grant T32AI007405. The spinning-disk confocal microscope employed for imaging was acquired through Shared Instrumentation Grant Award Number S10RR029218. The experimental procedures in this thesis were approved by and mice were handled in accordance with the guidelines of the National Jewish Health Institutional Animal Care and Use Committee. (Protocol Numbers: AS 2811-02-17 and AS2811-12-19)

TABLE OF CONTENTS

CHAPTER

I. INTRODUCTION	1
T Cell Migration and Function	1
Transendothelial Migration: The Process of Extravasation	2
Molecular and Physical Cues for Naive T cell TEM	4
Molecular and Physical Cues for Activated T cell TEM	5
Therapeutically Targeting T cell Migration	6
Transduction of Chemokine and Integrin Signaling by GTPases	7
Actin Filament Dynamics During Migration	8
Actin Networks and Effectors in T cells	9
Scope of Thesis.....	13
II. MATERIALS AND METHODS	21
Generation of FMNL1 KO Mice	21
Mice	22
Media	23
Antibodies for Flow Cytometry.....	23
Western Blotting.....	23
Flow Cytometry Characterization of FMNL1 KO Mice	24
T Cell Isolation	24
Polyclonal T Cell Activation and Culture	25
Fluorescent Dye-Labeling of T Cells	25
Lymphoid Organ T Cell Trafficking	26
Islet Trafficking	26

CNS Trafficking	27
T Cell Transfer Diabetes Model	28
T Cell Transfer EAE Model	29
Microscopy	29
T cell TEM Under Flow	29
FMNL1 Localization During TEM	30
Nucleus Localization During TEM	31
T cell Transwell Migration	31
Neutrophil Transwell Migration	32
Actin Polymerization Assay	32
FMNL1 Re-Expression	33
Statistical Analysis	34
III. FMNL1 IS DISPENSABLE FOR T CELL DEVELOPMENT AND HOMEOSTATIC TRAFFICKING	35
Introduction	35
Results	37
Deletion of FMNL1 Does Not Significantly Alter Major Immune Cell Populations	37
FMNL1 Deficiency Does Not Affect Naive T cell Trafficking to Secondary Lymphoid Organs	38
FMNL1 Deficiency Does Not Impair <i>Ex Vivo</i> T Cell Activation	38
Discussion	38
IV. FMNL1 DEFICIENCY IMPAIRS TRAFFICKING TO SITES OF INFLAMMATION AND T CELL DRIVEN AUTOIMMUNE DISEASE	51

Introduction	51
Results	52
FMNL1-deficient T cells Are Impaired in Trafficking to the Pancreatic Islets and Inducing Type 1 Diabetes.....	52
FMNL1-deficient T cells Are Impaired in Trafficking to the CNS and Inducing EAE	54
FMNL1-deficient T cells Are Not Impaired in Trafficking to Secondary Lymphoid Organs.....	55
Discussion.....	55
 V. FMNL1 PROMOTES NUCLEUS TRANSMIGRATION THROUGH RESTRICTIVE ENDOTHELIAL BARRIERS DURING DIAPEDESIS	61
Introduction	61
Results	63
FMNL1 Deficiency Impairs T cell TEM at the Diapedesis Step.....	63
FMNL1 Deficiency Impairs Transmigration of the Nucleus During TEM.	64
T cell Migration Through Narrow Pores Is FMNL1 Dependent	65
Discussion.....	68
 VI. MDIA1 DEFICIENCY IMPAIRS INDUCTION OF EAE AND T CELL DIAPEDESIS .	79
Introduction	79
Results	80
Self-reactive mDia1-deficient T Cells Are Impaired in Inducing EAE.....	80
mDia1 Deficiency Impairs T cell TEM at the Diapedesis Step.....	81
Discussion.....	81
 VII. DISCUSSION.....	88

Summary of Major Findings	88
Future Directions	92
Do Formins Regulate Interstitial T cell migration and Function?	92
How Do Formins Regulate Immune Responses To Pathogens?.....	94
How Do Formins Remodel Actin Cytoskeletal Networks During TEM?	95
How do Cytoskeletal Effectors Remodel the Actin Cytoskeleton to Facilitate Nucleus Passage Through Restrictive Barriers?	97
Proposed Model of Cytoskeletal Effector Function in TEM.....	98
Significance and Implications	100
REFERENCES	105

LIST OF ABBREVIATIONS

ADP	adenosine diphosphate
ANOVA	analysis of variance
APC	antigen presenting cell
ATP	adenosine triphosphate
BSA	bovine serum albumin
CCL	C-C motif chemokine ligand
CCR	C-C motif chemokine receptor
CD	cluster of differentiation
Cdc42	cell division cycle 42
CNS	central nervous system
CFA	complete Freund's adjuvant
CFP	cerulean fluorescent protein
CFSE	carboxyfluorescein succinimidyl ester fluorescent dye
CTY	CellTrace yellow fluorescent dye
CXCL	C-X-C motif chemokine ligand
CXCR	C-X-C motif chemokine receptor
DAD	diaphanous autoregulatory domain
DAPI	4',6-diamidino-2-phenylindole fluorescent dye
DC	dendritic cell
DID	diaphanous inhibitory domain
DMEM	dulbecco's modified eagle medium
DMSO	dimethyl sulfoxide
DN	double negative thymocyte
DP	double positive thymocyte
EAE	experimental autoimmune encephalomyelitis
ELISA	enzyme-linked immunosorbent assay
ES	embryonic stem cell
EVL	ena-VASP-Like (EVL)
FH1	formin homology 1 domain
FH2	formin homology 2 domain
F-actin	filamentous actin polymer
FMNL1	formin-like 1
FBS	fetal bovine serum
FSC	forward scatter
G-actin	globular actin monomer
GAP	GTPase activating protein
GBD	GTPase binding domain
GDP	guanosine diphosphate
GEF	guanine nucleotide exchange factor
GFP	green fluorescent protein
gMFI	geometric mean fluorescence intensity
GTP	guanosine triphosphate
HEPES	4-(2-hydroxyethyl)-1-piperazineethanesulfonic acid
HEV	high endothelial venule
ICAM-1	intracellular adhesion molecule-1
IL-2	interleukin-2

IRES	internal ribosome entry site
KO	knockout
LFA-1	lymphocyte function-associated antigen-1, integrin α L (CD11a) β 2(CD18)
LPAM-1	lymphocyte Peyer's patch adhesion molecule-1, integrin α 4 (CD49d)
MAdCAM1	mucosal vascular addressin cell adhesion molecule 1
MMLV	Moloney murine leukemia virus
MOG	myelin oligodendrocyte glycoprotein
MS	multiple sclerosis
MyoIIA	non-muscle myosin IIA
mDia1	diaphanous-related formin 1
NK	natural killer cell
OVA	ovalbumin
PALM	photoactivation localization microscopy
PNAd	peripheral node addressin
PSGL-1	p-selectin glycoprotein ligand-1
Rac1	ras-related C3 botulinum toxin substrate 1
Rap1	ras-related protein 1
RFP	red fluorescent protein
RhoA	ras homolog family member A
RIP-mOVA	membrane-bound ovalbumin expressed under the rat insulin promoter
ROCK	rho-associated coiled-Coil containing protein kinase
RPMI	Roswell Park Memorial Institute media
SMIFH2	small molecule inhibitor of formin homology 2 domain
SP	single positive thymocytes
STED	stimulated emission depletion microscopy
STORM	stochastic optical reconstruction microscopy
TCR	T cell receptor
Th	T helper cell
TNF- α	tumor necrosis factor- α
TEM	transendothelial migration
VASP	vasodilator-stimulated phosphoprotein
VCAM-1	vascular cell adhesion molecule-1
VLA-4	very late antigen-4, integrin α 4 (CD49d) β 1(CD29)
VPD	violet proliferation dye 450
WASP	Wiskott-Aldrich syndrome protein
WT	wild-type

CHAPTER I

INTRODUCTION

T Cell Migration and Function

Some of the earliest studies of lymphocytes identified them as migratory cells^{1,2}. In the over fifty years since then, it has become well established that migration both to and within tissues is essential for the function of lymphocytes, and in particular, T cells³⁻¹³. At every stage of the life of a T cell, T cells exhibit motile behavior. In development, premature T cells traffic to, migrate within, and upon maturation, exit the thymus^{5,14-17}. Naive T cells must circulate between and within secondary lymphoid organs to survey for their cognate antigens^{10,18-20}. While B cells can produce antibodies, enabling remote effects at distant sites, T cells must often directly interact with an antigen presenting cell (APC) and target cells in order to execute their effector function³, requiring them to act more locally. Consequently, T cell trafficking to sites of infection or tumors is essential for mediating T cell-dependent control and clearance^{7-9,18,21}. After clearance of a pathogen, different memory T cells subtypes localize to both lymphoid and non-lymphoid organs where they patrol for pathogen return^{10,18,22-25}. T regulatory cells must also migrate to and within tissues to execute their functions^{26,27}. Furthermore, in the context of autoimmune disease, infiltration of tissues by self-reactive T cells can be pathogenic²⁸. In multiple sclerosis (MS) and its mouse model, experimental autoimmune encephalomyelitis (EAE), self-reactive T cells invade the central nervous system (CNS) parenchyma to drive an inflammatory response that results in demyelination of neurons²⁹⁻³¹. Transfer of T cells specific for the myelin oligodendrocyte glycoprotein (MOG) is sufficient to drive EAE³². In type 1 diabetes T cells infiltrate the pancreatic islets of Langerhans to mount an autoimmune attack on the insulin-producing β cells^{33,34}. In mouse models of type 1 diabetes, transfer of T cells specific for islet antigens is sufficient to drive disease^{12,35}. Trafficking of T cells to sites of autoimmune

inflammation has also been shown to be involved in the pathogenesis of rheumatoid arthritis and inflammatory bowel disease^{28,36,37}. Thus, for T cells in both pathogenic and protective roles, migration is intrinsically coupled to their function.

Transendothelial Migration: The Process of Extravasation

To efficiently transit through an organism one hundred trillion times its volume, a T cell relies on the rapid circulation of the bloodstream through the extensive vascular network^{3,4,38}. Whether for a naive cell T cell entering the lymph node or an activated T cell trafficking to a site of inflammation, extravasation from the bloodstream is necessary for subsequent T cell functions. To enter tissues from the bloodstream T cells undergo the multistep process of transendothelial migration (TEM), typically in post-capillary venules³⁸. Canonically, TEM consists of four main sequential stages: rolling, adhering, crawling, and diapedesis (Fig. 1.1)³⁸.

Intravascular T cells are subject to substantial shear stress due to the rapid flow of the bloodstream, ranging from 1 dyne/cm² in the venules (HEVs) of lymph nodes to greater than 6 dyne/cm² in the venules of other tissues³⁹⁻⁴¹. Transient interactions between selectins and oligosaccharides related to sialyl-Lewis^x enable T cells to resist these forces and initiate TEM by rolling on the vascular endothelial cell wall (Fig. 1.1)⁴²⁻⁴⁴. Low-affinity interactions between integrins and their immunoglobulin super family ligands can also facilitate rolling in some tissue-specific contexts³⁰. This rolling process enables T cells to subsequently encounter chemokines attached to the glycocalyx of the endothelium⁴⁵⁻⁴⁷. Signaling by these chemokines as well as shear forces acting on the T cell serve to activate integrins into a high-affinity conformation^{44,46-48}. Subsequent binding of high-affinity integrins to their ligands on the endothelium promotes the full arrest and attachment of the T cell to vascular wall (Fig. 1.1)^{46,47,49}.

Post-arrest, T cells respond to chemotactic cues and crawl on the endothelial luminal surface, relying on integrin-mediated adhesions for traction (Fig 1.1)^{46,47}. During this process T cells adopt an amoeboid morphology and motility, with a ruffled, protrusive structure known as the lamellipodium at the leading edge of the cell and a contractile structure known as the uropod at the trailing edge (Fig 1.2)^{6,50,51}. Additionally, during crawling, micro-protrusions, known as filopodia or podosomes, extend from the ventral side and leading edge of the T cell into the endothelium, to probe for chemokine signals as well as permissive sites for transmigration across the endothelium^{46,49,52}.

In the final stage of TEM, diapedesis, T cells translocate across the vascular cell wall (Fig 1.1). This process predominantly occurs between endothelial cells at cell-cell junctions via the paracellular route. However, in certain tissues, such as the CNS, diapedesis also occurs through the endothelial cell body via the transcellular route⁵²⁻⁵⁷. Ligation of endothelial adhesion molecules, such as ICAM-1 (intracellular adhesion molecule-1) and VCAM-1 (vascular cell adhesion molecule-1), by T cell integrins drives signaling events within the endothelial cells that promote the internalization of VE-cadherin⁵⁷⁻⁵⁹. Internalization of VE-cadherin loosens endothelial cell-cell junctions and thus facilitates subsequent diapedesis of T cells⁵⁷⁻⁵⁹. Extension of protrusions, such as filopodia and podosomes, may also induce changes within the endothelial cells to initiate diapedesis^{46,52,56,57}. Following the initiation of diapedesis, the T cell extrudes its cell body through and underneath the endothelium^{46,56,57,60,61}. As the T cell migrates beneath the endothelium, it retracts its uropod to complete the process (Fig 1.1)^{51,56,57,60}. The nucleus is the most rigid cellular structure and, as such, presents a significant obstacle to the completion of diapedesis^{51,60-64}. It has been proposed that the segmented and deformable shape of the neutrophil nucleus facilitates the rapid migration of these cells through restrictive environments^{54,62,65}. In contrast, T cells exhibit a more rigid, ovoid nucleus and rely on

significant contractile forces in the uropod to transmigrate the nucleus through the endothelium during diapedesis^{50,60,63}. Thus, nucleus translocation can be a rate-limiting step for T cell migration through restrictive environments and, consequently, diapedesis^{66,67}.

Molecular and Physical Cues for Naive T cell TEM

The combination of differing adhesion molecules and chemokines along with specialized vascular endothelial environments serve to regulate T cell migration to various tissues^{3,4,38}. T cell subtypes differentially express adhesion molecules and chemokine receptors to preferentially home where needed^{3,4}. To facilitate surveillance and antigen recognition, the secondary lymphoid organs rapidly recruit naive T cells from the bloodstream^{68,69}. In the lymph nodes, the cuboidal structure of the HEVs, permissive endothelial junctions, and presence of low shear stress forces all promote efficient TEM⁶⁸. HEVs express oligosaccharide decorated glycoproteins collectively known as peripheral node addressin (PNAd). PNAd binds L-selectin (CD62L), which is highly expressed on naive T cells and thus mediates the rolling stage of TEM in these tissues^{42,68,70}. Circulating naive T cells also express high levels of the chemokine receptor CCR7 which recognizes the chemokines CCL21 and CCL19 expressed by the HEV endothelium and within the lymph node^{18,68}. ICAM-1, expressed on the HEV endothelium, binds the integrin lymphocyte function-associated antigen-1 (LFA1, integrin α L β 2) expressed by T cells to facilitate arrest and crawling (Fig 1.1). In the spleen, a sinusoidal vascular architecture reduces shear stress, and a fibroblastic reticular network expressing CCL21 guides naive T cell migration from the vasculature to the white pulp⁶⁹. A subset of memory T cells, known as central memory, also express CCR7 and CD62L, which promotes their migration to secondary lymphoid organs²².

Molecular and Physical Cues for Activated T cell TEM

Upon activation, many T cells downregulate CD62L and CCR7 and upregulate chemokine receptors and adhesion molecules that promote their preferential recruitment to inflamed non-lymphoid tissues^{3,4,71}. Activation upregulates enzymes in T cells that post-translationally glycosylate P-selectin glycoprotein ligand-1 (PSGL-1) to enable its binding to P- and E-selectins^{39,72}. Inflammatory mediators in tissues, such as tumor necrosis factor- α (TNF- α), stimulate the expression of P- and E-selectins on the endothelium, thus enabling recruitment of activated T cells to these inflamed tissues (Fig 1.1)^{73,74}. Similar to neutrophils⁷⁵, activated T cells are also capable of generating specialized membrane protrusions, known as tethers and slings, that stabilize rolling under the high shear stress conditions found in the vasculature of many non-lymphoid tissues³⁹. In addition, activated T cells upregulate expression of LFA-1 and VLA-4 (very late antigen-4, integrin $\alpha 4\beta 1$), which can then bind to ICAM-1 and VCAM-1, both of whose expression is induced on inflamed endothelium (Fig 1.1)^{73,76}. Activated T cells, particularly CD8 and Th1 T cells, upregulate the chemokine receptor CXCR3, which can drive T cell trafficking to a broad range of inflamed tissues that express the ligands CXCL9, CXCL10 and CXCL11 (Fig 1.1)^{71,77-82}. Tight junctions between endothelial cells in some non-lymphoid organs, such as in the CNS, can render the vasculature of these organs so restrictive to immune migration that they are often considered to be immune privileged⁸³. However, mediators produced by inflamed tissues can also reduce the tightness of junctional adhesions between endothelial cells, creating more permissive sites for leukocyte entry^{59,84}. Thus, changes in the properties of both T cells and endothelial cells orchestrate activated T cell recruitment to sites of inflammation.

In addition to these broad regulators of T cell trafficking to inflammatory sites, activation of T cells in specific contexts can induce the expression of more specific tissue homing adhesion

molecules and chemokine receptors^{3,4}. For instance, T cells that undergo activation in the gut-draining secondary lymphoid organs in the presence of vitamin A metabolites upregulate integrin $\alpha 4\beta 7$ (LPAM-1) and CCR9. These surface molecules can facilitate preferential TEM in the gut mucosa via their respective ligands, mucosal vascular addressin cell adhesion molecule 1 (MAdCAM1) and CCL25⁸⁵. In contrast, T cells activated in skin draining lymph nodes in the presence of vitamin D metabolites express CCR10, which can respond to CCL27 produced in the skin, while suppressing expression of LPAM-1⁸⁶. While the skin and gut homing programs are the best defined, there is evidence that other activation contexts may also promote specific trafficking to defined tissue sites. Dendritic cells (DCs) in the mediastinal lymph node have been suggested to activate T cells to express CCR4 to respond to CCL17 and CCL22 expressed in lung⁸⁷. A study in a rat model of EAE suggested that self-reactive T cells adopt an adhesive and migratory transcriptional profile that promotes their entry into the CNS⁸⁸.

Therapeutically Targeting T cell Migration

Disruption of T cell migration by targeting the surface molecules that guide TEM has shown therapeutic promise in a number of inflammatory and autoimmune diseases⁸⁹. A monoclonal antibody against the $\alpha 4$ integrin subunit has been used to block VLA-4-mediated trafficking to the CNS to treat MS as well as LPAM-1-mediated trafficking to gut mucosal sites to treat Crohn's disease^{90,91}. An antibody specific to LPAM-1, and therefore more selectively targeting trafficking to the gut, has shown promise for treating ulcerative colitis and Crohn's disease^{92,93}. A chemical antagonist of CCR5 has shown promise in treating graft-versus-host disease⁹⁴. A complication of therapeutically inhibiting T cell trafficking has been immune suppression and resulting pathologies⁸⁹, such as re-emergence of JC virus in treated MS patients⁹⁵, thus highlighting the central importance of T cell migration to function in both protective and pathologic contexts.

Transduction of Chemokine and Integrin Signaling by GTPases

To undergo the stages of TEM, T cells must translate the migratory cues given by adhesion molecules and chemokines into the morphological changes and force generation necessitated by the physical challenges of TEM^{6,47,96}. To mediate these changes, chemokine and integrin signals are transduced and coordinated by Rho- and Ras- GTPases, which convert between inactive GDP-bound and active GTP-bound forms (Fig. 1.3)⁹⁷⁻⁹⁹. This cycle is dynamically regulated by GTPase activation proteins (GAPs), and guanine nucleotide exchange factors (GEFs), which promote the inactive and active GTPase forms, respectively^{97,99}. After chemokine binding, chemokine receptors alter their conformation, transducing their signal via the activation of G protein heterotrimers, composed of the α , β , and γ subunits⁹⁹. G α subunits can interact directly or in a complex with GEFs to stimulate Rho GTPase activation⁹⁹. G protein activation can also stimulate phospholipase C isoforms, Ser/Thr-kinases, phosphatidylinositol 3-kinase isoforms, and c-Src-related non-receptor tyrosine kinases⁹⁹. Phosphoinositide production and kinase activity downstream of these molecules can also activate GEFs to in turn activate GTPases⁹⁹⁻¹⁰¹. TCR signaling and integrin signaling can also activate some of these same signaling cascades to activate GEFs and subsequently, RhoGTPases^{99,100}. Rap1, a Ras-GTPase, and four members of the Rho GTPase family, Rac1, Rac2, RhoA and Cdc42, have been implicated in TEM⁹⁷⁻⁹⁹. Rap1, which is activated by CALDAG-GEF1, forms a complex to trigger conformational activation of LFA-1 for high-affinity binding in response to chemokine stimulus. Rap1 in concert with Cdc42 has also been implicated in regulating T cell polarity¹⁰². Rac1 and Rac2 function mainly at the leading edge of the cell to generate the formation of the lamellipodium mediated by the activity of the Wiskott-Aldrich syndrome protein (WASP) family⁹⁹. In T cells, Rac1 and Rac2 activity is primarily controlled by the DOCK2 and Vav1 GEFs activated by chemokine receptors and the TCR⁹⁹. In the rear of the cell, RhoA, activated

by GEF-H1, promotes contraction of the uropod via the activity of Rho- associated coiled-coil containing protein kinase (ROCK), which in turn can regulate MyoIIa contractile activity^{51,103}. RhoA function has also been observed at the leading edge of the cell, where it has been proposed to be involved in extension and contraction of membrane protrusions^{98,103,104}. Cdc42, regulated in part by the DOCK8 GEF, has also been suggested to regulate membrane protrusions, in particular filopodia^{105,106}. While these Rho GTPase members have been well studied, less is known about the downstream cytoskeletal effectors that can be activated by these signaling pathways and that mediate the morphological changes inherent to TEM.

Actin Filament Dynamics During Migration

To traffic to tissues, T cells must adapt to diverse environments and respond to a variety of environmental cues^{6,38}. During TEM, T cells must convert these cues into coordinated morphological changes coupled with force generation to resist shear forces and to traverse vascular endothelial barriers (Fig 1.1)^{6,38,47}. The actin cytoskeleton serves as a dynamic network of filaments to provide both the structure and force to accomplish these tasks (Fig. 1.2)^{6,47}. Globular actin monomers (G-actin) bound to ATP polymerize into a filamentous actin (F-actin) double-stranded helix¹⁰⁷. Hydrolysis of ATP to ADP destabilizes actin monomer interactions leading to depolymerization¹⁰⁷. Nucleation of new actin filaments is thermodynamically unfavorable. However, once an initial oligomer has formed, actin polymerization can proceed in a polarized fashion, with polymerization occurring 10x faster at the dynamic barbed end than the less active pointed end¹⁰⁷. This spontaneous polymerization of actin is regulated by the local concentration of ATP bound G-actin¹⁰⁷. The protein profilin sequesters G-actin to both inhibit spontaneous polymerization and catalyze the exchange of ADP for ATP in the actin monomer¹⁰⁷. Recruitment of G-actin-bound profilin to an actin filament can thus provide a controlled means of promoting F-actin elongation or nucleation at a specific site within the cell (Fig 1.4B). A

variety of cytoskeletal effector proteins associate with actin to regulate the growth and turnover of filaments, thus enabling the cell to adaptively remodel the actin cytoskeleton to suit its needs¹⁰⁷. Such cytoskeletal effector functions include: nucleation of new filaments, elongation of existing filaments, capping to block elongation and stabilize filaments, severing of filaments and depolymerization of filaments¹⁰⁷. The ability of this versatile cytoskeletal system to dynamically create structural scaffolds, effect morphological changes, and generate force make it an essential participant in the migration of cells^{6,47}. However, the contribution of specific cytoskeletal effectors to T cell migration and extravasation has only recently begun to be understood.

Actin Networks and Effectors in T cells

Actin networks in T cells are comprised of branched and linear filaments that are cross-linked by the motor protein non-muscle Myosin IIA (MyoIIA) (Fig. 1.2)⁶. Immediately beneath the plasma membrane, a network of actin known as the cortical cytoskeleton is important for cell shape maintenance and changes (Figure 1.2)⁶. In the uropod, ROCK, activated by RhoA, phosphorylates the Myosin light chains to activate its motor activity and thus generate contractile forces. In the context of T cell migration these contractile forces have been shown to be important for the retraction of the uropod as the cell moves forward^{51,60,103,108}. Our lab has previously shown that contractile forces generated by MyoIIA also promote transmigration of the T cell nucleus across the endothelium during TEM (Fig. 1.1)⁶⁰. Additionally, our lab has previously demonstrated that MyoIIA deficiency impairs both naive and activated T cell trafficking to lymphoid and non-lymphoid organs^{60,109}.

Downstream of Rac and Cdc42 signaling, WASP family proteins bind to Arp2/3 (actin related protein 2/3 complex) to form an activated complex that can recruit profilin-bound actin monomers to nucleate new actin filaments. This complex binds to pre-existing actin filaments to nucleate new filaments at an angle of 70 degrees thus developing a branched actin network

(Fig 1.4B)¹⁰⁷. In migrating T cells, these branched actin networks expand at the leading edge of the cell, pushing the membrane forward to create the lamellipodium (Fig 1.2)⁹⁶. Arp2/3 and branched actin networks may also be involved in generating filopodia¹¹⁰. Mutations in WASP and other regulators of Arp2/3 function, such as WIP (WASP-interacting protein) and Coronin1A, cause immunodeficiency, in part due to impaired lymphocyte trafficking^{111–113}. Additionally, WASP and Arp2/3 contribute to the formation and maintenance of the immune synapse^{114,115}.

Linear actin polymerization is mediated by two major families in T cells: the Ena/VASP (vasodilator-stimulated phosphoprotein) family and the formin family¹¹⁶. These families can also participate in branched actin networks by elongating filaments nucleated by Arp2/3. The Ena/VASP family elongates actin filaments mainly through anti-capping activity and recruitment of G-actin and profilin^{117,118}. In T cells, two Ena/VASP members are expressed, VASP and Ena-Vasp-Like (EVL). While EVL and VASP function has not been extensively characterized in T cells, they have been shown to localize to filopodia and lamellipodia^{116,119} and may also be involved in actin rearrangement downstream of TCR signaling¹²⁰. We have recently shown that EVL and VASP modulate $\alpha 4$ integrin expression and function in activated T cells to promote diapedesis and trafficking to both lymphoid and non-lymphoid organs¹¹⁹.

Formins remodel the actin cytoskeleton both by nucleating new actin filaments and processively elongating them via recruitment of profilin-bound G-actin and by anti-capping activity (Fig 1.4B)¹²¹. While mammals have 15 formin family members¹²², two are highly expressed in primary T cells: Diaphanous-related formin-1 (mDia1, Diaph1) and Formin-like 1 (FMNL1, FRL1)^{104,116,123–125}. While FMNL1 and mDia1 only share 23% sequence homology, they are characterized by the same overall domain structure^{121,122}. Formins form homodimers to carry out their function^{121,122}. Dimerization of the formin homology 2 (FH2) domain creates a

toroid structure that encircles the actin filament to provide processive actin polymerase activity (Fig 1.4B)^{121,122}. This function is aided by a formin homology 1 (FH1) domain that recruits profilin-bound G-actin. Regulation of these formins is controlled by an autoinhibition mechanism^{121,122,126–128}. A C-terminal diaphanous autoregulatory domain (DAD) interacts with a N-terminal diaphanous inhibitory domain (DID) to inactivate actin polymerization (Fig 1.4A)^{121,122,126–128}. Binding of Rho GTPases to a GTPase binding domain (GBD) disrupts this DID-DAD inhibitory interaction to activate the formin (Fig 1.4A)^{121,122,127,128}. GTPase binding has also been suggested to regulate the localization of mDia1 and FMNL1¹²⁶. In this manner, formins serve as terminal cytoskeletal effectors for Rho GTPases to induce actin network remodeling (Fig 1.4B).

While mDia1 is expressed in a wide variety of tissues, it is upregulated by activated T cells and tissue infiltrating T cells^{104,129,130}. Biochemically, the GBD of mDia1 has been shown to be capable of binding Rac1 and Cdc42, though it has the highest affinity for RhoA¹³¹. Studies of mDia1 in T cells have further confirmed that mDia1 is primarily a RhoA effector^{103,104}. In crawling T cells, mDia1 localizes at the leading edge behind the lamellipodium to drive actin polymerization^{103,104}. mDia1 may also be involved in the formation of filopodia, though this has not been observed in primary T cells^{116,132}. In addition to its actin polymerization function, mDia1 has also been shown to interact with the microtubule cytoskeleton^{133,134}. Mice deficient in mDia1 have reduced numbers of T cells in secondary lymphoid organs as a result of impaired T cell thymic egress^{124,135}. Additionally, mDia1 has been suggested to mediate morphological changes and cytoskeleton remodeling in response to TCR stimulus and within the immunological synapse^{104,116,135,136}. These findings may explain prior observations that mDia1-deficient T cells are impaired in proliferation in response to anti-CD3 and anti-CD28 stimulus^{124,135}. Loss of mDia1 in T cells impairs trafficking to both lymphoid organs as well as inflamed skin^{124,134}.

Consistent with these trafficking defects, mDia1-deficient T cells display impaired chemotaxis even though chemokine receptor expression levels are unaltered.^{124,134,135} Likewise, integrin expression appears to be unaltered in mDia1-deficient T cells, although adhesion to integrin ligands appears to be impaired^{104,134,135}. While the specific requirement for mDia1 in T cell TEM for T cells is unknown, we have recently shown that mDia1 promotes completion of diapedesis in leukemia cells¹³⁷. Thus, mDia1 may act in number of capacities to promote T cell migration. However, precisely how these effects combine to regulate T cell function during an immune response is not fully understood.

Unlike mDia1, which is expressed in a wide variety of cell types, FMNL1 expression is largely restricted to cells of the hematopoietic lineage^{123,129,130,138}. There are conflicting reports as to which GTPases regulate FMNL1 activity. The initial pulldown assays of FMNL1 in a mouse macrophage cell line suggested it interacts with Rac1, but not Cdc42 or RhoA¹²³. Pulldown assays in a human B cell lymphoma line also suggested a FMNL1-Rac1 interaction¹³⁹. However, another report using a different mouse macrophage cell line and *in vitro* biochemical assays reported that FMNL1 was specifically regulated by Cdc42 but not Rac1 or RhoA¹²⁶. In the Jurkat T cell leukemia line, FMNL1 was reported to bind Rac1 and RhoA but not Cdc42¹¹⁶. Thus, the regulation of FMNL1 may be cell type- and organism-specific. In addition to actin polymerization and anti-capping activity, biochemically, FMNL1 has been also suggested to have filament bundling and interestingly, filament severing activity¹⁴⁰. FMNL1 is not well characterized in T cells, but previous studies have identified roles in macrophage phagocytosis, membrane protrusion formation, and migration^{123,126,141,142}. In leukemic cells, FMNL1 has been suggested to be involved in membrane dynamics, proliferation, and migration^{139,143,144}. In the Jurkat T cell leukemia line, FMNL1 contributes to the reorientation of the centrosome to the immune synapse and Golgi apparatus structure^{116,145}. Knockdown of FMNL1 in human CD8 T

cells was reported to marginally impair non-specific cytotoxic activity¹¹⁶. FMNL1 has been reported to be transcriptionally upregulated in self-reactive T cells that are licensed for CNS entry in a rat model of EAE⁸⁸. Additionally, FMNL1 expression is increased in T cells in equine spontaneous autoimmune uveitis¹⁴⁶. However, the mechanistic role of FMNL1 in primary lymphocytes and *in vivo* is unknown.

Scope of Thesis

The migration of T cells is essential to their role in immune surveillance and effector function in tissues^{3,4}. Targeting of T cell trafficking has proven to have therapeutic benefit in controlling T cell driven autoimmune and inflammatory pathologies⁸⁹. The critical role of selectins, chemokines and integrins in enabling T cell TEM is well established³⁸. Additionally, the role of Rho GTPases in transducing these external signals to mediate the shape changes involved in TEM has been well characterized^{97,98}. However, the role of downstream cytoskeletal remodeling proteins in effecting these changes is less well understood. Previous studies by our lab and others identified roles for Arp2/3, MyoIIA, and Ena/Vasp proteins in T cell migration and function. In the work presented in this thesis, we sought to identify the role of the formins, FMNL1 and mDia1, in T cell TEM and autoimmune disease.

Previous studies of FMNL1 had used RNAi knockdown^{116,126,139,142,143} or myeloid specific depletion to investigate the function of FMNL1¹⁴¹. Therefore, we developed a germline FMNL1 knockout (KO) mouse to more fully examine the function of FMNL1 in primary lymphocytes. Given that previous studies found a role for the formin mDia1 in promoting T cell egress from the thymus and trafficking to lymphoid organs¹²⁴, we hypothesized that FMNL1 KO mice would also be lymphopenic and have T cell trafficking defects. Chapter III details how we targeted the *Fmnl1* gene and confirmed deletion of the FMNL1 protein. We also present the characterization of the immune cell populations in the thymus, blood, and secondary lymphoid

organs of FMNL1 KO mice at steady state. Contrary to our initial hypothesis, we found equivalent levels of both developmental and mature populations of T cells in FMNL1 KO and wild-type (WT) mice. Additionally, we found equivalent populations of other lymphocytes and myeloid cells at steady state. Chapter III also highlights that co-transfer experiments with naive FMNL1 KO and WT T cells revealed no differences in homing to lymphoid organs. Additionally, we found that FMNL1 KO T cells activated equivalently to WT T cells *ex vivo*. Together, our findings in this chapter indicate that FMNL1 is dispensable for lymphocyte development, homeostatic trafficking, and activation.

Activated T cell trafficking to non-lymphoid tissues occurs in physiologically distinct vascular environments and involves different chemokines and adhesion molecules compared to homeostatic T cell trafficking to lymphoid organs^{3,4}. Thus, we hypothesized that FMNL1 would be required for activated T cell trafficking to non-lymphoid tissues with more restrictive vascular barriers. Chapter IV examines the ability of activated FMNL1 KO T cells to traffic to inflamed pancreatic islets in a murine type 1 diabetes model or the inflamed CNS in the murine EAE model of MS. We found that *ex vivo* activated FMNL1 KO T cells were impaired in homing to both the islets and the CNS. In contrast, *ex vivo* activated FMNL1 KO and WT T cells migrated equivalently to secondary lymphoid organs. Chapter IV also presents our findings that self-reactive FMNL1 KO T cells are impaired in inducing type 1 diabetes and EAE in T cell transfer disease models. Combined, our results suggest FMNL1 selectively promotes activated T cell trafficking to inflamed non-lymphoid organs and, consequently, promotes T cell-driven autoimmune disease.

Given our observation of impaired trafficking by activated FMNL1 KO T cells, we hypothesized that FMNL1 KO T cells would be impaired in transendothelial migration. Chapter V examines the requirement for and mechanism of action of FMNL1 in the various stages of

TEM, as well as FMNL1 localization in migrating T cells. We found that while FMNL1 was dispensable for adhesion, crawling and initiation of diapedesis, it was important for the completion of diapedesis. Additionally, we found that FMNL1 was enriched behind the nucleus in transmigrating T cells and that FMNL1 KO T cells were impaired in transmigrating their nucleus through the endothelium during TEM. Based on these results, we hypothesized that FMNL1 would be selectively required for migrating through narrow pores. In Chapter V, we also present our findings that FMNL1 deficiency impaired T cell transwell chemotaxis through 3 μ m pores but not 5 μ m pores. Additionally, we found that FMNL1 was dispensable for neutrophil migration through 3 μ m pores, suggesting that nuclear rigidity determines the requirement for FMNL1 in migrating through restrictive barriers. Strikingly, co-inhibition of FMNL1 and MyoIIA entirely eliminated T cell chemotaxis through 3 μ m pores. Furthermore, we found that FMNL1 KO T cells are impaired in actin polymerization in response to chemokine. Finally, in this chapter, we also present our finding that varying the expression level of FMNL1 in T cells positively correlates with their ability to migrate through restrictive barriers. Taken together, our data in this chapter suggest that the requirement for FMNL1 is pore size-dependent and that T cell migration through restrictive barriers relies on both FMNL1 and MyoIIA.

Based on previous reports that mDia1 promotes T cell trafficking^{124,134,135}, we hypothesized that self-reactive mDia1 KO T cells would be impaired in inducing EAE. We also hypothesized that mDia1 KO T cells would be impaired in TEM. Chapter VI details our examination of the behavior of mDia1 KO T cells in EAE and TEM. We found that mDia1 KO T cells were impaired in inducing EAE and at the diapedesis step of TEM. Our results from this chapter suggest that mDia1-deficient T cells have similar autoimmune and TEM phenotypes to FMNL1-deficient T cells despite their different localization and upstream regulation.

Together, the data presented in this thesis identify a previously unknown role for FMNL1 in promoting the transmigration of the nucleus through restrictive barriers during T cell TEM. Additionally, we show that both FMNL1 and mDia1 are important for T cell driven induction of autoimmune disease. These findings may provide insights for targeting actin cytoskeletal effectors to therapeutically modulate T cell function in autoimmune and inflammatory diseases.

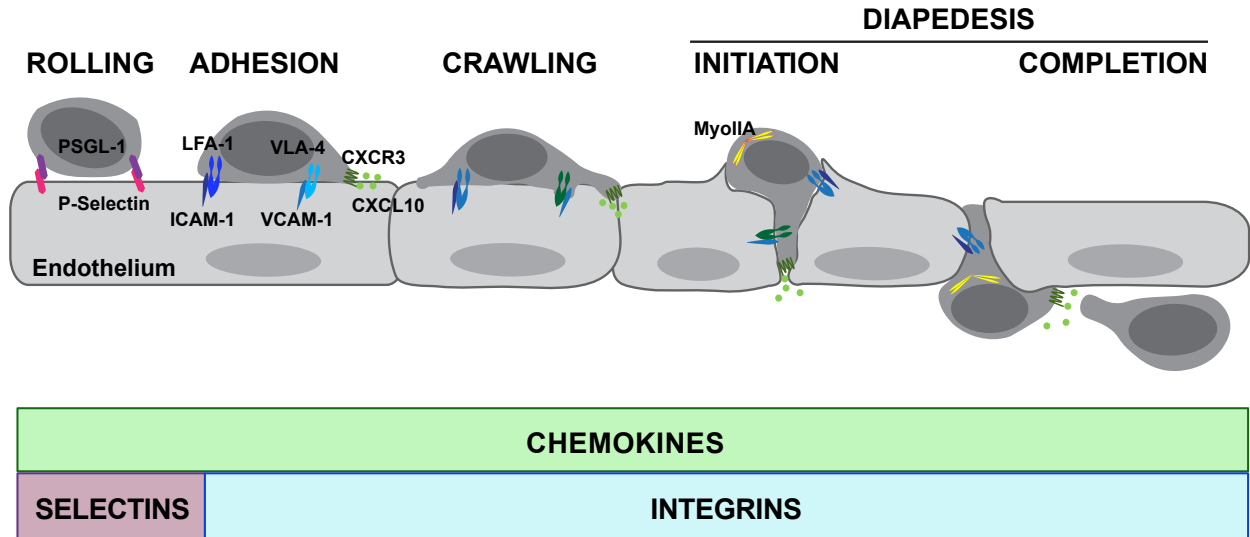


Figure 1.1: The process of T cell transendothelial migration (TEM). A model of the four sequential stages of TEM and some of the key molecular regulators of this process. The colored bars denote the stages of TEM during which the indicated types of molecular regulators are involved. T cells are initially captured from the blood flow to begin selectin-mediated (1) rolling along the vascular endothelial wall followed by (2) firm adherence in a chemokine-driven integrin-mediated process. After (3) crawling along the endothelium probing for permissive sites for extravasation, T cells initiate the (4) diapedesis step and squeeze through the vascular endothelium.

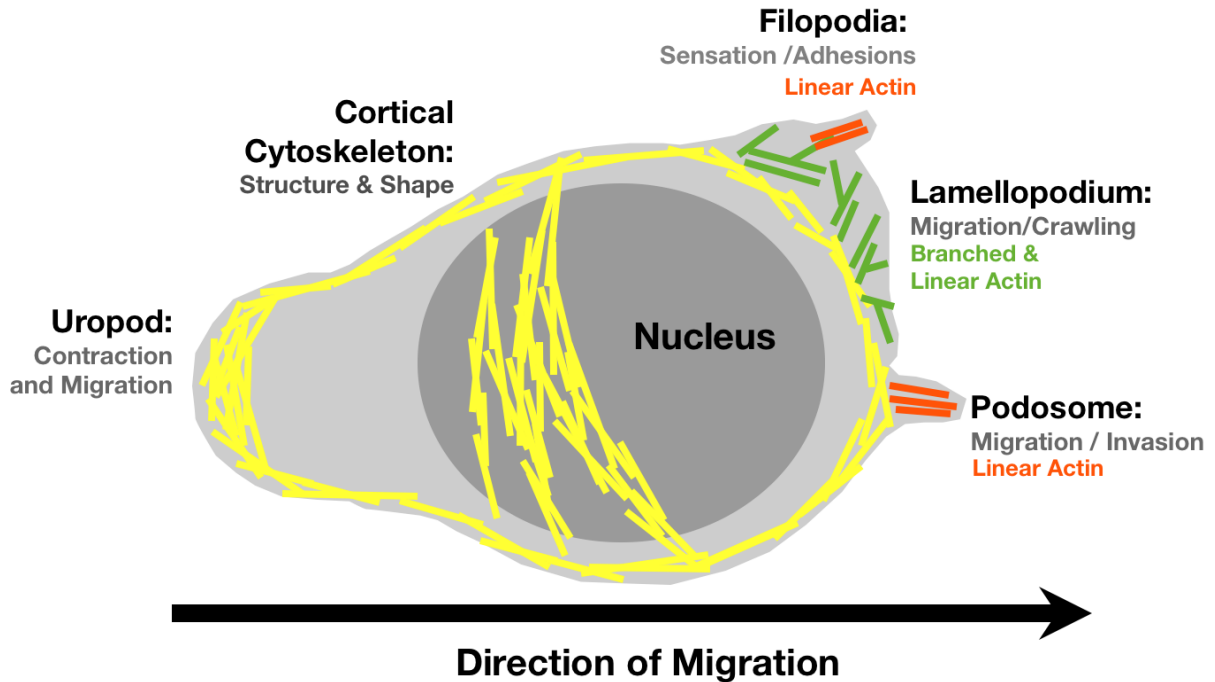


Figure 1.2: Morphology and actin networks in a crawling T cell. A schematic depicting the morphological structures present in a migrating T cell and the actin networks that regulate them. Crawling T cells adopt an amoeboid morphology. Extension of branched and linear actin networks generates a ruffled, protrusive structure known as the lamellopodium at the leading edge of the cell. Additionally, during crawling, linear actin-rich micro-protrusions, known as filopodia or podosomes, extend from the T cell to probe for chemokine signals as well as permissive sites for transmigration across the endothelium. The cortical cytoskeleton lies immediately beneath the plasma membrane and provides structure and shape to the cell. A contractile structure known as the uropod defines the trailing edge.

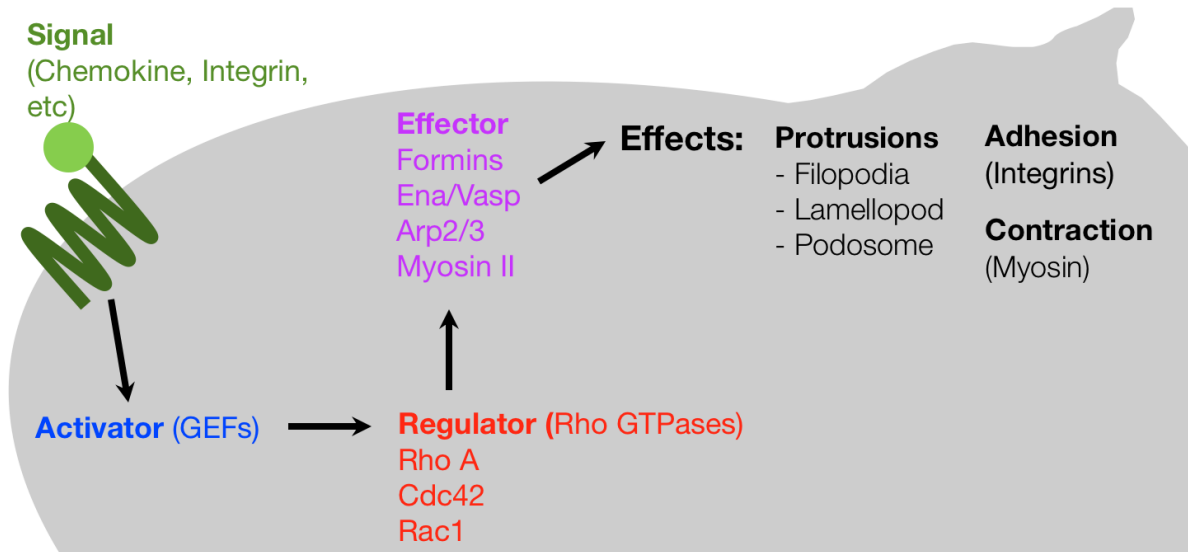


Figure 1.3: Transduction of migratory signals to generate morphological changes.

Generalized schematic depicting how external signals from chemokines and integrin ligands are transduced to generate force and morphological changes. Upon binding their ligands, chemokine receptors and integrins induce local phosphoinositide production and kinase activity to activate guanine nucleotide exchange factors (GEFs). The GEFs in turn activate Rho GTPases which orchestrate cytoskeletal rearrangements through the activation of terminal effector proteins that directly interact with the actin cytoskeleton.

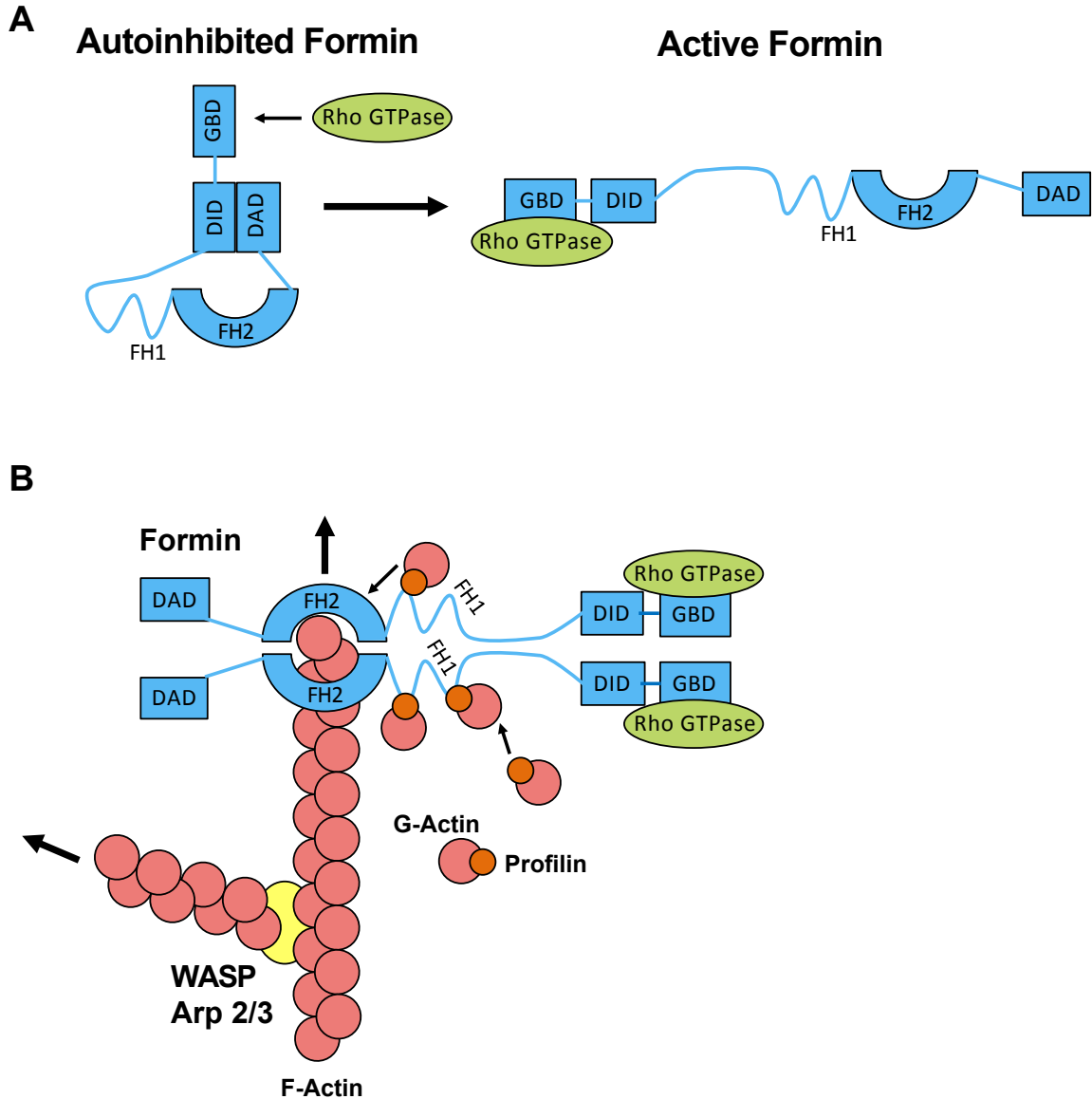


Figure 1.4: Formin domain organization and regulation of activity. **A)** Schematic of formin domain organization in autoinhibited and active states. A C-terminal diaphanous autoregulatory domain (DAD) interacts with a N-terminal diaphanous inhibitory domain (DID) to inactivate actin polymerization activity of the the formin holomorphy 1 (FH1) and formin homology 2 (FH2) domains (Fig 1.4A). Binding of Rho GTPases to a GTPase binding domain (GBD) disrupts this DID-DAD inhibitory interaction to activate the formin. **B)** Schematic of actin polymerizing activity by a formin dimer and the WASP Arp 2/3 complex. Dimerization of the FH2 domain creates a toroid structure that encircles the actin filament to provide processive actin polymerase activity. This function is aided by the FH1 domain that recruits profilin-bound G-actin. The WASP Arp2/3 complex creates branched actin networks by binding to existing filaments to nucleate new filaments at an angle of 70 degrees .

CHAPTER II

MATERIALS AND METHODS

Generation of FMNL1 KO Mice

To obtain FMNL1 KO mice, we targeted the *Fmnl1* gene via homologous recombination by inserting, after exon 3 of *Fmnl1*, a strong splice acceptor and a LacZ tag followed by a Neomycin selection cassette into C57BL/6 embryonic stem (ES) cells. The targeting construct was purchased from EUCOMM. This construct also inserts loxP sites flanking exons 4 to 6 as well as FRT sites flanking the LacZ tag and Neomycin cassette. This can enable future conversion of the targeted allele into a conditional KO after crossing with Flp recombinase mice to eliminate the LacZ-Neomycin cassette and then crossing to mice expressing Cre recombinase to excise exons 4-6. To target the *Fmnl1* allele, C57BL/6N (JM8.F6) ES cells were electroporated with the targeting construct and selected using G418. Individual ES cell colonies were isolated, and putative positive homologous recombinants were identified using loss of allele analysis followed by long range PCR through both the 5' and 3' ends of the targeting construct into the *Fmnl1* locus. The homologous recombinant ES cell clones were chromosome counted, and clones with the best euploidy were microinjected into C57BL/6 albino blastocysts. High percentage male chimeras generated from these injections were bred to C57BL/6 albino females. Offspring with black coat color were genotyped for the desired *Fmnl1* targeting by PCR. For these PCRs the following primer sequences were used (Fig 3.1): GF4, ACCATATTGTTATCTAGGTCTCCTTG; LAR3, CAACGGGTTCTTCTGTTAGTCC; RCF, GGTCTGAGCTCGCCATCAGTTCA; GR4, GCCTACATGGTGTTCATCAGGATCCAC. Mice containing the *Fmnl1* targeted allele were selected as breeders to propagate the FMNL1 KO transgenic line. Dr. Jennifer Matsuda and the National Jewish Mouse Genetics Core carried out the gene targeting, ES cell manipulation, and chimera generation. Targeting of the *Fmnl1*

gene was further confirmed by western blot comparing lysates from T cells derived from control and homozygous FMNL1 KO mice, which show a complete loss of FMNL1 protein.

Mice

For characterization experiments and experiments with polyclonal T cells, FMNL1 KO mice were paired with age and sex matched WT C57BL/6 mice bred in-house. FMNL1 KO mice were crossed with OT-I (C57BL/6-Tg(TcraTcrb)1100Mjb/J)¹⁴⁷, OT-II (B6.Cg-Tg(TcraTcrb)425Cbn/J)¹⁴⁸, or 2D2 (C57BL/6-Tg(Tcra2D2,Tcrb2D2)1Kuch/J)¹⁴⁹ TCR transgenic mice bred in-house to create respective FMNL1 KO TCR transgenic mice. Age and sex matched WT TCR transgenic mice bred in-house were used as controls. CD45.1/.1 (B6.SJL-*Ptprc^a Pepc^b*/BoyJ)¹⁵⁰ mice were purchased from Charles River and bred in-house. RIP-mOva (C57BL/6-Tg(Ins2-TFRC/OVA)296Wehi/WehiJ)¹⁵¹ mice were purchased from Jackson Labs. Mice deficient in mDia1 (mDia1 KO) on the C57BL/6 background, generated by Sakata et al. as described previously¹²⁴, were generously provided by Dr. Shuh Narumiya (Kyoto University, Kyoto, Japan) and bred in-house. For experiments with polyclonal T cells, mDia1 KO mice were paired with age and sex matched WT C57BL/6 mice bred in-house. 2D2 TCR transgenic mice bred in-house were crossed with mDia1 KO mice to create mDia1 KO 2D2 TCR transgenic mice. Age and sex matched WT 2D2 TCR transgenic mice were used as controls. All mice used in experiments were 8-16 weeks old. In all experiments except for the EAE trafficking experiments both male and female mice were used, alternating between genders for experimental repeats. For EAE trafficking experiments, as the EAE induction protocol (Hooke Labs) requires female mice, only female mice were used. The experimental procedures were approved by and mice were handled in accordance with the guidelines of the National Jewish Health Institutional Animal Care and Use Committee. (Protocol Numbers: AS 2811-02-17 and AS2811-12-19)

Media

T cells were cultured in R10 media: RPMI 1640 (Corning) supplemented with L-glutamine (292 $\mu\text{g}/\text{mL}$), penicillin (100 U/mL), streptomycin (100 $\mu\text{g}/\text{mL}$), and β -mercaptoethanol (50 μM) (all purchased from Gibco) and 10% Fetal Bovine Serum (FBS, Corning lot # 35010150). The bEnd.3 endothelial cell line¹⁵² was cultured in D10 media: DMEM (Corning) supplemented with 10mM HEPES (Corning), L-glutamine, penicillin, streptomycin, and β -mercaptoethanol and 10% Fetal Bovine Serum (as above). For microscopy experiments, cells were resuspended in imaging media: RPMI 1640 without phenol red (Gibco) supplemented with 2% bovine serum albumin (BSA, Millipore Sigma) and 10mM HEPES (Corning). Imaging media was also used for actin polymerization and transwell assays.

Antibodies for Flow Cytometry

The following monoclonal antibodies were used for flow cytometry staining: CD4 (GK1.5), CD8a (53-6.7), CD3 (145-2C11), CD19 (6D5), NK1.1 (PK136), CD11b (M1/70), Ly6C (HK1.4), Ly6G(1A8), Siglec F(E50-2440), CD11c (N418), MHCII IA/IE (M5.114.15.2), F4/80 (BM8), CD64 (X54-5/7.1), CD44 (IM7), , CD62L (Me114), CD49d (R1.2), CD11a (M17/4), CXCR3 (CXCR3-173), CXCR4 (L276F12), CD45.1 (A20), CD45.2 (104). These antibodies were purchased from Biolegend, eBioscience, or BD Bioscience. For all experiments involving flow cytometry, cells were blocked with anti-CD16/CD32 antibodies (2.4G2, BioXcell) prior to staining.

Western Blotting

FMNL1 was detected using either a goat polyclonal antibody (Santa Cruz Catalog # sc-66757) or rabbit polyclonal antibody (Abcam Catalog # ab97456). As a loading control, α -tubulin was detected using a mouse monoclonal antibody (B-1-5-2, Millipore Sigma). Antibody staining was visualized using the Odyssey near-infrared imaging system with IRDye-680 or-800

secondary antibodies (Li-cor Biosciences). Band intensities were quantified with densitometry using Odyssey 2.1 software (Li-cor Biosciences).

Flow Cytometry Characterization of FMNL1 KO Mice

Thymus, blood, spleen, and inguinal lymph nodes were collected from FMNL1 KO mice or age and sex matched WT C57BL/6 mice. Blood was lysed in 175 mM ammonium chloride (Millipore Sigma) for 30 min on ice. Spleen and LN were mechanically dissociated and then digested with Collagenase D (0.4 Wunsch U/mL) and DNase (250 μ g/mL) (both from Roche) for 30 min at 37 °C. After preparations of single cell suspensions, cells were stained with fluorescently labeled antibodies. For quantification of cell numbers, a known number of CountBright Absolute Counting Beads (ThermoFisher Scientific) were added to each sample. Samples were then analyzed by flow cytometry on a BD LSR Fortessa. Thymic populations were identified as follows: CD4 single positive (SP): CD4⁺, CD8⁻; CD8 SP: CD4⁻, CD8⁺; double positive (DP): CD4⁺, CD8⁺; double negative (DN) CD4⁻, CD8⁻. Lymphocyte populations were identified as follows: CD4 T cells: CD3⁺, CD4⁺; CD8 T cells: CD3⁺, CD8⁺; B Cells: CD3⁻, CD19⁺; natural killer (NK) cells: CD3⁻, NK1.1⁺. Myeloid populations were identified as follows: monocytes: CD11b⁺, Ly6C^{high}; eosinophils: CD11b⁺, Siglec F⁺; neutrophils CD11b⁺, Ly6G⁺; dendritic cells (DCs): CD11c⁺, MHCII^{high}; macrophages: CD11b⁺, Ly6C^{int}, F4/80⁺, CD64⁺.

T Cell Isolation

Naive CD4, total CD4, or total CD8 T cells were isolated from dissociated and pooled spleen, axillary, brachial, inguinal and mesenteric lymph nodes using magnetic negative selection kits (Stemcell Technologies) as described previously¹¹⁹. Naive CD4 T cells were used for naive T cell trafficking experiments. Isolated CD8 T cells were used for OT-I experiments and islet trafficking experiments. Isolated CD4 T cells were used for all other trafficking experiments, microscopy experiments, and *in vitro* experiments.

Polyclonal T Cell Activation and Culture

Polyclonal T cells were activated *ex vivo* as described previously¹¹⁹. In brief: isolated T cells were activated with plate-bound anti-CD3 (2C11, 1 μ g/well of 24 well plate) and soluble anti-CD28 (PV-1) (2 μ g/mL) antibodies (both from BioXCell) in the presence of irradiated CD45.1/.1 feeder splenocytes for two days in R10. Cells were then removed from the plate and cultured with 10 U/mL recombinant human interleukin 2 (rIL2, AIDS Research and Reference Reagent Program, Division of AIDS, National Institute of Allergy and Infectious Diseases, National Institutes of Health, from M. Gately, Hoffmann-La Roche) for 3 days with addition of fresh R10 media and rIL2 on day 4 post-activation. By day 5, all CD45.1/.1 irradiated splenocytes have died. Prior to use dead cell and debris were removed from the culture using a Histopacque-1119 (Millipore Sigma) density gradient.

Fluorescent Dye-Labeling of T Cells

For lymphoid organ and islet trafficking experiments, WT or FMNL1 KO T cells were differentially dye-labeled with either Cell Proliferation Dye eFluor670 (ThermoFisher Scientific) or Violet Proliferation Dye 450 (VPD) (BD Biosciences) and then mixed at a 1:1 ratio prior to transfer as described previously¹². For CNS trafficking experiments WT or FMNL1 KO T cells were differentially dye-labeled with VPD or CFSE (ThermoFisher Scientific) and then mixed at a 1:1 ratio prior to transfer as described previously¹¹⁹. For microscopy experiments WT and FMNL1 T cells were differentially dye-labeled with either CFSE or CellTrace Yellow (CTY) (ThermoFisher Scientific) and mixed at a 1:1 ratio. For all experiments involving dye-labeled T cells dyes were swapped between WT and FMNL1 KO T cells between experimental repeats to control for potential effects of the dyes. To achieve fluorescent labeling, T cells were incubated at 37°C for 30 min with the following dye concentrations and incubation media: eFluor670 5 μ M in HBSS (Corning); VPD 1 μ M in HBSS; CFSE 2 μ M in RPMI (Corning); CTY 5 μ M in HBSS.

After incubation with the indicated dye in the indicated media, an equal volume of FBS was added to absorb excess dye and samples were incubated for 2 min at room temperature. Cells were then washed 2 times with R10, prior to resuspension in the appropriate buffer or media for injection or imaging.

Lymphoid Organ T Cell Trafficking

WT and FMNL1 KO T cells were differentially dye-labeled, mixed at a 1:1 ratio (2.5 x 10⁶ cells each) ratio and transferred intravenously (i.v.) into CD45.1/.1 recipient mice. 24 h post-transfer mice were euthanized with CO₂. Blood was collected by cardiocentesis and red blood cells were lysed for 30min on ice with 175mM ammonium chloride. Spleen was collected and mechanically dissociated, and red blood cells were lysed for 5 min at room temperature in 175mM ammonium chloride. Inguinal lymph nodes were collected and mechanically dissociated. After preparation of single-cell suspensions, isolated cells were stained with anti-CD45.2 antibodies. For quantification of cell numbers, a known number of CountBright Absolute Counting Beads (ThermoFisher Scientific) were added to each sample. Samples were then analyzed on a CyAn ADP flow cytometer (Beckman Coulter). Transferred T cells were identified as CD45.2⁺ and either VPD⁺ or efluor670⁺.

Islet Trafficking

Adam Sandor and Victor Lui performed the islet trafficking experiments. OT-I T cells (10⁷) were isolated and transferred i.v. into RIP-mOVA recipient mice 7 days prior to harvest to induce immune infiltration of the islets. *Ex vivo* activated, polyclonal, WT and FMNL1 KO CD8 T cells were differentially dye-labeled, mixed at a 1:1 ratio (10⁷ cells each) and transferred i.v. into these RIP-mOVA mice 24 h prior to harvest. Mice were anesthetized with intraperitoneal (i.p.) ketamine (50 mg/g, Vedco) and xylazine (5 mg/g, JHP) prior to euthanasia by cardiocentesis and cervical dislocation. Blood was collected and processed as above. Pancreatic

islets were harvested as described previously^{12,35}. In brief: the pancreas was inflated via the common bile duct with ~3 mL of 0.8 mg/mL Collagenase P (Roche) and 10 µg/mL Dnase I (Roche) in HBSS (Corning). Following inflation, the pancreas was removed and incubated at 37 °C for 10–16 min, and the islets were isolated by density centrifugation. Intact islets were then handpicked under a dissecting microscope and subsequently digested with Collagenase D (0.4 Wunsch U/mL, Roche) for 30 min, followed by 30 min in Cell Dissociation Buffer (Millipore Sigma) to prepare a single cell suspension. Isolated cells were stained with anti-CD45.2, and anti-CD8 antibodies. For quantification of cell numbers, a known number of CountBright Absolute Counting Beads (ThermoFisher Scientific) were added to each sample. Samples were then analyzed on a BD LSR Fortessa. Transferred T cells were identified as CD45.2⁺, CD8⁺, and either efluor670⁺ or VPD⁺.

CNS Trafficking

First, EAE was induced in recipient mice using induction kits (Hooke Laboratories) according to the manufacturers protocol. Briefly, WT female CD45.1/.1 mice were immunized with MOG35–55 peptide emulsified in complete Freund's adjuvant injected subcutaneously, followed by intraperitoneal injection of pertussis toxin on the day of induction and the following day. EAE onset was within 10–15 d post-immunization. Mice were monitored and scored daily for development of EAE based on the following 0–5 scoring criteria: 0, no disease; 1 limp tail; 2, weakness or partial paralysis of hind limbs; 3, full paralysis of hind limbs; 4, complete hind limb paralysis and partial front limb paralysis; 5, complete paralysis of front and hind limbs or moribund state. Mice with a score ≥ 4 were euthanized immediately. Experiments to quantify trafficking to the brain and spinal cord were performed as described previously¹¹⁹. In brief: *ex vivo* activated, polyclonal WT and FMNL1 KO CD4 T cells were differentially dye-labeled, mixed at a 1:1 ratio (10^7 cells each) and transferred i.v. into mice with an EAE score of 2.0-3.0.

24 h later mice were euthanized for tissue collection. To distinguish transferred cells in the vasculature from those fully extravasated into the parenchyma of tissues, mice were injected via tail vein with 3 μ g of anti-CD4-allophycocyanin 4 min prior to euthanasia as described previously^{153,154}. After euthanasia, blood was collected by cardiocentesis and the vasculature of the mouse was perfused with saline through the heart. Blood was processed as above. Brain and spinal cord were mechanically dissociated and total leukocytes were then isolated with a 70%/30% Percoll gradient (Millipore Sigma). After preparation of single-cell suspensions, isolated cells were stained with anti-CD45.2, and anti-CD45.1 antibodies. For quantification of cell numbers, a known number of CountBright Absolute Counting Beads (ThermoFisher Scientific) were added to each sample. Samples were then analyzed on a BD LSR Fortessa. Transferred T cells were identified as CD45.2⁺, CD45.1⁻, and either CFSE⁺ or VPD⁺. In the brain and spinal cord samples, extravasated cells were identified as intravascular CD4⁻.

T Cell Transfer Diabetes Model

WT and FMNL1 KO OT-I T cells were activated *ex vivo* with OVA peptide 257 – 264 (Pi Proteomics) for 2 days in the presence of irradiated CD45.1/.1 splenocytes and then cultured with IL-2 as above for 4 days. WT and FMNL1 KO OT-II T cells were activated with OVA peptide 323-339 (GenScript) for 2 days in the presence irradiated CD45.1/.1 splenocytes and then cultured with IL-2 as above for 4 days. On day 6 post-antigen stimulus, dead cells were removed by Histopacque-1119 (Millipore Sigma) density gradient. OT-I (5×10^6) and OT-II (2.5×10^6) T cells of the same FMNL1 genotype (WT with WT, KO with KO) were then combined and transferred i.v. into RIP-mOVA recipient mice. The blood glucose of the recipient mice was then monitored daily from days 4-28 post-transfer. Mice with blood glucose levels of greater than 350 mg/dL on two consecutive days were considered to be diabetic and were euthanized.

T Cell Transfer EAE Model

WT or KO (FMNL1 KO or mDia1 KO) 2D2 T cells were activated with MOG peptide 35-55 (20 µg/mL) (CHI Scientific) for two days in the presence of irradiated CD45.1/.1 splenocytes and then cultured with IL-2 as above for 5 days. On day 7 post-antigen stimulus, dead cells were removed by Histopacque-1119 (Millipore Sigma) density gradient. Cells were then restimulated with plate-bound anti-CD3 (2C11, 1µg/well of 24 well plate) and plate-bound anti-CD28 (PV-1, 1µg/well of 24 well plate) antibodies (both from BioXCell) for two days. Cells were then removed from the plate and rested for an additional day in R10. 5×10^6 of these activated WT or KO 2D2 T cells were then transferred i.v. into sub-lethally irradiated (300 rads) CD45.1/.1 recipient mice. From days 7-28 post-transfer mice, were monitored and scored for development of EAE as described above. The researchers performing the disease scoring were blinded as to the experimental group of the mice.

Microscopy

All microscopy experiments employed a 3i (Intelligent Imaging Innovations) Marianas spinning-disk confocal microscope system equipped with a Zeiss inverted stand and a Yokogawa spinning disk unit. The microscope is housed in an environmental control chamber and all imaging of live-cells was performed at 37 °C.

T cell TEM Under Flow

TEM experiments were performed as described previously^{119,137,155}. In brief: a 1:1 mixture of *ex vivo* activated, differentially fluorescently dye-labeled WT and KO (FMNL1 KO or mDia1 KO) T cells was resuspended in imaging media at 2×10^6 cells/mL. T cells were perfused at 0.2 dyne/cm² shear-flow into a flow chamber (µ-slide VI, IBIDI) coated with a monolayer of bEnd.3 brain-derived endothelial cells¹⁵², that had been activated with 40ng/mL TNF-α (ThermoFisher Scientific) 24 h before imaging and treated with 10 ng/mL CXCL10

(Peprotech) 30 min before imaging. After 5 min of accumulation, the shear-flow was raised to 2 dyne/cm². Phase contrast and fluorescence images were acquired every 20 s for 30 min using a spinning-disk confocal microscope with a 20x phase objective (Zeiss). Time-lapse images were then analyzed using SlideBook 6 (3i) and the stages of TEM manually scored as described previously^{119,137,155}. Briefly, T cells that lose a portion of the phase halo localized to a small protrusion of the cell, detected by fluorescence, are considered to have attempted diapedesis, with completion being scored as complete loss of the phase halo. Diapedesis data were filtered to exclude all cells that were not present in the field of view for at least 13 min (twice the mean time from the start of imaging until the completion of diapedesis). This filtering is applied to prevent biased scoring of cells that were not present in the imaging field of view for very long as being failed attempts at diapedesis.

FMNL1 Localization During TEM

Ex vivo activated WT T cells dye-labeled with CTY were perfused into flow chambers containing b.End3 monolayers for 5 min as above. Cells were allowed to migrate under 2 dyne/cm² shear flow for 5 min and then fixed with 4% (w/v) paraformaldehyde (Electron Microscopy Sciences) in PBS for 10 min. Cells were then permeabilized and blocked for 1 h at room temperature with the following saponin buffer: 0.5% (w/v) saponin (Millipore Sigma) 2% (v/v) FBS (Corning) 2% (v/v) normal donkey serum (Jackson ImmunoResearch Laboratories) with 0.05% (w/v) sodium azide (Millipore Sigma) in PBS (Millipore Sigma). Cells were stained overnight at 4 °C with a mouse monoclonal antibody against FMNL1 (A4, Santa Cruz) diluted 1:100 in the saponin solution. To visualize the FMNL1 antibody, cells were subsequently stained with a Dylight-649 conjugated Donkey anti-mouse secondary antibody (Jackson ImmunoResearch) diluted 1:100 in saponin buffer for 1 h at room temperature. To visualize the nucleus, cells were additionally stained with 250ng/mL DAPI (ThermoFisher Scientific) during

the secondary antibody step. Multi-plane images were then acquired across a 10 μm range using a spinning-disk confocal microscope with a 40x Water/Oil objective (Zeiss). Maximum Z-projections and side-view reconstruction images were compiled using SlideBook 6 (Intelligent Imaging Innovations). After background fluorescence subtraction, the linescan intensities were then used to categorize the level of FMNL1 enrichment adjacent to the back of nucleus as follows: perinuclear enrichment: ≥ 1.33 x fold peak of FMNL1 fluorescence intensity behind the nucleus compared to other peaks of FMNL1 fluorescence in the rest of the cell; no enrichment: lack of a main peak of FMNL1 fluorescence behind the nucleus; partial enrichment: presence of a FMNL1 peak behind the nucleus with additional peaks of similar intensities in other locations of the cell

Nucleus Localization During TEM

Ex vivo activated, differentially dye-labeled WT and FMNL1 KO T cells were perfused into flow chambers with b.End3 monolayers, allowed to migrate, and then fixed as above. Cells were stained with DAPI as above and then imaged using a spinning-disk confocal microscope (3i) with a 40x phase objective (Zeiss). Similar to the live cell analysis above, phase contrast imaging was analyzed with SlideBook 6 and manually scored to determine the position of the nucleus relative to the plane of the endothelium as follows: above – nucleus completely surrounded by the phase halo; in process – nucleus partially surrounded by the phase halo; below – nuclei with complete absence of the phase halo.

T cell Transwell Migration

Wells of a 24-well plate were prepared containing either 5 μm or 3 μm transwell inserts (Corning) and imaging media with either 100ng/mL CXCL10 or 1 μg /mL CXCL12 (both from Peprotech) in the bottom chamber. 1×10^6 WT or FMNL1 KO T cells were added to the top chambers and allowed to migrate for 1 h at 37 $^{\circ}\text{C}$ into the lower well. 2×10^5 cells (20% of input

cells added to transwells) were placed directly into bottom wells with no transwell as a standard to calculate the percentage of migrated cells. Each condition was set up in duplicate. Migrated T cells were collected from the bottom wells and 25 μ L of CountBright Absolute Counting Beads (ThermoFisher Scientific) were added to each sample to enable quantification of migrated cells. Each sample was quantified for a fixed period (30 s) using a flow cytometer (CyAn ADP Beckman Coulter). The number of cells counted during this time was normalized to the number of beads counted to adjust for any variations in flow rate during the run. For chemical inhibition experiments, T cells were incubated for 30 min at 37 °C with 100 μ M blebbistatin (Millipore Sigma) or an equivalent amount of DMSO vehicle prior to the transwell assay. During the assay, this concentration was maintained in both transwell chambers, as well as the 20% standard wells used to calculate the percentage of migrated cells.

Neutrophil Transwell Migration

Wells of a 24 well plate were prepared with 3 μ m transwell inserts as above and with 100ng/mL CXCL1 (Peprotech) in the bottom chamber. Neutrophils were isolated from the bone marrow of WT or FMNL1 KO mice using magnetic negative selection kits (StemCell Technologies), and then 1×10^6 cells were added to the top chambers of the transwells. Cells were allowed to migrate for 1 h at 37 °C and then quantified as above.

Actin Polymerization Assay

Quantification of actin polymerization in response to chemokine was performed as described previously¹¹⁹. In brief: *ex vivo* activated WT or FMNL1 KO T cells were stimulated with either no chemokine, 1 μ g/mL CXCL12 or 100 ng/mL CXCL10 (Peprotech) for 5, 15, or 60 s at 37 °C in imaging media. All conditions were set up in duplicate. The reaction was stopped using 4% (w/v) paraformaldehyde (Electron Microscopy Sciences) in PBS, and the cells were fixed for 10 min. T cells were then permeabilized with saponin buffer (as in microscopy

experiments) for 30 min at room temperature. Cells were stained with a 1:50 dilution of Phalloidin Alexa Fluor 647 (ThermoFisher Scientific), and fluorescence was quantified using a CyAn ADP flow cytometer (Beckman Coulter). Geometric mean fluorescence intensities (gMFI) were normalized to the values of the unstimulated samples.

FMNL1 Re-Expression

WT or FMNL1 KO T cells were activated with anti-CD3 and anti-CD28 antibodies as above and then on day two post-activation transduced with Moloney murine leukemia retrovirus (MMLV) constructs either expressing FMNL1 and GFP (under an IRES) or fluorescent protein alone. To maximize expression, cells were transduced a second time with the same viral vectors on day 3 post-activation. On day 4 post-activation, GFP⁺ T cells were sorted using an ICyte Synergy (Sony). After 24 h of culture, cells were used in transwell assays or for western blot as described above.

Flow Cytometry Analysis

Flow cytometry gating, analysis and graph preparation were performed using FlowJo v.10 software. To determine fluorescence spillover and compensation, single stains for each fluorescent antibody or dye used in a given experiment were prepared and fluorescence intensities in each channel were recorded. The percentage compensation for each combination of channels was then calculated using FlowJo. This compensation matrix was then applied to samples and manually checked to ensure appropriate compensation at all levels of fluorescence and for over/under-compensation. Flow cytometry gates were based on previous reports for the indicated population, or unstained or fluorescence-minus-one controls to determine a true positive population. For comparisons of expression levels between WT and either FMNL1 KO or mDial KO T cells, the geometric mean fluorescence intensity (gMFI) was calculated for the indicated channel using FlowJo. Then the gMFI of a given channel for the KO cells was

divided by the gMFI of the same channel for the WT cells to determine a gMFI ratio.

Statistical Analysis

Graphpad Prism 7.0 software was used to create graphs and to perform all statistical analyses. Specific statistical tests and n for each experiment are indicated in the corresponding figure legend. In experiments directly analyzing WT or FMNL1 KO mice, such as the leukocyte population characterization experiments, the individual mice were considered to be the independent experimental unit (n). In experiments where WT or KO T cells were transferred into multiple recipient mice, the source mouse for transferred cells was considered the independent experimental unit and statistics were performed on the mean values from mice receiving the same source of cells. Similarly, for microscopy experiments, the source mouse was considered to be the independent experimental unit, and statistics were performed on the mean values from cells from the same source.

CHAPTER III

FMNL1 IS DISPENSABLE FOR T CELL DEVELOPMENT AND HOMEOSTATIC TRAFFICKING

Introduction

T cells are inherently migratory and motile cells during both their development in the thymus and their subsequent immune surveillance in lymphoid organs^{3,4}. In T cell development lymphoid progenitor cells traffic to the thymus where they undergo positive and negative selection to produce mature T cells^{14,16}. During this process of thymic selection, thymocytes migrate within the thymus to efficiently scan and interact with specialized thymic APCs^{5,15,16}. Positive and negative selection occur in distinct microenvironments, and thus as thymocytes develop they must migrate between areas of the thymus as well^{15,16}. The strength of thymocyte-APC interactions is thought to dictate the ultimate fate of a developing T cell¹⁶. Mature T cells must then exit the thymus and egress into the bloodstream^{17,156}. From the bloodstream, these mature naive T cells circulate to and within secondary lymphoid organs to survey for the presence of their cognate antigens on APCs. Peptide-MHC recognition by the TCR triggers the formation of an immune synapse between the T Cell and the APC, accompanied by dramatic changes to cell morphology and receptor organization¹⁵⁷. Synapse formation regulates T cell activation and proliferation in response to antigenic stimulus^{157,158}. These T cell migratory behaviors and morphological transformations are facilitated by a dynamic actin cytoskeleton that enables rapid physical changes in response to environmental stimuli^{6,47}. T-APC interactions and organization of the immune synapse are also mediated by cytoskeletal remodeling^{11,116,136,158}. Prior studies of cytoskeletal effector proteins have demonstrated that disruption of normal actin dynamics can alter both lymphocyte development and homeostatic trafficking^{11,111,124,134,135,159}.

Indeed, several immune deficiencies are a result of aberrant regulation of the actin cytoskeleton^{6,111-113,160}.

Actin networks in T cells consist of branched and linear filaments that are cross-linked by the motor protein MyoIIA⁶. Our lab has previously shown that MyoIIA deficiency alters T cell trafficking to and within lymph nodes^{60,109}. Branched actin networks, which are generated by the Arp2/3 complex and its upstream regulators, WASP family proteins, play a role in T cell trafficking as well as in generation of membrane protrusions during TEM¹¹¹. Additionally, WASP and Arp2/3 contribute to formation and maintenance of the immune synapse^{114,115}. Mutations in WASP and other regulators of Arp2/3 function cause immunodeficiency in part due to impaired lymphocyte trafficking¹¹¹⁻¹¹³. Formins generate linear actin filaments by both nucleating new actin filaments and processively elongating them through recruitment of profilin-bound actin monomers and protection from anti-capping proteins¹²¹. Two members of the formin family are highly expressed in T cells: mDia1 and FMNL1^{104,116,123-125}. Previous studies have identified a broad role for mDia1 in regulating T cell trafficking, thymic egress, chemotaxis, and activation^{104,124,134,135}. We have recently shown that mDia1 promotes the dissemination and transendothelial migration of leukemia cells¹³⁷. Unlike mDia1, which is expressed in a wide variety of cell types, FMNL1 expression is largely restricted to cells of the hematopoietic lineage^{123,129,130,138}. FMNL1 has previously been implicated in macrophage phagocytosis, membrane protrusion formation, and migration^{123,126,141,142}. In leukemic cells, FMNL1 has been suggested to be involved in membrane dynamics, proliferation and migration^{139,143,144}. FMNL1 is not well characterized in T cells. Previous studies have suggested that FMNL1 contributes to the reorientation of the centrosome to the immune synapse and Golgi apparatus structure in Jurkat transformed T cells as well as the cytotoxic behavior of CD8 T cells^{116,145}. However, the role of FMNL1 in primary lymphocytes is unknown.

Since previous studies relied on RNAi approaches^{116,126,139,142,143} or myeloid specific deletion to investigate FMNL1¹⁴¹, we developed a novel germline FMNL1 KO mouse to more fully investigate the function of FMNL1 in primary lymphocytes. Given that disruption of the cytoskeleton can potentially alter immune cell development, we began our studies by examining the immune cell populations in the blood and lymphoid organs of FMNL1 KO mice. Since the cytoskeleton can also impact T cell trafficking and activation, we subsequently investigated the ability of FMNL1 KO T cells to migrate to lymphoid organs and be activated *ex vivo*. Here, we report that FMNL1 is dispensable for lymphocyte development, T cell trafficking to lymphoid organs, and *ex vivo* T cell activation.

Results

Deletion of FMNL1 Does Not Significantly Alter Major Immune Cell Populations

To determine the role of FMNL1 in immune cell function we generated FMNL1 KO mice, with the assistance of Jen Matsuda and the National Jewish Mouse Genetics Core, by inserting a LacZ-neomycin cassette into the *Fmnl1* locus of C57BL/6 mice (Fig. 3.1A). We confirmed the correct insertion of this cassette via PCR (Fig. 3.1B, C) and verified deletion of FMNL1 at the protein level via western blot (Fig. 3.1D). We then examined whether FMNL1 deficiency altered the number and frequency of major immune cell populations in the thymus, blood, and secondary lymphoid organs. Flow cytometric analysis of the blood as well as the primary and secondary lymphoid tissues revealed no major differences in the number and proportions of either lymphoid (Figs. 3.2-3.5) or myeloid populations (Fig. 3.6) between FMNL1 KO and age matched control mice. These data suggest that deficiency in FMNL1 does not result in substantial alterations to the major immune cell compartments at steady state.

FMNL1 Deficiency Does Not Affect Naive T cell Trafficking to Secondary Lymphoid Organs

Similar lymphocyte populations in the WT and KO mice at steady state suggested that FMNL1 is not required for homeostatic T cell trafficking. To confirm this we used co-adoptive transfer of differentially fluorescently labeled naive CD45.2 WT control and FMNL1 KO T cells into CD45.1/.1 congenic WT recipient mice (Fig. 3.7A). Twenty-four hours post-intravenous transfer, we found equivalent ratios and numbers of transferred control and FMNL1 KO T cells in the spleen, lymph nodes, and blood of recipient mice (Fig. 3.7B, C). Taken together with our observations of similar T cell numbers at steady state (Figs. 3.2-3.5), our data suggest that FMNL1 is dispensable for homeostatic T cell trafficking to secondary lymphoid organs.

FMNL1 Deficiency Does Not Impair *Ex Vivo* T Cell Activation

Since the cytoskeleton can impact T cell activation^{124,135,136,158}, we next wanted to examine whether T cell activation would be altered by FMNL1 deficiency. We incubated WT and FMNL1 KO T cells with a strong APC-independent stimulus *ex vivo* using anti-CD3 and anti-CD28 antibodies. We found no major differences in the proliferation (Fig. 3.8A), the expression of canonical markers of activation (Fig. 3.8B, C) and chemokine receptors (Fig. 3.8D, E), or the size (Fig. 3.8F, G) of FMNL1 KO T cells compared to WT T cells. These data suggest that FMNL1 KO T cells activate equivalently to WT T cells *ex vivo*.

Discussion

Both T cell development and immune surveillance rely on the migration of T cells to and within primary and secondary lymphoid organs. Inherent to this motile behavior is dynamic remodeling of actin filaments by cytoskeletal effectors. While deficiency in other cytoskeletal effectors has been shown to impair the development, trafficking, and activation of T cells^{104,111-115,124,135}, our data suggest that FMNL1 is dispensable for these processes.

A prior report suggested that complete FMNL1 deficiency in mice would be genetically lethal¹⁴¹. However, our FMNL1-deficient mice are viable and breed normally. This discrepancy may be due to differences in the targeting approach and use of a ubiquitously expressed Cre recombinase in the earlier approach. Furthermore, the small sample size of litters in the previous report suggests that the determination of embryonic lethality may not have been statistically robust. Formins and linear actin networks have been previously implicated in the formation of the cytokinetic ring during cell division¹²¹. For example, FMNL1 is reported to be involved in proliferation of leukemia cells¹³⁹. Our observation of normal populations of immune cells within the blood, spleen, and lymph nodes of FMNL1-deficient mice suggests that FMNL1 is dispensable for hematopoiesis. Even in the case of rapid proliferation of T cells after a strong activation stimulus, we observed no difference in proliferation between WT and FMNL1-deficient mice *in vitro*. It is possible that, in the case of constant division by transformed lymphocytes, other Formins, such as mDia1, are unable to compensate. It is also likely that the requirements for FMNL1 differ between primary and transformed lymphocytes.

Previous investigations of the other primary formin expressed in T cells, mDia1, observed defects in the development, trafficking, and *ex vivo* activation of mDia1-deficient T cells^{104,124,134,135}. In contrast, in FMNL1-deficient mice, we observed normal populations of both thymic precursors and mature T cells, as well as unimpaired T cell trafficking to secondary lymphoid organs and *ex vivo* activation. These data suggest that FMNL1 may play a distinct role from mDia1 in T cell development, trafficking, and activation.

Given the previously proposed roles for FMNL1 and formins in cell polarization and actin organization during T-APC interactions in Jurkat cells^{116,136}, one might predict impaired thymic selection or activation in FMNL1-deficient T cells. However, as mentioned above, in FMNL1-deficient mice we observed normal numbers of thymic precursors and mature T cells, as

well as equivalent *ex vivo* T cell activation. These discrepancies may be due to differences between *in vitro* Jurkat-APC interactions and T cells and anti-CD3 and anti-CD28 antibodies. Additionally, the nature of the immune synapse and T cell-APC interactions is likely different between thymocytes and mature T cells¹⁶¹. Future *in vivo* studies of T cell activation in response to vaccination or pathogen challenge in FMNL1 KO mice will further clarify the role for FMNL1 in T cell activation.

While our data do not currently suggest any substantial alterations to the numbers of the major immune populations in FMNL1-deficient mice, our population characterization in this study is limited to the numbers and proportions of broadly defined immune cell populations in the lymphoid organs and the blood. It is possible that although T cell numbers in these tissues are equivalent between WT and FMNL1 KO mice, there are alterations in the TCR repertoire or specific sub-populations of T cells. Additionally, a number of specialized T cells reside in non-lymphoid tissues^{162–164}, and it is possible their numbers and function could be altered in FMNL1-deficient mice. While we observed equivalent numbers of myeloid cells in the blood and lymphoid organs of FMNL1-deficient mice, many innate immune populations exist within non-lymphoid tissue^{163–165}. As has been suggested previously with macrophages^{123,141,142,166}, FMNL1-deficiency may alter the number and function of innate immune cells in non-lymphoid organs. Further characterization of the immune cell populations in the non-lymphoid organs of FMNL1-deficient mice may reveal additional roles for FMNL1 in immune function. While additional immune cell phenotypes may be identified in FMNL1-deficient mice, our observations here present the opportunity to examine the function of FMNL1 in T cell trafficking and autoimmune disease without the potential confounding effects of substantially altered lymphocyte development and proliferation.

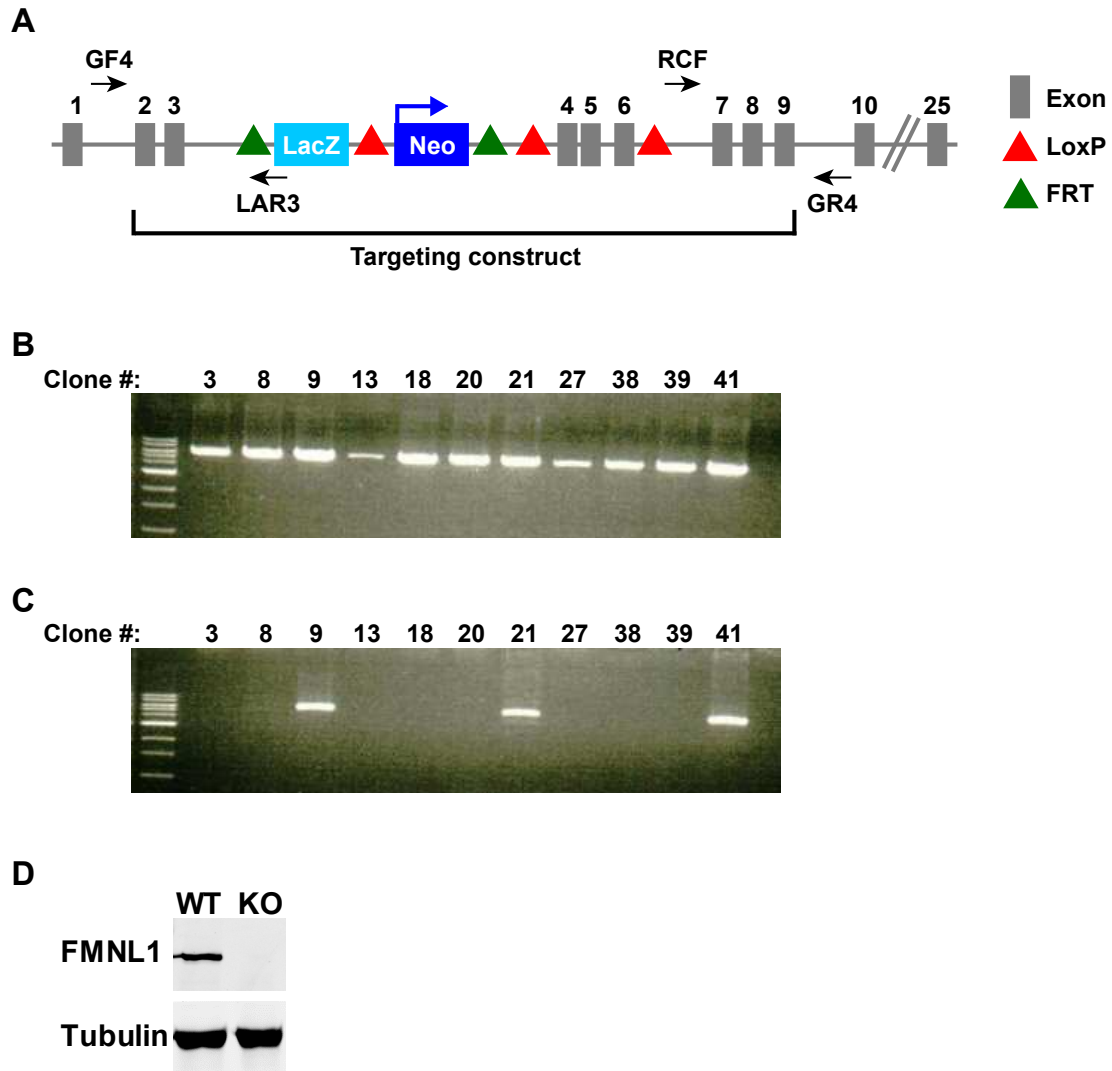


Figure 3.1: *Fmn1* targeting strategy and knock-out confirmation. **A)** Schematic of the targeted *Fmn1* allele after homologous recombination with the targeting construct. **B)** PCR reaction (with GF4 and LAR3 primers) showing ES cell clones positive for the insertion at the 5' end of the targeting construct. **C)** PCR reaction (with RCF and GR4 primers) showing ES cell clones positive for the insertion at the 3' end of the targeting construct confirming that the complete targeting construct was recombined into the *Fmn1* locus. Clone 9 was ultimately selected to establish the FMNL1 KO line. **D)** Representative western blot showing complete loss of FMNL1 protein expression in T cells from mice homozygous for the *Fmn1* KO allele. Tubulin staining is shown as a loading control.

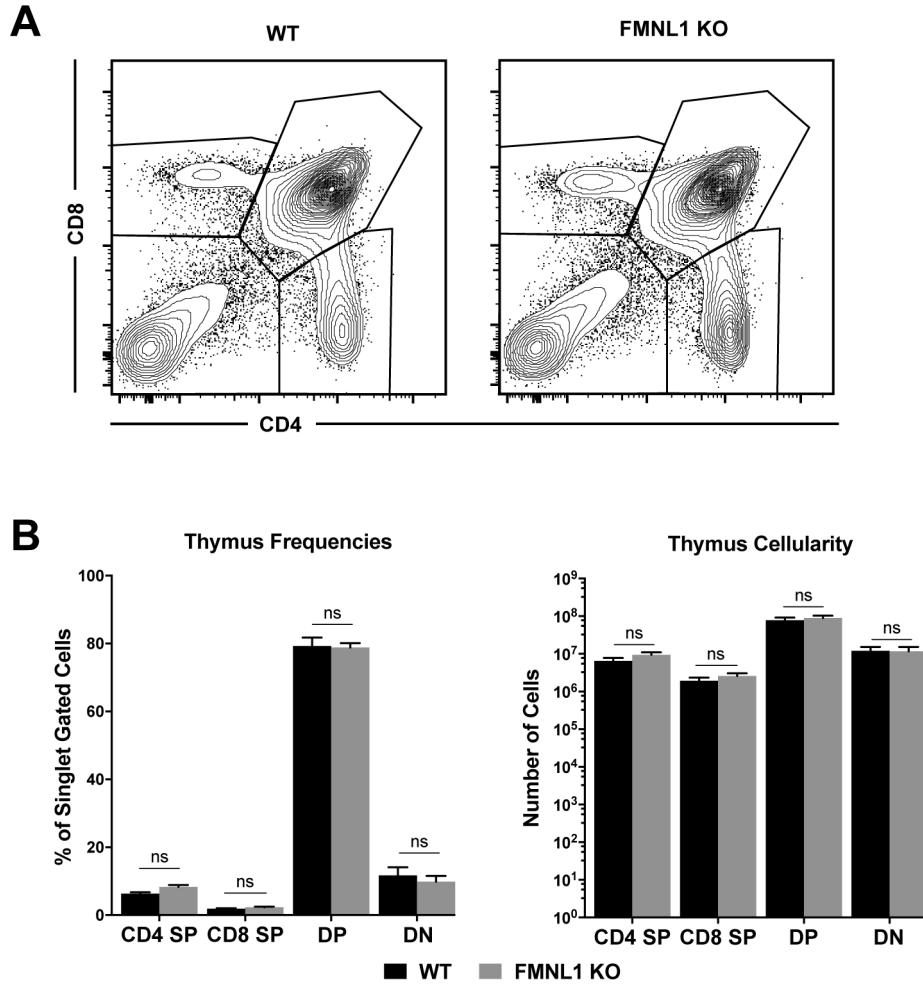


Figure 3.2: Thymic populations are not altered in FMNL1 KO mice. **A)** Representative CD4 by CD8 flow cytometry plots of single cell gated populations from the thymus of WT or FMNL1 KO mice. Thymic populations were identified as follows: CD4 single positive (SP): CD4⁺, CD8⁻; CD8 SP: CD4⁻, CD8⁺; double positive (DP): CD4⁺, CD8⁺; double negative (DN) CD4⁻, CD8⁻. **B)** Quantification of the populations in A. Frequencies of singlet gated cells (left) and total numbers per thymus (right). Data in B are the mean \pm the SEM from 8 independent mice for each group. Statistics were calculated using two-way ANOVA with Sidak's multiple comparisons test. n.s. = not significant.

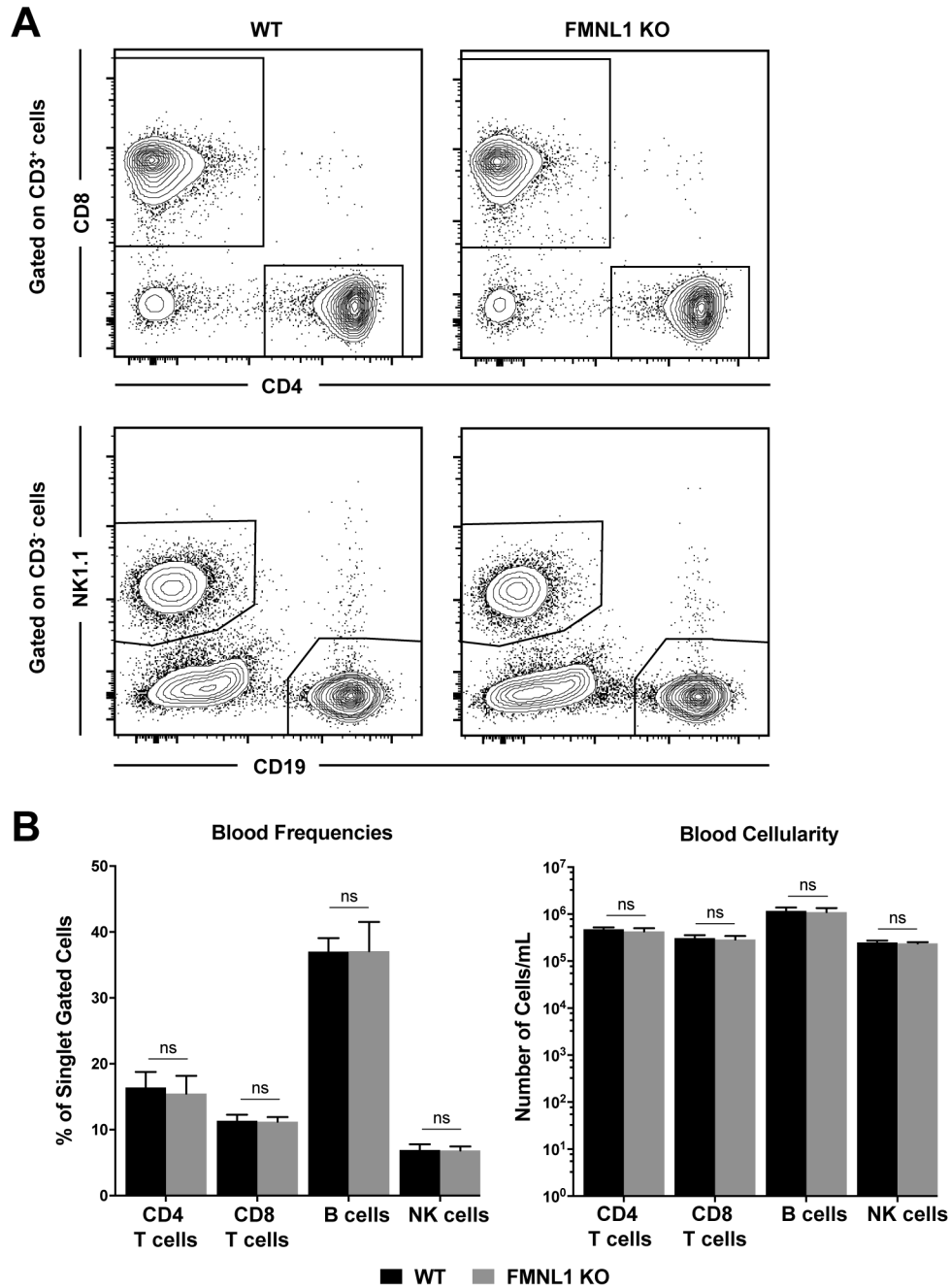


Figure 3.3: Blood lymphocyte populations are not altered in FMNL1 KO mice. A) Representative CD4 by CD8 flow cytometry plots of CD3⁺ gated cells from the blood of WT or FMNL1 KO mice (top). Representative CD19 by NK1.1 flow cytometry plots of CD3⁻ gated cells from the blood of WT or FMNL1 KO mice (bottom). Lymphocyte populations were identified as follows: CD4 T cells: CD3⁺, CD4⁺; CD8 T cells: CD3⁺, CD8⁺; B Cells: CD3⁻, CD19⁺; natural killer (NK) cells: CD3⁻, NK1.1⁺. **B)** Quantification of the populations in A. Frequencies of singlet gated cells (left) and total numbers per ml of blood (right). Data in B are the mean ± the SEM from 8 independent mice for each group. Statistics were calculated using two-way ANOVA with Sidak's multiple comparisons test. n.s. = not significant.

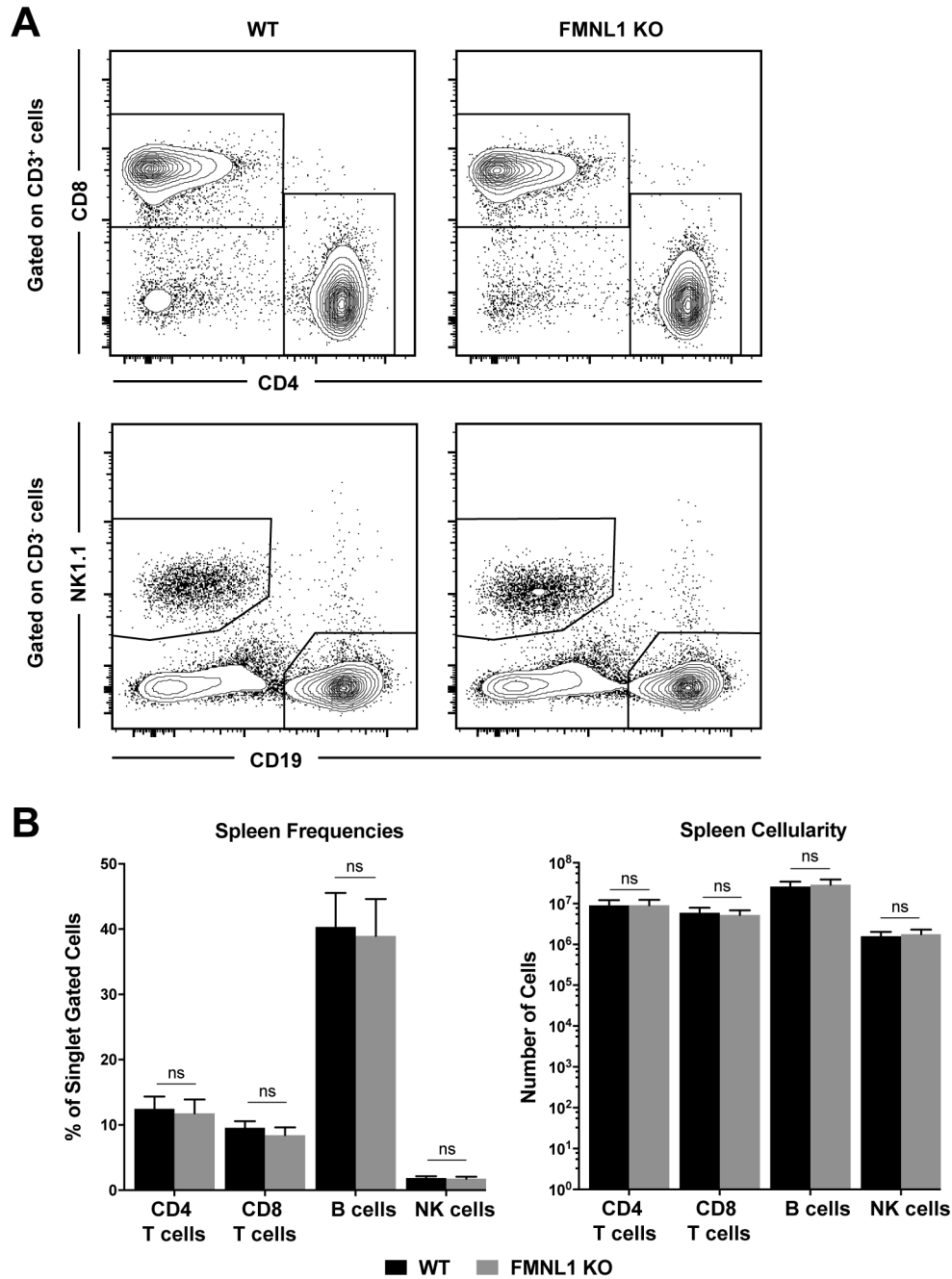


Figure 3.4: Splenic lymphocyte populations are not altered in FMNL1 KO mice. A) Representative CD4 by CD8 flow cytometry plots of CD3⁺ gated cells from the spleen of WT or FMNL1 KO mice (top). Representative CD19 by NK1.1 flow cytometry plots and of CD3⁻ gated cells from the spleen of WT or FMNL1 KO mice (bottom). Lymphocyte populations were identified as follows: CD4 T cells: CD3⁺, CD4⁺; CD8 T cells: CD3⁺, CD8⁺; B Cells: CD3⁻, CD19⁺; natural killer (NK) cells: CD3⁻, NK1.1⁺. **B)** Quantification of the populations in A. Frequencies of singlet gated cells (left) and total numbers per spleen (right). Data in B are the mean \pm the SEM from 8 independent mice for each group. Statistics were calculated using two-way ANOVA with Sidak's multiple comparisons test. n.s. = not significant.

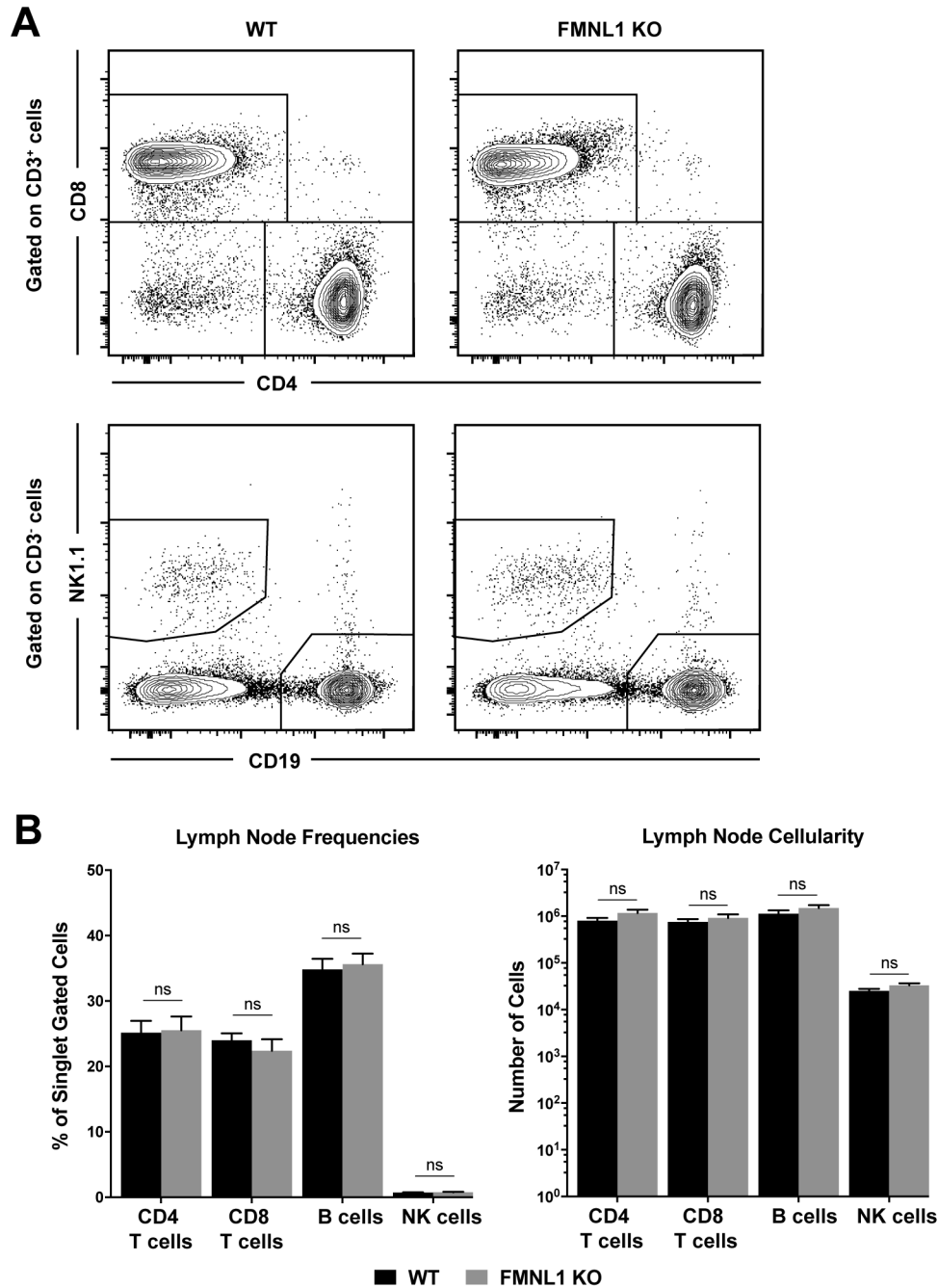


Figure 3.5: Lymph node lymphocyte populations are not altered in FMNL1 KO mice. A) Representative CD4 by CD8 flow cytometry plots of CD3⁺ gated cells from the inguinal lymph nodes of WT or FMNL1 KO mice (top). Representative CD19 by NK1.1 flow cytometry plots and of CD3⁻ gated cells from the inguinal lymph nodes of WT or FMNL1 KO mice (bottom). Lymphocyte populations were identified as follows: CD4 T cells: CD3⁺, CD4⁺; CD8 T cells: CD3⁺, CD8⁺; B Cells: CD3⁻, CD19⁺; natural killer (NK) cells: CD3⁻, NK1.1⁺. **B)** Quantification of the populations in A. Frequencies of singlet gated cells (left) and total numbers per spleen (right). Data in B are the mean \pm the SEM from 8 independent mice for each group. Statistics were calculated using two-way ANOVA with Sidak's multiple comparisons test. n.s. = not significant.

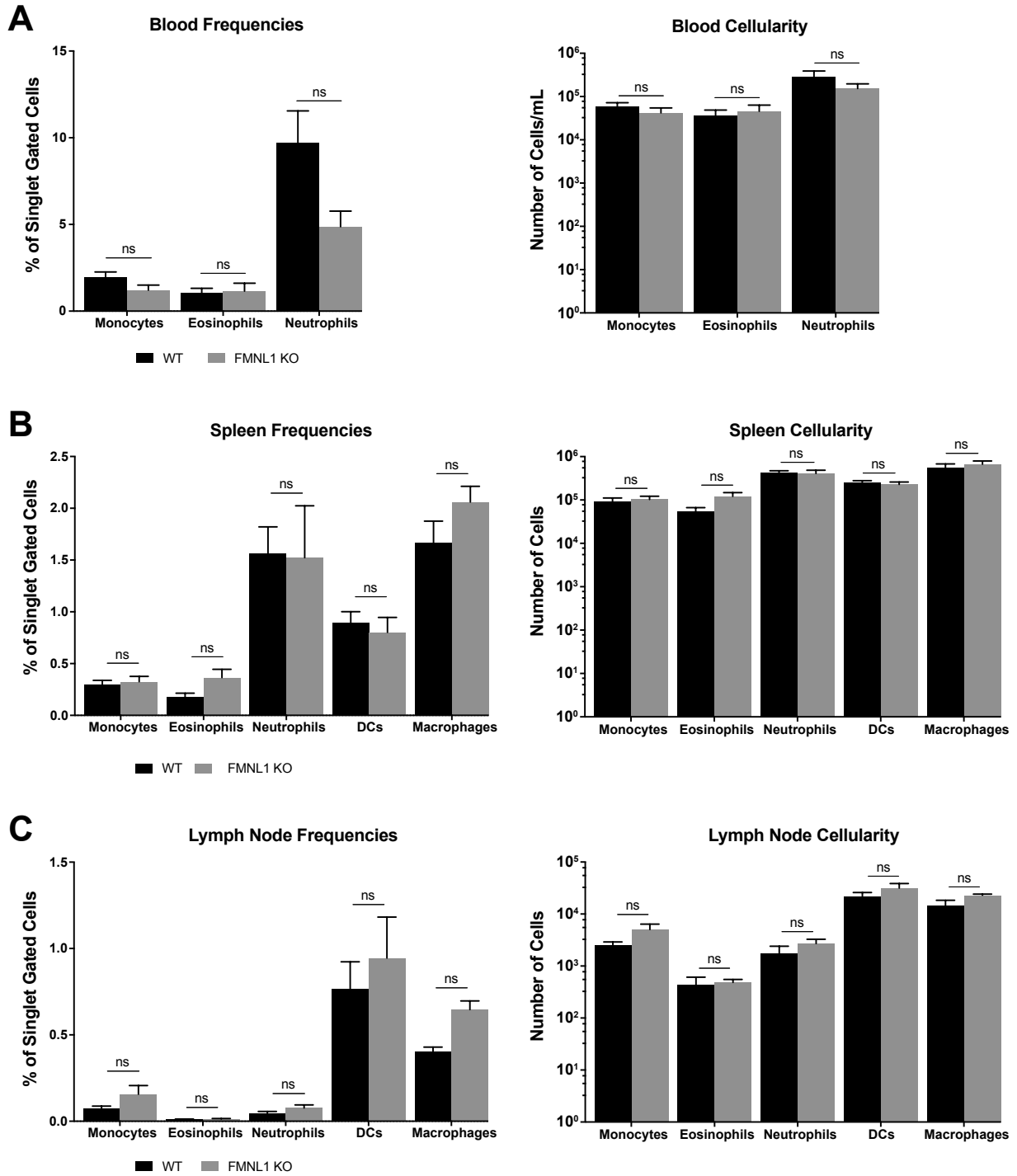


Figure 3.6. Myeloid populations in peripheral lymphoid organs are not altered in FMNL1 KO mice.

Figure 3.6. Myeloid populations in peripheral lymphoid organs are not altered in FMNL1 KO mice. Myeloid populations were identified as follows: monocytes: CD11b⁺, Ly6C^{high}; eosinophils: CD11b⁺, Siglec F⁺; neutrophils CD11b⁺, Ly6G⁺; dendritic cells (DCs): CD11c⁺, MHCII^{high}; macrophages: CD11b⁺, Ly6C^{int}, F4/80⁺, CD64⁺. **A)** Blood myeloid populations are not altered in FMNL1 KO mice. Frequencies of singlet gated cells (left) and total numbers of the indicated populations per ml of blood (right). **B)** Splenic myeloid populations are not altered in FMNL1 KO mice. Frequencies of singlet gated cells (left) and total numbers of the indicated populations per spleen (right). **C)** Lymph node myeloid populations are not altered in FMNL1 KO mice. Frequencies of singlet gated cells (left) and total numbers of the indicated populations per inguinal lymph node (right). Data in A-C are the mean \pm the SEM from 6 independent mice for each group. Statistics were calculated using two-way ANOVA with Sidak's multiple comparisons test. n.s. = not significant.

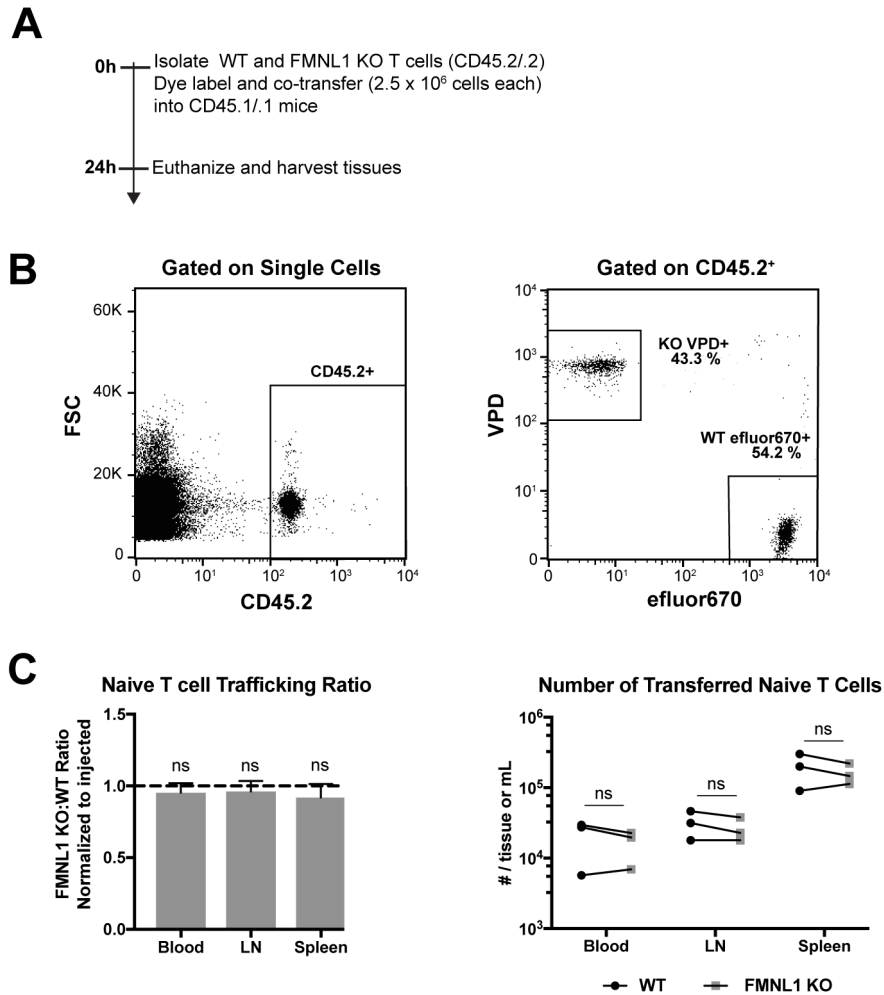


Figure 3.7: FMNL1 deficiency does not impair naive T cell trafficking to lymphoid tissues. **A)** Experimental set-up to quantify naive T cell trafficking to lymphoid organs. Differentially fluorescent dye-labeled naive WT and FMNL1 KO T cells were co-transferred intravenously at a 1:1 ratio into CD45.1/.1 congenic recipient mice and T cell trafficking to lymphoid tissues was quantified by flow cytometry 24 h post-transfer. **B)** Representative lymph node flow plots and gating strategy for identifying co-transferred dye-labeled T cells. **C)** Ratio of co-transferred FMNL1 KO to WT T cells in the indicated tissues (left). Values were normalized to the FMNL1 KO:WT ratio in the injected sample. A ratio below 1.0 (dashed line) indicates impaired trafficking to the tissue. Number of transferred WT or FMNL1 KO T cells recovered from the indicated tissues (right). Data in C are the mean \pm SEM (left) or individual means (right) from 3 independent experiments with 2 recipient mice each per experiment. Statistics in C were calculated using a one-sample two-tailed t-test against a theoretical FMNL1 KO:WT ratio of 1.0 (left) or repeated measures one-way ANOVA with Sidak's multiple comparisons test (right). n.s. = not significant.

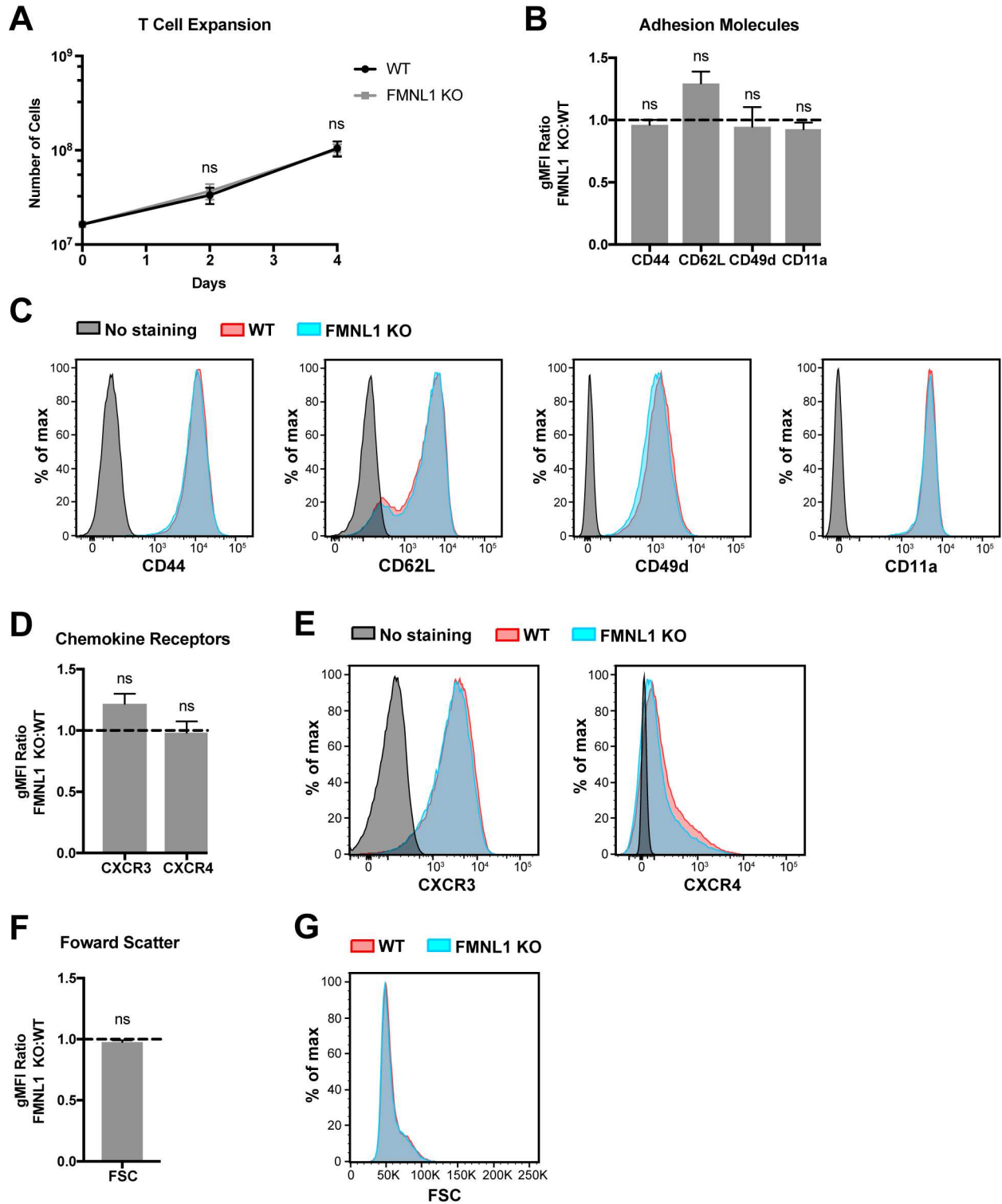


Figure 3.8: FMNL1 deficiency does not impair *ex vivo* T cell activation.

Figure 3.8: FMNL1 deficiency does not impair *ex vivo* T cell activation. T cells from WT or FMNL1 KO mice were isolated and then activated *ex vivo* with anti-CD3 and CD28 antibodies in the presence of WT irradiated CD45.1/.1 congenic splenocytes. After two days, T cells were removed from CD3 stimulus and cultured with IL-2. **A)** WT and FMNL1 KO T cells proliferate equivalently in response to CD3 stimulus. Total number of WT or KO T cells on days 0, 2 and 4 post-stimulus. **B)** Activated WT and FMNL1 KO T cells express equivalent levels of adhesion molecules and activation markers. Ratio of geometric mean fluorescent intensity (gMFI) of antibody staining of indicated surface molecules of FMNL1 KO T cells compared to WT T cells 5 days after activation. A ratio above or below 1.0 (dashed line) indicates a respective increase or decrease in expression of the indicated marker on FMNL1 KO T cells relative to WT. **C)** Representative overlay histograms of antibody staining for the indicated surface molecules quantified in B. **D)** Activated WT and FMNL1 KO T cells express equivalent levels of chemokine receptors. Ratio of gMFI of antibody staining of indicated chemokine receptors of FMNL1 KO T cells compared to WT T cells 5 days after activation. **E)** Representative overlay histograms of antibody staining for the indicated surface molecules quantified in D. **F)** Activated WT and FMNL1 KO T cells are the same size. Ratio of gMFI for forward scatter (FSC) of FMNL1 KO T cells compared to WT T cells 5 days after activation. **G)** Representative overlay histogram for forward scatter intensities quantified in F. Data in A, B, D and F are the mean \pm SEM from 4 independent experiments. Statistics in A were calculated using repeated measures two-way ANOVA with Sidak's multiple comparisons test; statistics in B, D and F were calculated using a one-sample two-tailed t-test against a theoretical FMNL1 KO:WT gMFI ratio of 1.0. n.s. = not significant.

CHAPTER IV

FMNL1 DEFICIENCY IMPAIRS TRAFFICKING TO SITES OF INFLAMMATION AND T CELL DRIVEN AUTOIMMUNE DISEASE

Introduction

Activated T cell trafficking and extravasation into tissues are required for execution of effector functions against pathogens and malignant cells³⁴. However, in the context of aberrant immune function, T cell entry into target tissues can be a driver of autoimmune and inflammatory diseases^{34,36,167}. For example, in type 1 diabetes, CD8 T cells invade the pancreatic islets to destroy β cells³⁴, while in multiple sclerosis and its mouse model, EAE, pathogenic CD4 T cells invade the central nervous system leading to neuronal damage¹⁶⁷. As such, disruption of T cell trafficking by targeting integrins or chemotactic stimuli appears to be a promising approach to achieving immune regulation in certain disease contexts^{89–94,168,169}.

The permissiveness of vasculature to lymphocyte entry varies widely from tissue to tissue. Differential expression of adhesion molecules and chemokines at vascular sites within tissues as well as the physical properties of the vascular endothelium itself can all regulate the ability of T cells to extravasate^{4,38,83}. In the lymph node, the specialized structure of the HEV facilitates the rapid entry of lymphocytes from the bloodstream. In the spleen, the sinusoidal vascular architecture and specialized fibroblastic reticular networks also make for a relative permissive site for lymphocyte entry^{69,170}. In contrast, the vascular endothelium of peripheral organs, such as the central nervous system, can be highly restrictive to lymphocyte entry as a result of tight cell-cell junctions between endothelial cells⁸³. The expression of chemokines as well as selectins and integrins on the vascular endothelium can also vary by tissue type⁴.

Given the difference in ligands as well as physical properties between tissue vascular endothelia, it is possible that the requirement and role for different T cell cytoskeletal effectors in

regulating tissue entry also varies based on the tissue site. Our group's previous study of activated T cells deficient in the cytoskeletal motor protein MyoIIA demonstrated substantially impaired trafficking to tumors and the inflamed spinal cord, compared to only mildly impaired trafficking to the lymph nodes or unimpaired trafficking to the spleen⁶⁰. Our prior investigation of T cells deficient in the Ena/VASP family of linear actin effector proteins showed impaired trafficking of activated T cells to the lymph nodes, spleen, inflamed CNS, and inflamed skin¹¹⁹. However, the trafficking of naive T cells deficient in Ena/VASP proteins to secondary lymphoid organs was unimpaired¹¹⁹. Previous studies of T cells deficient in the formin mDial1 demonstrated trafficking defects in both naive T cells to the lymphoid organs^{124,135} as well as activated T cells to the inflamed skin¹³⁴. FMNL1 has been reported to be upregulated by T cells trafficking to immune privileged sites during autoimmune attack^{88,146}.

Given the potential for different roles for cytoskeletal effectors in regulating trafficking to lymphoid organs versus non-lymphoid organs, in this chapter, we investigated the ability of activated FMNL1-deficient T cells to traffic to the pancreatic islets or the CNS in two different models of autoimmune inflammation. Since trafficking of self-reactive T cells to target tissues can drive autoimmune damage, we also examined the ability of transferred self-reactive FMNL1 KO T cells to induce either type 1 diabetes or EAE. Here, we report that FMNL1 KO T cells were impaired in both their ability to traffic to the islets and CNS as well as their ability to induce autoimmune disease.

Results

FMNL1-deficient T cells Are Impaired in Trafficking to the Pancreatic Islets and Inducing Type 1 Diabetes

Activated T cells are distinct from naive cells in both size and expression of adhesion molecules and chemokine receptors^{3,4}. Therefore, we hypothesized that the requirements for

FMNL1 in activated T cell trafficking might be different than in naive T cells. While the vasculature of secondary lymphoid organs is permissive for lymphocyte entry (e.g. HEVs)^{68,69}, the vasculature in other tissues and organs poses a more stringent barrier to extravasation⁸³. For example, extravasation into the pancreatic islets of Langerhans during type 1 diabetes can take over an hour (Adam Sandor, Rachel Friedman unpublished observation), whereas entry into secondary lymphoid tissues occurs within minutes^{69,171}. Thus, we investigated whether FMNL1 deficiency affects activated T cell trafficking to sites of inflammation. With the assistance of Adam Sandor and Victor Lui, we first examined T cell trafficking to the islets in the RIP-mOVA inducible model of type 1 diabetes in which membrane bound Ovalbumin (mOVA) is expressed in beta cells under the rat insulin promoter (RIP). To establish specific inflammation in the islets, we transferred ovalbumin specific OT-I transgenic T cells into RIP-mOVA mice. Six days later, *ex vivo* activated polyclonal WT and FMNL1 KO CD8 T cells were differentially fluorescently labeled and co-transferred into these RIP-mOVA mice, and the blood and islets were isolated twenty-four hours after transfer (Fig. 4.1A). Activated FMNL1 KO T cells displayed a 3.8-fold reduction on average in trafficking to the islets compared to control T cells (Fig. 4.1B).

Since type 1 diabetes is driven by destruction of beta cells by islet-infiltrating antigen specific T cells, we next wanted to investigate whether the observed trafficking defects in FMNL1-deficient T cells would affect their ability to induce diabetes. To test this, we activated control or FMNL1 KO OT-I and OT-II T cells *ex vivo* with their cognate peptides and then transferred these cells into RIP-mOVA recipients (Fig. 4.1C). Recipient mice were then monitored for 28 days for signs of diabetes (2 consecutive blood glucose readings >350 mg/dL). While 100% of mice receiving control T cells developed diabetes, only 44% of mice receiving FMNL1 KO T cells developed diabetes (Fig. 4.1D).

FMNL1-deficient T cells Are Impaired in Trafficking to the CNS and Inducing EAE

We next wanted to determine whether our observations on FMNL1 regulation of T cell trafficking to the islets extend to other inflamed tissues and autoimmune disease settings. The CNS also has highly restrictive vascular endothelial barriers. Direct observation of extravasation into the CNS suggests that T cells can take several hours to access the parenchyma of the brain and spinal cord^{30,31}. We therefore sought to examine how FMNL1 deficiency would affect CD4 T cell trafficking to the CNS in the EAE model of CNS inflammation. We used a standard model of EAE induction by immunizing with myelin oligodendrocyte glycoprotein (MOG) peptide in Complete Freund's Adjuvant (CFA) followed by two injections with pertussis toxin. After development of overt EAE symptoms in recipient mice (disease score ≥ 2), we co-transferred differentially dye-labeled *ex vivo* activated polyclonal WT and FMNL1 KO CD4 T cells (Fig. 4.2A). Twenty-four hours post-transfer, we quantified the number of transferred cells in the blood, brain, and spinal cord of the recipient mice. Activated FMNL1 KO T cells had a 1.4-fold reduction in trafficking to the brain and a 2.2-fold reduction in trafficking to the spinal cord compared to control T cells (Fig. 4.2B).

Transfer of MOG specific 2D2 T cells can drive EAE in recipient mice in a manner that relies on T cell trafficking to the CNS^{32,149}. Therefore, we sought to examine whether the observed trafficking defects of FMNL1-deficient T cells would affect their ability to induce EAE in WT recipient mice. We activated control or FMNL1 KO 2D2 CD4 T cells with MOG peptide *ex vivo*, transferred these cells into recipient mice, and then monitored these mice for development of EAE (Fig. 4.2C). While 100% of mice receiving control 2D2 T cells developed EAE, only 33% of mice receiving FMNL1 KO 2D2 T cells developed EAE (Fig. 4.2D). Mice receiving control T cells displayed an average peak disease score of 3.5 compared to an average peak score of 0.67 for mice receiving FMNL1 KO T cells (Fig. 4.2E). Given that similar

trafficking and disease induction defects were observed in two different autoimmune models, together, our data suggest that FMNL1 broadly promotes trafficking of activated T cells to sites of inflammation enabling them to cause autoimmune disease.

FMNL1-deficient T cells Are Not Impaired in Trafficking to Secondary Lymphoid Organs

We next wanted to investigate whether the impairment in FMNL1-deficient activated T cell trafficking was specific to restrictive non-lymphoid tissues or would apply to more permissive lymphoid tissues as well. To examine activated T cell trafficking to secondary lymphoid organs, we co-transferred differentially dye-labeled *ex vivo* activated WT and FMNL1 KO T cells into CD45.1/.1 congenic WT recipient mice (Fig. 4.3A). Twenty-four hours later, we quantified the number of transferred WT and FMNL1 KO T cells in the blood, spleen, and lymph nodes of recipient mice. While the ratio of KO to WT T cells was slightly lower than the expected value of 1 in the blood and greater than the expected value of 1 in the spleen, comparison of the number of cells present in these locations revealed no significant differences (Fig. 4.3B). These data suggest that FMNL1 is not required for the *ex vivo* activation of T cells or activated T cell trafficking to lymphoid organs.

Discussion

T cell trafficking and extravasation into tissues can drive both protective responses against pathogens as well as pathogenic responses during autoimmune attack^{3,4,34,36,167}. While in Chapter III we observed that FMNL1 was dispensable for T cell trafficking to secondary lymphoid organs, in this chapter, we report that FMNL1-deficient T cells are impaired in trafficking to the pancreatic islets and the CNS in the context of autoimmune inflammation. Together, these data suggest that FMNL1 selectively regulates trafficking to non-lymphoid organs.

Our observations of T cell-induced EAE and type 1 diabetes models suggest that reduced trafficking of FMNL1-deficient T cells to sites of inflammation can impair the induction of autoimmune disease. While we observed a partial but significant inhibition of trafficking, we observed complete disease protection in a subset of mice in both disease phenotypes. The differences between these findings may be due to the fact that, in the activated T cell transfer disease models, no prior immune infiltration has occurred, and thus, the vascular endothelial barriers are more intact. Consequently, these barriers are much more restrictive compared to the trafficking models where immune cell recruitment is ongoing. Additionally, there may be a thresholding effect whereby trafficking is reduced such that the number of FMNL1-deficient T cells capable of entering the tissue are not sufficient to induce disease. While, in this chapter, we have examined the function of FMNL1 in T cell extravasation, it is also possible that, in these disease contexts, FMNL1 may have additional roles. Some non-lymphoid tissues offer secondary barriers to cell entry, such as the glia limitans, a restrictive basement membrane in the CNS^{56,83}. It is possible that FMNL1 deficiency impairs migration through these restrictive secondary barriers as well. Additionally, FMNL1 may play a role in T cell motility and, consequently, the ability of T cells to execute effector functions within potentially restrictive tissue parenchyma. Furthermore, it has been previously reported that knockdown of FMNL1 slightly impaired human CD8 T cell killing *in vitro*¹¹⁶, thus FMNL1 deficiency may also play a role in OT-I T cell effector function in the RIP-mOVA model. Future study of FMNL1-deficient T cells within tissues may identify additional mechanisms by which FMNL1 contributes to pathogenic T cell behavior in autoimmune settings.

Inhibition of T cell trafficking has shown therapeutic promise in the treatment of autoimmune and inflammatory disease^{89,90,94,168,169,172}. For example, antibody blockade of $\alpha 4$ integrin to block T cell trafficking to the CNS has proven to be an effective treatment for

multiple sclerosis⁹⁰. Our observations that FMNL1 deficiency in T cells impairs their ability to traffic to autoimmune inflammatory sites and induce autoimmune disease in both EAE and type 1 diabetes suggest that FMNL1 may be a potential therapeutic target for autoimmune disease treatment. As immune cell development and homeostatic trafficking appear unaltered by global FMNL1 deficiency, targeting of FMNL1 may offer the possibility of selectively impairing activated T cell trafficking to specific tissue sites while leaving systemic immune surveillance intact. A recent report has suggested that selectively inhibiting activated T cell trafficking may be particularly beneficial in the context of graft-versus-host disease¹⁶⁹. However, given that our data demonstrated that FMNL1-deficiency impaired T cell trafficking to multiple inflamed tissue sites, it is likely that T cell responses to pathogens in non-lymphoid organs would also be affected. Future studies examining the ability of FMNL1-deficient T cells to control either systemic or tissue-confined infections will provide insight into the degree that FMNL1-deficiency may impair protective immune responses. While previously studied cytoskeletal effectors of T cell migration, such as Arp2/3, mDia1, MyoIIA, and Ena/Vasp proteins, are expressed in most tissues and cell types, FMNL1 expression is largely restricted to hematopoietic cells^{123,129,138}. Additionally, FMNL1 expression has been reported to be upregulated by pathogenic T cells in autoimmune settings^{88,146}. These expression patterns may offer the possibility of a more targeted approach to therapeutically altering cytoskeletal function in immune cells.

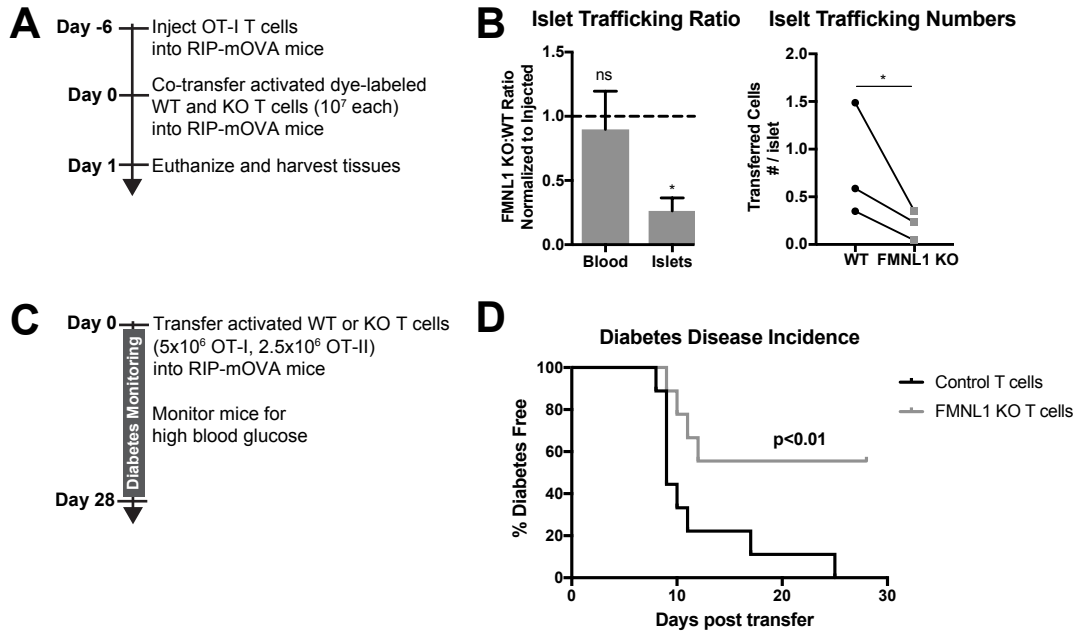


Figure 4.1: FMNL1-deficient T cells are impaired in trafficking to the pancreatic islets and inducing type 1 diabetes. **A)** Experimental set-up to quantify activated T cell trafficking to the inflamed pancreatic islets. To induce inflammation of the pancreatic islets, 7 days prior to harvest, WT OT-I transgenic T cells were transferred intravenously into RIP-mOVA mice. *Ex vivo* activated, differentially dye-labeled, polyclonal WT and FMNL1 KO T cells were then co-transferred intravenously at a 1:1 ratio into these RIP-mOVA mice, and T cell trafficking to the indicated tissues was quantified by flow cytometry 24 h post-transfer. **B)** FMNL1-deficient T cells are impaired in trafficking to the inflamed pancreatic islets. Ratio of co-transferred FMNL1 KO to WT T cells in the indicated tissues (left). Values were normalized to the FMNL1 KO:WT ratio in the injected sample. A ratio below 1.0 (dashed line) indicates impaired trafficking to the tissue. Number of transferred WT or FMNL1 KO T cells recovered from the islets (right). **C)** Experimental set up for induction of type 1 diabetes in RIP-mOVA mice. Control or FMNL1 KO OT-I and OT-II T cells were activated *ex vivo* and then transferred into RIP-mOVA recipients. Recipient mice were then monitored for 28 days for glycemia. **D)** FMNL1 deficiency in self-reactive T cells delays and partially protects from diabetes. Diabetes incidence of mice receiving control or FMNL1 KO OT-I and OT-II T cells. Data in B are the mean \pm SEM (left) or individual means (right) from 3 independent experiments with at least 3 recipient mice per experiment; data in D are pooled from 3 independent experiments with cohorts of 3 mice/group each. Statistics in B were calculated using a one-sample two-tailed t-test against a theoretical FMNL1 KO:WT ratio of 1.0 (left) or a two-tailed paired t test (right); statistics in D were calculated by Log-rank test. n.s. = not significant, * = $p < 0.05$.

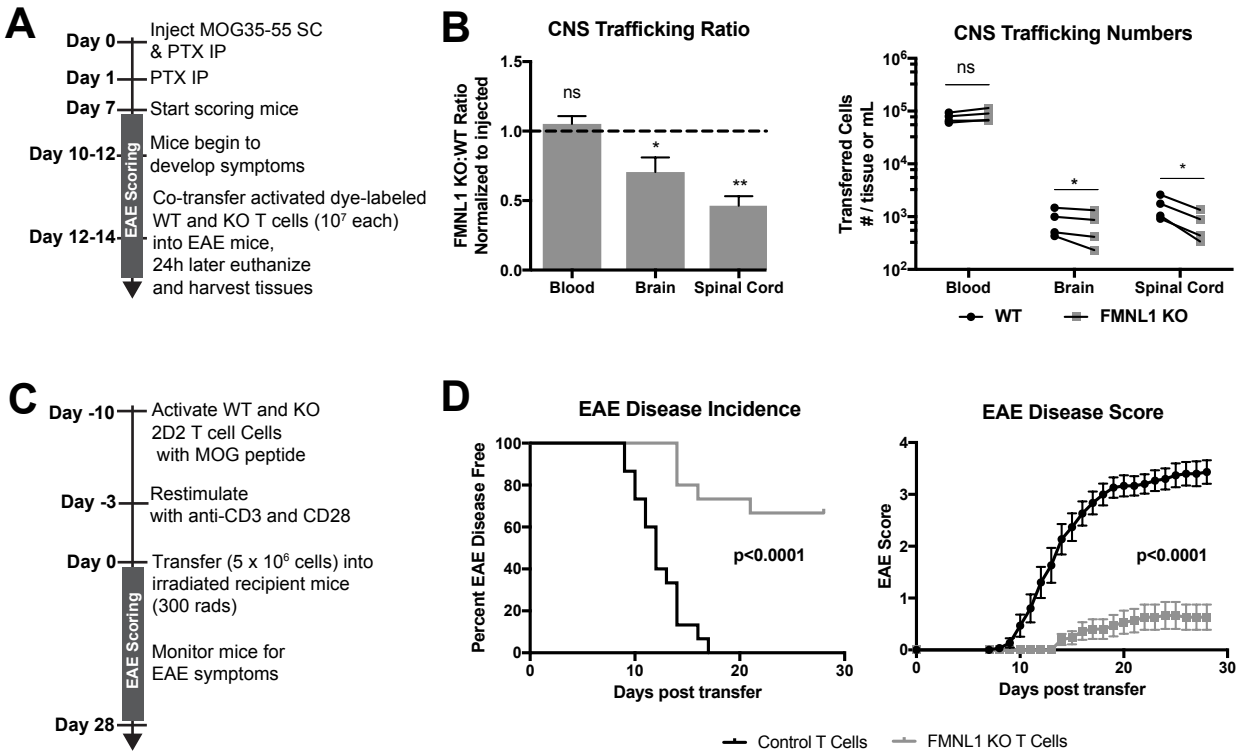


Figure 4.2: FMNL1-deficient T cells are impaired in trafficking to the inflamed CNS and inducing EAE. **A)** Experimental set-up to quantify activated T cell trafficking to the inflamed CNS. Activated, differentially dye-labeled, polyclonal WT and FMNL1 KO T cells were co-transferred intravenously at a 1:1 ratio into mice with ongoing EAE (score ≥ 2.0) and T cell trafficking to the indicated tissues was quantified by flow cytometry 24 h post-transfer. **B)** FMNL1-deficient T cells are impaired in trafficking to the inflamed CNS. Ratio of co-transferred FMNL1 KO to WT T cells in the indicated tissues (left). Values were normalized to the FMNL1 KO:WT ratio in the injected sample. A ratio below 1.0 (dashed line) indicates impaired trafficking to the tissue. Number of transferred WT or FMNL1 KO T cells recovered from the indicated tissues (right). **C)** Experimental set-up for induction of EAE via T cell transfer. Control or FMNL1 KO MOG-specific 2D2 T cells were activated *ex vivo* and then transferred into WT recipient mice. EAE disease severity was scored daily for 28 days. **D)** FMNL1 deficiency in T cells delays EAE onset and partially protects from disease. EAE incidence (score ≥ 1.0) in mice receiving control or FMNL1 KO 2D2 T cells (left). Mean EAE score \pm SEM over time in mice receiving control or FMNL1 T cells 2D2 T cells (right). Data in B are the mean \pm SEM (left) or individual means (right) from 4 independent experiments with 2 recipient mice per group; data in D are pooled from 3 independent experiments with cohorts of 5 mice/group each. Statistics in B were calculated using a one-sample two-tailed t-test against a theoretical FMNL1 KO:WT ratio of 1.0 (left) or repeated measures one-way ANOVA with Sidak's multiple comparisons test (right); statistics in D (left) were calculated by Log-rank test; statistical interaction of genotype with disease severity over time in D (right) was calculated by repeated measures two-way ANOVA. n.s. = not significant, * = $p < 0.05$, ** = $p < 0.01$.

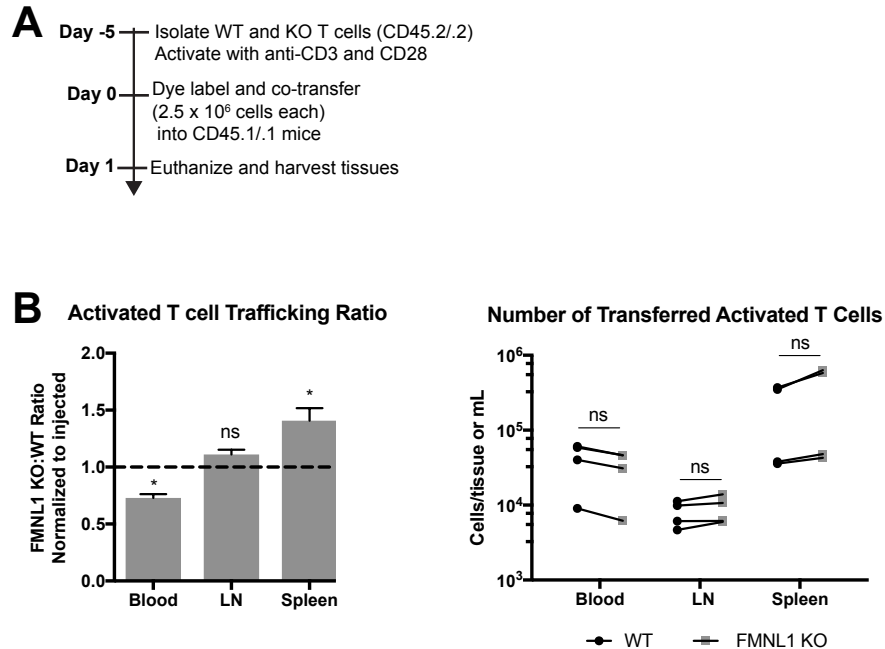


Figure 4.3: Activated FMNL1 T cells are not impaired in trafficking to peripheral lymphoid organs. **A)** Experimental set-up to quantify activated T cell trafficking to lymphoid organs. Differentially dye-labeled *ex vivo* activated WT and FMNL1 KO T cells were co-transferred intravenously at a 1:1 ratio into CD45.1/1 recipient mice and T cell trafficking to lymphoid tissues was quantified by flow cytometry 24 h post-transfer. **B)** Ratio of co-transferred FMNL1 KO to WT T cells in the indicated tissues (left). Values were normalized to the FMNL1 KO:WT ratio in the injected sample. A ratio below 1.0 (dashed line) indicates impaired trafficking to the tissue. Number of transferred WT or FMNL1 KO T cells recovered from the indicated tissues (right). Data in B are the mean \pm SEM (left) or individual means (right) from 4 independent experiments with 2 recipient mice each per experiment. Statistics in B were calculated using a one-sample two-tailed t-test against a theoretical FMNL1 KO:WT ratio of 1.0 (left) or by repeated measures one-way ANOVA with correction with Sidak's multiple comparisons test (right). n.s. = not significant, * = $p < 0.05$.

CHAPTER V

FMNL1 PROMOTES NUCLEUS TRANSMIGRATION THROUGH RESTRICTIVE ENDOTHELIAL BARRIERS DURING DIAPEDESIS

Introduction

To exit blood vessels and enter tissues, T cells undergo the multistep process of TEM. T cells are initially captured from the blood flow to begin selectin-mediated rolling along the vascular endothelial wall followed by firm adherence in a chemokine driven integrin-mediated process. After crawling along the endothelium probing for permissive sites for extravasation, T cells initiate the diapedesis step and squeeze through the vascular endothelium³⁸. To undergo the stages of TEM, T cells rely on morphological changes and generation of force mediated by remodeling of the actin cytoskeleton^{6,47,96}. Previous studies have identified a key role for the Rho family of GTPases in transducing chemokine and integrin signaling during TEM^{97,103}. However, the contribution of specific downstream cytoskeletal effectors to this process has only recently begun to be understood.

The different stages of TEM impose different physical requirements on the cell³⁸ and thus potentially different roles for the actin cytoskeletal effectors in mediating morphological changes and mechanotransduction during this process. In the initial stage of TEM, activated T cells form transient interactions by the glycosylated carbohydrate ligand PSGL-1 and P- or E-selectins on the vascular endothelium enabling them to resist the shear stress of the bloodstream and roll along the endothelium. Specialized adhesive membrane protrusions known as tethers and slings arise from T cell microvilli to stabilize the cell during this rolling step³⁹. While no specific cytoskeletal effectors or structures in these protrusions have been characterized, RNA sequencing data has suggested the potential involvement of the actin cytoskeleton in tether and sling formation³⁹.

Subsequent to the rolling stage, activation of integrins to a high affinity conformation by chemotactic stimuli enables T cells to firmly adhere to ICAM-1 and VCAM-1 ligands on the vascular endothelium⁴⁶. Anchoring of integrins to the actin cytoskeleton by adaptor proteins such as paxillin and talin-1 has been shown to be important for integrin activation and subsequent force transmission necessary for adhesion to endothelium and subsequent crawling^{173,174}. In the crawling stage of TEM, T cells migrate along endothelium following chemotactic signals. At the leading edge of the T cell, branched actin networks created by Arp2/3 extend the plasma membrane forward in a ruffled structure known as the lamellipodium⁹⁶. Actin polymerization by mDia1 has also been proposed to contribute to the protrusion of lamellipodia in T cells^{98,103,104}. At the rear of the cell, the uropod, contractile forces mediated by MyoIIA are important for retracting the cell body as it moves forward^{51,60,103,108}. Additionally, during this crawling phase, T cells extend actin-rich exploratory structures, known as filopodia or podosomes, which are thought to be involved in scanning the endothelium for permissive sites for diapedesis^{46,49,52}. Arp 2/3, Ena/VASP proteins, and formins have all been implicated in the formation of filopodia, though it is not clear which of these effectors performs this role in T cells^{96,110,175,176}.

In the final stage of TEM, diapedesis, T cells extend their cytoplasm beneath the endothelium and then squeeze through this vascular wall to exit the bloodstream^{38,57}. We have previously shown that contraction of the cytoskeleton by MyoIIA in the uropod is important for passage of the T cell nucleus through the endothelium and the completion of diapedesis⁶⁰. We have also observed an integrin-dependent role for Ena/VASP proteins in promoting completion of diapedesis¹¹⁹. Integrin-mediated crosstalk between T cells and the endothelium has been suggested to loosen endothelial cell-cell junctions to promote permissive openings for diapedesis⁵⁷⁻⁵⁹. However, the role of the T cell actin cytoskeleton and membrane protrusions in regulating this aspect of diapedesis has not been elucidated.

Given the trafficking defects we observed in Chapter IV and the roles for cytoskeletal remodeling in multiple stages of TEM, in this chapter, we sought to determine the function of FMNL1 in activated T cell TEM. To further determine the mechanism of FMNL1 action in T cell migration, we also examined the ability FMNL1-deficient T cells to undergo chemotaxis and polymerize actin. Here we report that FMNL1 localizes behind the nucleus during TEM and promotes the passage of this rigid structure through the endothelium during diapedesis. Furthermore, we report that the requirement for FMNL1 in chemotaxis is pore-size dependent and that expression levels of FMNL1 dictate the ability of T cells to transmigrate through restrictive barriers.

Results

FMNL1 Deficiency Impairs T cell TEM at the Diapedesis Step

Having established a role for FMNL1 in activated T cell trafficking in Chapter IV, we investigated the requirement for FMNL1 in the different stages of TEM: rolling, adhering, crawling, and diapedesis. For these experiments, we employed a previously established *in vitro* flow chamber system to visualize and quantify T cell TEM under shear flow using time-lapse microscopy^{60,119,137,155}. After culturing an endothelial cell monolayer within the flow chamber, we perfused in differentially dye-labeled activated control and FMNL1 KO T cells and imaged them under physiological shear flow for 30 minutes. With phase-contrast imaging, T cells above the plane of the endothelium display a white halo, which is progressively lost as the cells undergo diapedesis (Fig. 5.1A). Cells that lose a portion of the white phase halo localized to a small protrusion of the cell, detected by fluorescence, are considered to have initiated diapedesis. Completion of diapedesis is scored as complete loss of the phase halo (Fig. 5.1A, B). Quantification of the number of cells adhering to the endothelium and subsequently detaching under flow revealed no differences between WT and FMNL1 KO T cells (Fig. 5.1C, D).

Similarly, both WT and FMNL1 KO T cells were equally capable of crawling on the endothelial monolayer (Fig. 5.1E), suggesting that FMNL1 is dispensable during the first stages of TEM. While FMNL1 KO T cells were equivalent to WT cells in their ability to initiate diapedesis (Fig. 5.1F), they were 3.8-fold reduced in their ability to complete the TEM process (Fig. 5.1G). Furthermore, those few FMNL1 KO T cells that were able to complete TEM took more than twice as long on average to do so compared to WT T cells (Fig. 5.1H). These data indicate a specific role for FMNL1 in completion of the diapedesis step of the TEM process.

FMNL1 Deficiency Impairs Transmigration of the Nucleus During TEM.

To further elucidate the role of FMNL1 in T cell diapedesis, we examined its localization within T cells during TEM. Using the same flow chamber system as above, dye-labeled activated T cells were introduced into the flow chamber and allowed to migrate on the endothelial monolayer under shear flow for 5 minutes before fixing the cells. We then stained for FMNL1 and the nucleus (Fig. 5.2A). We confirmed that the FMNL1 antibody staining was specific for FMNL1 using similar staining conditions on control and FMNL1 KO T cells (Fig. 5.3). Using the plane of the endothelium as a reference, we identified cells that were actively undergoing diapedesis, i.e. with a portion of their cytoplasm below the endothelial monolayer (Fig 5.2B). In these cells, we then quantified the fluorescence intensity of the nucleus, FMNL1, and cytoplasmic staining from the back to the front of the cell (Fig. 5.2C). Cells were scored as having perinuclear FMNL1 enrichment, partial perinuclear enrichment, or no enrichment (see Methods for analysis). On average, we found perinuclear enrichment of FMNL1 in 64% of transmigrating WT T cells, with an additional 12.5% displaying a partial perinuclear enrichment (Fig. 5.2D).

The rigid structure of the nucleus can impede completion of migration through restrictive barriers such as the endothelium^{60,62}. Given the localization of FMNL1 directly behind the

nucleus of transmigrating T cells, we examined whether FMNL1 deficiency would impact the ability of activated T cells to translocate their nuclei across the endothelium during TEM. Using differentially dye-labeled WT and FMNL1 KO T cells in the same flow chamber system as above, after 5 minutes of migration, we fixed the cells and quantified the position of the nucleus relative to the endothelium. FMNL1 KO T cells were significantly impaired in their ability to transmigrate their nuclei, with only 7% of transmigrating FMNL1 KO T cells having migrated their nuclei below the endothelium compared to 32% for WT T cells (Fig. 5.2E). This finding is consistent with our earlier observation that FMNL1 KO T cells are able to initiate diapedesis but are substantially impaired in completing the process. Taken together with the localization data, these findings suggest that FMNL1 facilitates completion of diapedesis by promoting the transmigration of the nucleus through the endothelial barrier.

T cell Migration Through Narrow Pores Is FMNL1 Dependent

Based on our observations that FMNL1 deficiency impaired activated T cell trafficking selectively to tissues with restrictive endothelial barriers and impaired TEM specifically at the diapedesis step, we hypothesized that the requirement for FMNL1 in migration would be dependent on the physical restriction of the barrier. To test this idea, we performed transwell assays with inserts containing pore sizes of different diameters. In response to either CXCL10 or CXCL12, activated FMNL1 KO T cells were impaired in their ability to migrate across 3 μ m transwell inserts compared to activated WT T cells (Fig. 5.4A). However, FMNL1 KO cells migrated equivalently as WT T cells to these same chemokines across 5 μ m transwell inserts (Fig. 5.4A). The nuclei of lymphocytes have been estimated to be approximately 5-7 μ m in diameter⁶². Thus, our observation that FMNL1-deficient T cells are impaired in transmigration of their nuclei across restrictive endothelial barriers is consistent with our finding that FMNL1-deficient T cells are impaired in transmigrating through small openings.

Neutrophils also express FMNL1 at similar levels to T cells¹⁷⁷ but are characterized by a multi-lobed, more flexible, nuclear structure^{54,64,65}. Therefore, we examined whether FMNL1-deficient neutrophils would be impaired in migrating through 3µm transwell pores. In response to the neutrophil chemoattractant CXCL1, FMNL1 KO neutrophils displayed equivalent migration compared to WT neutrophils (Fig. 5.4B). These findings suggest that, in cells with more flexible nuclei, the need for FMNL1 in transmigrating through restrictive openings is reduced.

Similar to FMNL1, the motor protein MyoIIA displays a perinuclear localization during activated T cell TEM and promotes nucleus transmigration during the completion of diapedesis⁶⁰. As in our experiments with FMNL1, the requirement for MyoIIA in T cell transwell chemotaxis is pore-size dependent^{51,60}. Thus, we hypothesized that FMNL1 may be acting either in parallel or in conjunction with MyoIIA to facilitate transmigration through restrictive barriers. If FMNL1 and MyoIIA operate entirely within the same mechanism, then co-inhibition should have no greater affect than single inhibition. If the mechanisms are distinct, then co-inhibition should have additive effects. To examine the relationship between MyoIIA and FMNL1, we performed chemotaxis assays to CXCL10 across 3µm transwell membranes using activated WT and FMNL1 KO T cells treated with the MyoIIA inhibitor blebbistatin. While FMNL1-deficiency or inhibition of MyoIIA alone similarly reduced chemotaxis to CXCL10 by 20%, the combination of the two impaired chemotaxis 99% (Fig. 5.4C). This synergistic impairment of chemotaxis suggests that FMNL1 and MyoIIA operate through distinct mechanisms that can compensate for the inhibition of the other to promote T cell transmigration through narrow pores.

One possible mechanism by which FMNL1 could promote chemotaxis through narrow pores is through polymerization of actin in response to chemokine. Therefore, we next examined the ability of activated FMNL1-deficient T cells to polymerize actin in response to chemokine

using fluorescent phalloidin staining to quantify filamentous actin. In response to 15 seconds of CXCL10 stimulus, WT T cells increased their total polymerized actin an average of 1.9-fold, while FMNL1 KO T cells only increased their total polymerized actin an average of 1.6-fold (Fig 7C). Similarly, in response to 15 seconds of CXCL12 stimulus, WT T cells increased their total polymerized actin an average of 1.8-fold, while FMNL1 KO T cell only increased their total polymerized actin an average of 1.4-fold (Fig 5.4D). Thus, while FMNL1 KO T cells are capable of polymerizing actin in response to chemokines, their ability to respond is 15-20% reduced compared to WT T cells. Given the presence of other actin polymerizing proteins such as Arp2/3 and mDia1, this partial rather than complete inhibition is not surprising, while still indicating an effect on actin remodeling by FMNL1 in response to chemokine stimulation.

Finally, to quantitatively test the dependence of T cell transmigration on FMNL1 expression, we expressed FMNL1 in activated WT or FMNL1 KO T cells using retroviral constructs. As expected, FMNL1 KO T cells receiving a control construct were impaired in 3 μ m transwell migration to CXCL12 compared to WT T cells receiving the same construct (Fig. 5.4E). However, re-expression of FMNL1 in FMNL1 KO T cells restored their ability to transmigrate through 3 μ m pores (Fig. 5.4E). To determine if there was a correlation between FMNL1 levels and the ability of T cells to transmigrate, we measured, in parallel, in a sample of the same T cell populations, the level of FMNL1 expression in WT and FMNL1 KO T cells receiving either the control or FMNL1-expressing constructs using western blotting (Fig. 5.4F). We then graphed the level of FMNL1 expression against the ability of cells from the same population to migrate in a 3 μ m transwell assay. We found a strong positive correlation between the level of FMNL1 expressed by a given population of T cells and their ability to transmigrate through restrictive pores (Fig. 5.4G). This finding further supports that FMNL1 regulates the ability of activated T cells to navigate restrictive barriers

Discussion

The remodeling of the actin cytoskeleton is critical for morphological changes and mechanotransduction throughout the TEM process^{6,47,96}. Anchoring of integrins to the actin cytoskeleton is critical for firm adhesion and crawling upon to the endothelial monolayer, while the generation of actin-rich membrane protrusions is important for probing the endothelial monolayer and initiating diapedesis^{6,47,96}. Surprisingly, despite displaying reduced actin polymerizing capacity in response to chemokine, FMNL1-deficient T cells were equivalent to WT cells in their ability to adhere and crawl on to the endothelial monolayer and initiate diapedesis. These observations differ from previous studies of macrophages where FMNL1 was reported to promote the adhesion and migration of macrophages through the formation of membrane protrusions known as podosomes^{123,141}. While similar membrane structures in T cells have been suggested to play an important role in sensing of chemokine and initiating diapedesis^{46,49,52}, our observations of normal crawling and diapedesis initiation in FMNL1-deficient T cells suggest that FMNL1 may not be required for these functions in T cells. The cellular localization of FMNL1 also seems to be different between macrophages and T cells, with FMNL1 appearing enriched in ventral podosomal structures in macrophages¹⁴¹ but enriched behind the nucleus in T cells as shown herein. These observations argue for a distinct or additional role for FMNL1 in T cells compared to macrophages.

Completion of diapedesis also relies on actin remodeling and force generation as our previous work with the actin polymerizing Ena/VASP proteins and the cytoskeletal motor protein MyoIIA has demonstrated^{60,119}. Similar to the Ena/VASP proteins, FMNL1 is dispensable for the early stages of T cell TEM, instead being required for efficient completion of diapedesis. Our data also suggest that FMNL1, like the Ena/VASP proteins, has a selective role in the trafficking of activated cells. However, despite both being propagators of linear actin

filaments, Ena/VASP proteins and FMNL1 appear to have distinct mechanisms of action. Whereas Ena/VASP proteins mediate diapedesis through regulating the expression and function of $\alpha 4$ integrin¹¹⁹, our data suggest that FMNL1 mediates diapedesis by promoting transmigration of the nucleus. Thus, while Ena/VASP deficiency impairs the trafficking of activated T cells to both lymphoid tissue and inflammatory sites, where $\alpha 4$ integrin can be involved¹⁷⁸, FMNL1 deficiency only impairs trafficking to tissue sites with more restrictive endothelial barriers. As supported by our transwell migration data, the role for FMNL1 appears to be pore size dependent, consistent with the idea that it is involved in promoting the transmigration of the rigid structure of the nucleus during the completion of diapedesis.

Our FMNL1-deficient T cell TEM data show a striking phenotypic resemblance to inhibition of MyoIIA in transmigrating T cells from previous studies^{51,60}. Both proteins localize behind the nucleus during activated T cell TEM and promote nucleus transmigration through restrictive endothelial barriers⁶⁰. Furthermore, deletion of either FMNL1 or MyoIIA selectively impairs transmigration through narrow pores^{51,60}. Our observation that co-inhibition of FMNL1 and MyoIIA synergistically impairs chemotaxis suggests that they act through distinct but compensatory mechanisms. Since virtually no transmigration occurred when MyoIIA was inhibited in FMNL1 KO T cells, it is likely that FMNL1 and MyoIIA are the two primary mechanisms for activated T cell migration through restrictive barriers. Future live imaging studies looking at actin dynamics and the localization of FMNL1 and MyoIIA within transmigrating T cells will further delineate the nature of their mechanisms.

The use of FMNL1 by T cells to promote transmigration of the nucleus may represent a unique mechanism compared to those employed by other immune cell types. For example, DCs have been suggested to use actin polymerization by Arp2/3 instead of by formins to facilitate nucleus deformation when migrating through restrictive environments¹⁷⁹. Nuclear flexibility may

also dictate the requirement for actin-mediated nucleus manipulation. It has been reported that neutrophils, which have multi-lobed deformable nuclei, or cells with induced nuclear flexibility do not display perinuclear actin accumulation when encountering restrictive spaces, while cells with rigid nuclei do¹⁷⁹. Interestingly, unlike in activated T cells, inhibition of MyoIIA in neutrophils does not impair nucleus transmigration but rather affects retraction of the uropod at the trailing edge of the cell¹⁸⁰. Consistent with this literature, we observed that FMNL1 was dispensable for neutrophil migration through narrow pores, while in activated T cells, varying the level of FMNL1 expression strongly correlated with narrow pore transmigration. After activation, the nuclear volume of T cells increases but still maintains a rigid ovoid structure in contrast to the flexible segmented nuclear structure of neutrophils^{62,63}. However, similar to neutrophils, effector T cells must rapidly migrate into tissues to execute their functions⁴. Thus, we propose that perinuclear FMNL1 in activated T cells compensates for their increased nuclear size and rigidity by facilitating nucleus migration through the restrictive endothelial barriers of non-lymphoid tissues. Future studies examining FMNL1-deficiency in other immune cell types that migrate to sites of inflammation, such as monocytes, will establish whether, this mechanism applies to other cells with rigid nuclei. A family of intermediate filaments known as nuclear lamins are important structural determinants of nuclear shape and rigidity, in particular lamin A/C⁶². Neutrophils downregulate lamin A/C during their development and decreasing lamin A/C expression has been shown to decrease nuclear rigidity in neutrophils as well as other cell types^{62,64,179}. Additionally neutrophils upregulate the Lamin B receptor during development, and overexpression of Lamin B receptor has been suggested to promote a lobular nuclear morphology^{62,181}. We have attempted to modulate T cell nuclear rigidity and morphology directly by decreasing Lamin A/C expression via an RNAi approach or overexpressing Lamin B receptor via retroviral vector, but to date these approaches have not been successful. Future

studies and methods that can directly alter nuclear rigidity will establish more completely whether the requirement for FMNL1 in migration is directly linked to nuclear rigidity.

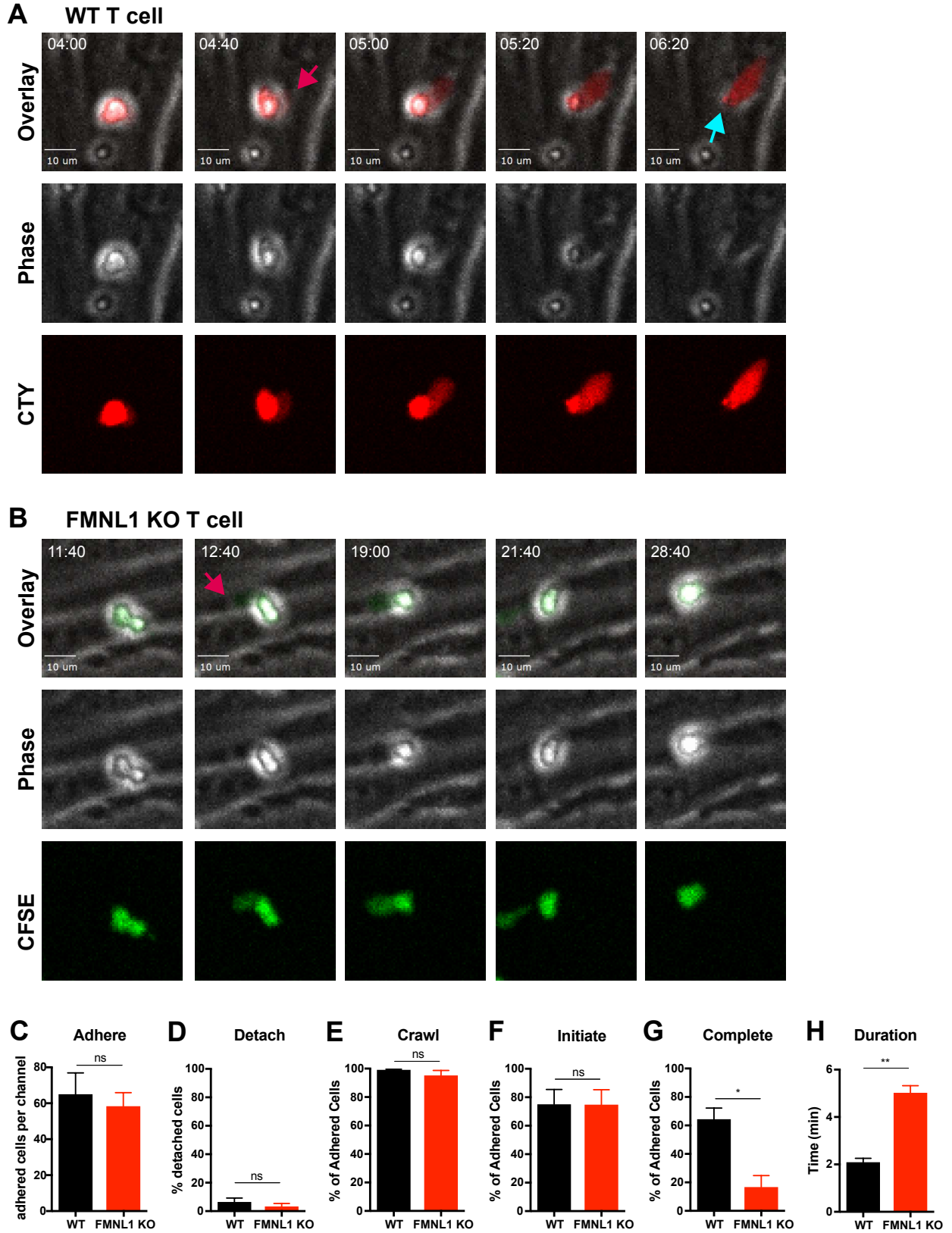


Figure 5.1: FMNL1 deficiency impairs TEM at the diapedesis step.

Figure 5.1: FMNL1 deficiency impairs TEM at the diapedesis step. *Ex vivo* activated CFSE or CellTrace Yellow (CTY) dye-labeled T cells were perfused into flow chambers containing bEnd.3 brain endothelial cell monolayers and kept under shear flow (2 dyne/cm²) for up to 30 min. During this time, phase contrast and fluorescence images were acquired every 20 sec using a spinning-disk confocal microscope. **A)** Selected time-points of a representative WT T cell during transmigration. This transmigrating T cell undergoes trans-endothelial migration (TEM), evidenced by a stepwise darkening in the Phase contrast channel during the time-lapse. The red arrow points to the formation of membrane protrusions under the endothelial monolayer; the blue arrow points to the completion of TEM as shown by the disappearance of the phase halo. Time in min:s. **B)** Selected time-points of a representative FMNL1 KO T cell attempting transmigration. The red arrow points to the formation of membrane protrusions under the endothelial monolayer. However, this FMNL1 KO T cell never completes TEM, as evidenced by the preservation of the phase halo. Time in min:s. **C)** FMNL1 deficiency does not alter the ability of T cells to adhere to the endothelial monolayer. Number of T cells adhered to the endothelial monolayer. **D)** FMNL1 deficiency does not affect T cell detachment from the endothelial monolayer. Percentage of adhered T cells that detached from the endothelial monolayer. **E)** WT and FMNL1 KO T cells have similar crawling behavior. Percentage of adhered T cells that crawled on the endothelial monolayer. **F)** FMNL1 deficiency does not impair the ability of T cells to attempt TEM. Percentage of adhered cells that attempted TEM as evidenced by extension of membrane protrusions underneath the endothelial monolayer. **G)** FMNL1 deficiency strongly impairs the ability of T cells to complete TEM. Percentage of adhered cells that completed TEM as evidenced by complete loss of the phase halo. **H)** FMNL1 deficiency prolongs TEM duration. For cells able to complete TEM, the time in minutes from first attempt to completion was quantified. Statistics in C-H calculated using two-tailed paired t-tests. Data in C-H are the mean \pm SEM from 3 independent experiments with >100 cells analyzed per experiment. n.s. = not significant, * = $p < 0.05$, ** = $p < 0.01$.

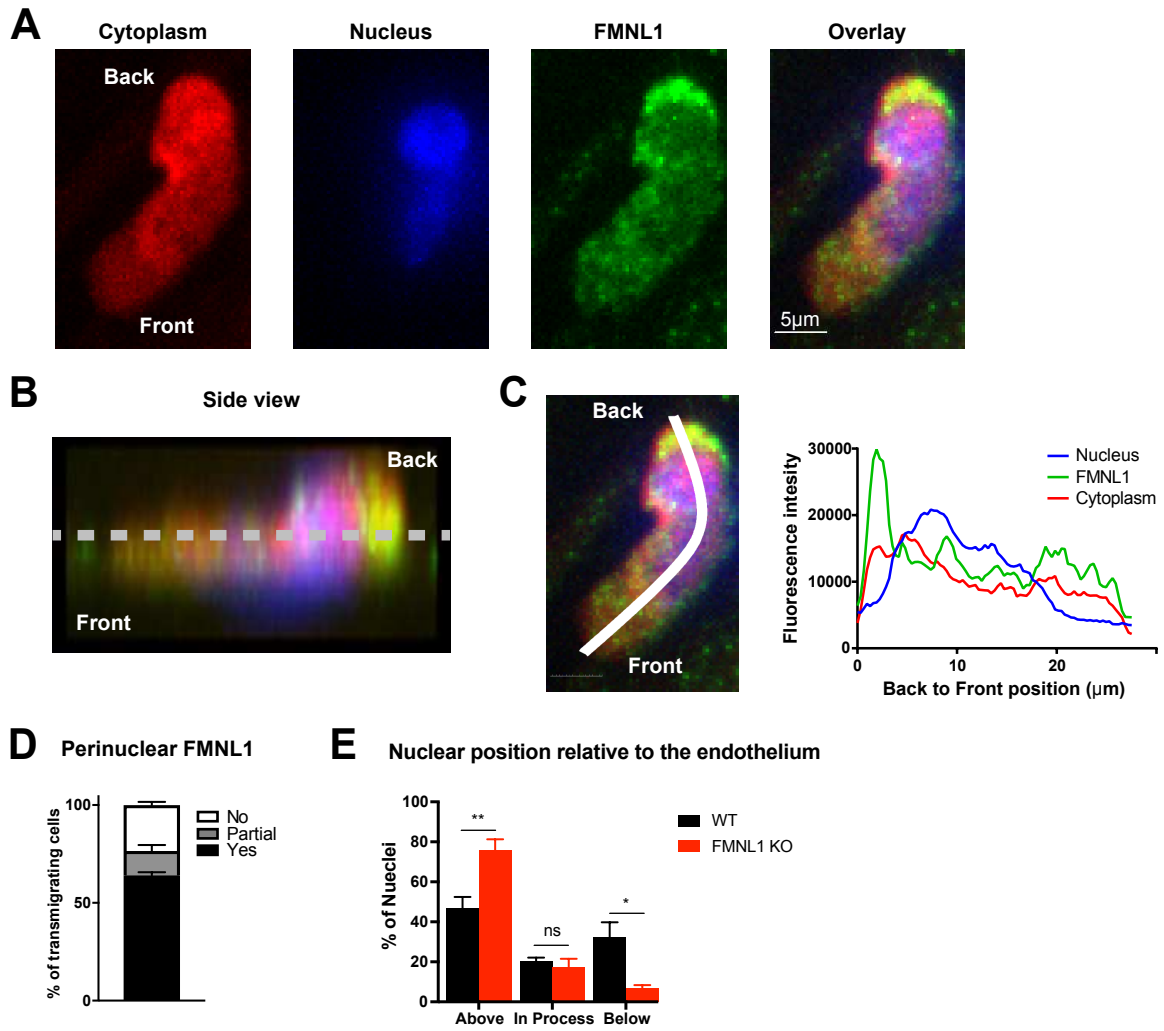


Figure 5.2: FMNL1 promotes nucleus transmigration in T cells undergoing TEM.

Figure 5.2: FMNL1 promotes nucleus transmigration in T cells undergoing TEM.

TEM of dye-labeled WT T cells was set up as in Figure 5. After 5 minutes of TEM under flow, cells were fixed, permeabilized, and stained with DAPI and an anti-FMNL1 antibody **A)** Representative maximum Z projections of a transmigrating T cell, defined as a cell with a portion of the cytoplasm underneath the endothelial monolayer. **B)** Representative 3D side view reconstruction of the transmigrating T cell in A. Dashed line indicates position of the endothelial monolayer. **C)** Representative linescan quantification of fluorescence intensities in a transmigrating T cell. Graph of the fluorescence intensities along the depicted line in each channel relative to the position within the cell. **D)** FMNL1 is enriched behind the nucleus in transmigrating T cells. Percentage of transmigrating T cells with perinuclear enrichment, partial enrichment of FMNL1 behind the nucleus, or no enrichment (see Methods for analysis). **E)** FMNL1 deficiency impairs transmigration of the T cell nucleus across endothelial barriers. Position of T cell nuclei in fixed WT or FMNL1 KO T cells after 5 min of TEM under flow. Using spinning-disk confocal microscopy and DAPI staining, the nuclei were scored as being above the plane of the endothelium, in the process of transmigration, or below. Data in D are the mean \pm SEM from 3 independent experiments with >15 cells analyzed per experiment; data in E are the mean \pm SEM from 4 independent experiments with > 50 cells analyzed per experiment. Statistics in E were calculated using repeated-measures ANOVA with Sidak's multiple comparisons test. n.s. = not significant, * = $p < 0.05$, ** = $p < 0.01$.

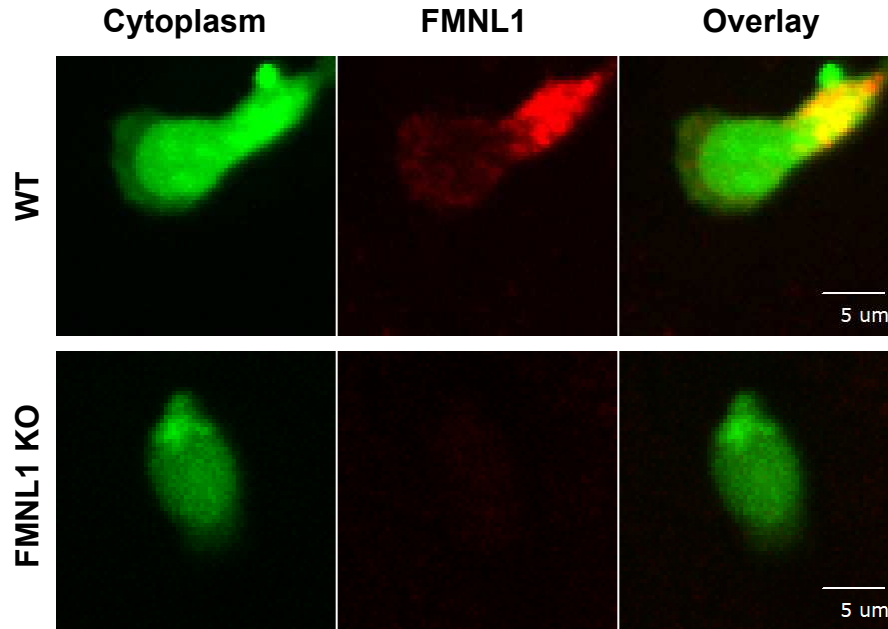


Figure 5.3: Immunofluorescent FMNL1 antibody staining is specific for FMNL1. TEM under flow of differentially dye-labeled WT and FMNL1 KO T cells was set up as in Figure 4. After 5 minutes of TEM under flow cells were fixed, permeabilized, and stained with an anti-FMNL1 antibody. Representative images of a WT (top) or FMNL1 KO T cell (bottom). Images are maximum Z projections of the indicated channel and a composite overlay image.

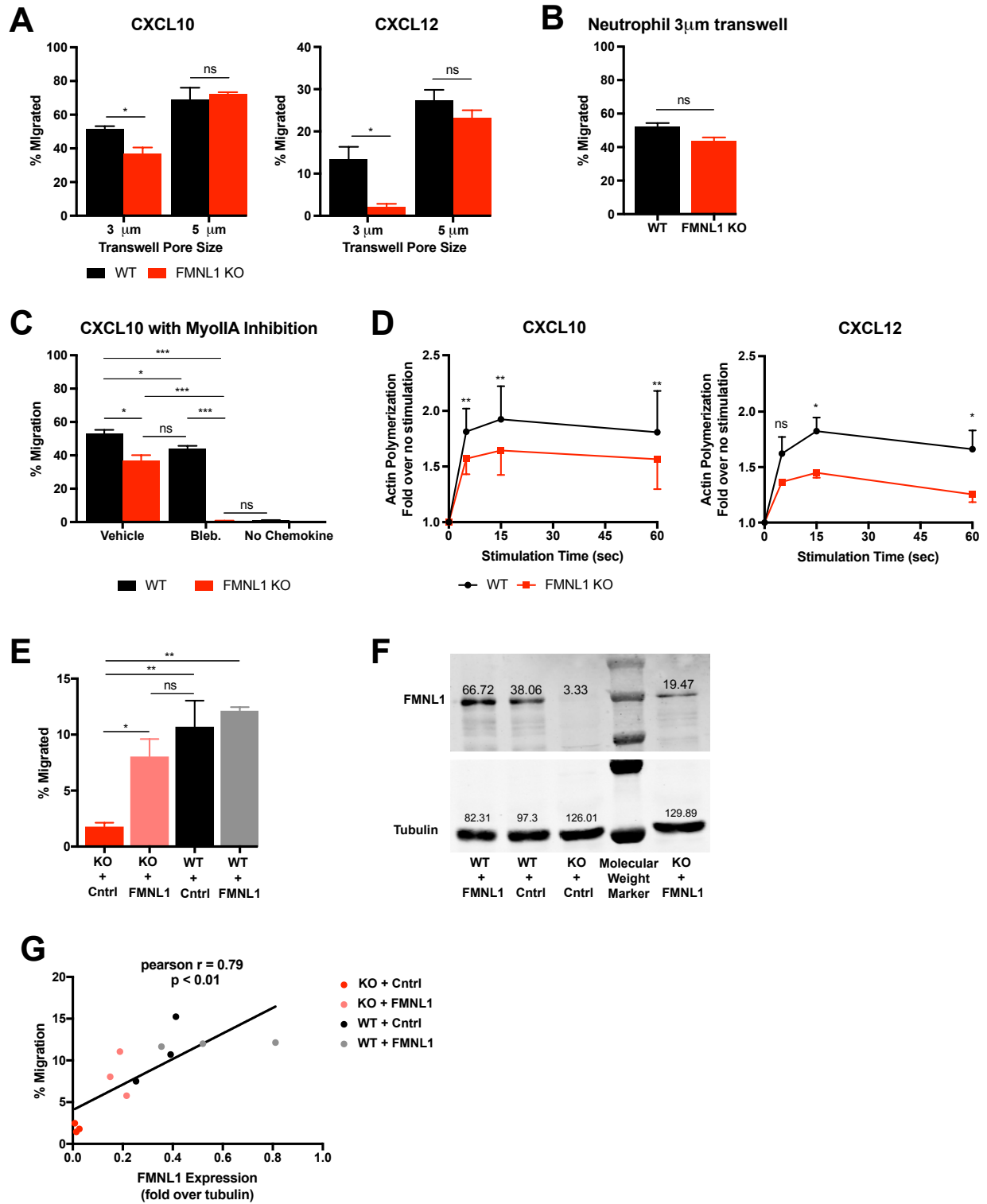


Figure 5.4: T cell migration through narrow pores is FMNL1 dependent.

Figure 5.4: T cell migration through narrow pores is FMNL1 dependent. **A)** FMNL1-deficient T cells are impaired in chemotaxis through narrow pores. Percentage of activated T cells migrating through transwell membranes of the indicated pore size in response to the indicated chemokine. **B)** Neutrophil chemotaxis through narrow pores is not impaired by FMNL1 deficiency. Percentage of neutrophils migrating through 3 μ m transwell membrane pores in response to CXCL1. **C)** Inhibition of MyoIIA in FMNL1-deficient T cells eliminates migration through narrow pores. Percentage of activated T cells with the indicated treatment migrating through 3 μ m transwell membrane pores in response to CXCL10. Bleb = blebbistatin. **D)** FMNL1-deficient T cells are impaired in actin polymerization in response to chemokine. Time course of fold increase in filamentous actin (as determined by flow cytometry of fluorescent phalloidin staining) of activated T cells in response to the indicated chemokine. **E)** Re-expression of FMNL1 in FMNL1 KO T cells restores migration through narrow pores. Activated WT or FMNL1 KO T cells were transduced using either a FMNL1-expressing or control retroviral construct. Percentage of indicated T cells migrating through 3 μ m transwell membrane pores in response to CXCL12. **F)** FMNL1 re-expression in FMNL1 KO T cells. Representative western blot showing expression levels of FMNL1 in FMNL1 KO or WT T cells transduced with FMNL1-expressing or control retroviral constructs. Tubulin staining is shown as a loading control. Numbers next to bands indicate densitometry quantification. **G)** Transwell migration correlates with FMNL1 expression. Percentage of T cells migrating through 3 μ m transwell membrane pores in response to CXCL12 vs level of FMNL1 expression as determined by densitometry of western blot staining in F. The line indicates simple linear regression of the data. Data in A, B and E are the mean \pm SEM from 3 independent experiments; data in C and D are the mean \pm SEM from 4 independent experiments; data in G are the individual values from 3 independent experiments. Statistics in A and E were calculated by repeated measures one-way ANOVA with Sidak's multiple comparisons test; statistics in B were calculated using a two-tailed paired t-test; statistics in C and D were calculated by repeated-measures two-way ANOVA with Sidak's multiple comparisons test; statistics in G were calculated using Pearson's correlation. n.s. = not significant, * = $p < 0.05$, ** = $p < 0.01$, *** = $p < 0.001$.

CHAPTER VI

MDIA1 DEFICIENCY IMPAIRS INDUCTION OF EAE AND T CELL DIAPEDESIS

Introduction

In addition to FMNL1, the formin mDia1 is highly expressed by T cells^{104,116,123-125}. While FMNL1 is primarily expressed by hematopoietic cells, mDia1 is expressed more ubiquitously^{123,129,130,138}. However, mDia1 protein expression is upregulated in activated T cells and tissue-infiltrating T cells¹⁰⁴. Compared to FMNL1, the function of mDia1 in T cells has been more extensively characterized. Mice deficient in mDia1 have reduced numbers of T cells in peripheral lymphoid organs, which has been attributed to an impairment in T cell thymic egress^{124,135}. However, numbers of B cells and myeloid cells in the secondary lymphoid organs and blood of mDia1-deficient T cells appear to be normal¹²⁴. mDia1 has also been implicated in morphological changes and cytoskeleton remodeling in response to TCR stimulus and within the immunological synapse^{104,116,135,136}. Previous studies have suggested that mDia1-deficient T cells are impaired in proliferation in response to anti-CD3 and anti-CD28 stimulus^{124,135}. mDia1-deficient T cells are impaired in trafficking to both lymphoid organs as well as inflamed skin^{124,134}. A number of studies have shown that, while expression levels of chemokine receptors are normal in mDia1-deficient T cells, chemotaxis is impaired^{124,134,135}. Integrin expression has also been reported to be unaltered on mDia1-deficient T cells, although adhesion to integrin ligands appears to be impaired depending on the context^{104,134,135}. While a specific role for mDia1 in T cell TEM has not been identified, we have recently shown that mDia1 promotes completion of diapedesis by leukemia cells¹³⁷. While one report has demonstrated impaired contact hypersensitivity in mDia1-deficient mice, it is not clear whether this is due to the impairment of T cell-intrinsic or -extrinsic mDia1 function^{124,182}. Consequently, the requirement

for mDia1 in T cell driven immune responses in autoimmune or infectious settings remains unknown.

Having established a role for FMNL1 in T cell migration and induction of autoimmune disease in Chapters III, IV, and V, in this chapter, we sought to also investigate the roles of mDia1 in these processes. Here, we report that self-reactive mDia1-deficient T cells are impaired in their ability to induce EAE. We further demonstrate that while activated mDia1-deficient T cells are capable of adhering to and crawling on the endothelium, they are impaired in their ability to complete diapedesis.

Results

Self-reactive mDia1-deficient T Cells Are Impaired in Inducing EAE

To investigate the requirement for mDia1 in T cell driven autoimmune disease, we used the MOG specific 2D2 T transfer model of EAE as in Chapter IV. We first activated control or mDia1 KO 2D2 CD4 T cells with MOG peptide *ex vivo* using WT CD45.1/.1 congenic irradiated splenocytes as APCs (Fig 6.1A). Since mDia1-deficient T cells had previously been reported to be impaired in T cell proliferation in response to an activating stimulus^{124,135}, we measured the number of control and mDia1 KO 2D2 T cells in response to MOG peptide activation. However, we found no differences in the expansion of control and mDia1 KO T cells (Fig 6.1 B). We also compared the level of canonical markers of T cell activation and found no differences between activated WT and mDia1 KO 2D2T cells (Fig. 6.1C). After *ex vivo* activation and expansion, we then transferred these T cells into recipient mice, and monitored these mice for development of EAE (Fig. 6.1A). While 90% of mice receiving control 2D2 T cells developed EAE, only 25% of mice receiving mDia1 KO 2D2 T cells developed EAE (Fig. 6.1D). Mice receiving control T cells displayed an average peak disease score of 2.3 compared to an average peak score of 0.35

for mice receiving FMNL1 KO T cells (Fig. 4E). These data suggest that mDia1-deficient T cells are impaired in inducing autoimmune disease.

mDia1 Deficiency Impairs T cell TEM at the Diapedesis Step

While mDia1 has been suggested to be important for T cell trafficking^{124,134,135}, its specific role in T cell TEM has not been elucidated. For these experiments, we employed an *in vitro* flow chamber system to visualize and quantify T cell TEM under shear flow as in Chapter V. After culturing an endothelial cell monolayer within the flow chamber, we perfused in differentially dye-labeled activated control and mDia1 KO T cells and imaged them under physiological shear flow for 30 minutes (Fig. 6.2A,B). Quantification of the number of cells adhering to the endothelium and subsequently detaching under flow revealed no differences between WT and mDia1 KO T cells (Fig. 6.2C, D). Similarly, both WT and mDia1 KO T cells were equally capable of crawling on the endothelial monolayer (Fig. 6.2E), suggesting that mDia1 is dispensable during the first stages of TEM. While mDia1 KO T cells were equivalent to WT cells in their ability to initiate diapedesis (Fig. 6.2F), they were 1.9-fold reduced in their ability to complete the TEM process (Fig. 6.2G). Furthermore, those mDia1 KO T cells that were able to complete TEM took 1.6 times as long, on average, to do so compared to WT T cells (Fig. 6.2H). These data indicate a role for mDia1 in completion of the diapedesis step of the TEM process.

Discussion

T cells primarily express two members of the formin family of cytoskeletal effectors, FMNL1 and mDia1^{104,116,123,125}. In chapters III-V, we characterized a specific role for FMNL1 in selectively mediating T cell trafficking to sites of inflammation by promoting transmigration of the T cell nucleus through restrictive endothelial barriers. Previous studies have identified a broad role for mDia1 in regulating T cell trafficking, thymic egress, chemotaxis and activation

^{104,124,134,135}. In contrast to prior reports^{124,135}, we observed normal T cell expansion and activation in response to TCR stimulus. This discrepancy may be due to the method of stimulation or the nature of the T cells used, as the previous systems used anti-CD3 and anti-CD28 antibodies to stimulate polyclonal T cells. In this study, we activated 2D2 TCR transgenic T cells using MOG peptide and WT irradiated splenocytes as APCs. As the nature of immune synapse formation is likely different between these two methods, it is possible that mDia1 is less required TCR-peptide-MHC-mediated activation compared to CD3/CD28 cross-linking activation. Another study used a similar method as the one employed in our study to activate mDia1 KO OT-II T cells with OVA peptide¹³⁴. Though clearly enough cells were generated from this activation method to perform trafficking experiments, the similarity or differences between control and mDia1 KO T cells were not reported¹³⁴. Future examination of the activation of mDia1-deficient T cells in physiological environments will better elucidate the exact requirement and specific role for mDia1 in T cell activation.

Even though mDia1-deficient 2D2 T cells activated equivalently to WT T cells *ex vivo*, when transferred into WT recipient mice they were substantially impaired in their ability to induce EAE. This is consistent with a previous report that showed that activated mDia1-deficient T cells are impaired in trafficking to an inflammatory site¹³⁴. This finding also mirrors our results from Chapter IV, where we showed that FMNL1-deficient 2D2 T cells were impaired in their ability to induce EAE. Together, these findings suggest that formins are critical for T cell driven autoimmune disease. While in this report we identified a role for mDia1 in T cell TEM, it is possible that other defects in mDia1-deficient T cells contribute to their impaired ability to induce autoimmunity. Some non-lymphoid tissues offer secondary barriers to cell entry, such as the glia limitans in CNS^{56,83}. It is possible that mDia1 deficiency impairs migration through these secondary barriers as well as through the endothelium. mDia1-deficient T cells have been

reported to have impaired motility within the lymph node, moving at a slower speed and surveying a smaller area than WT control T cells¹³⁴. Thus, it is possible that transferred mDia1-deficient 2D2 T cells would be impaired in migrating within the lymph nodes or the CNS parenchyma of recipient mice to find APCs and carry out their effector functions. Future study of mDia1-deficient T cells within tissues will better define the mechanisms by which mDia1 contributes to pathogenic T cell behavior in autoimmune settings.

Our finding that mDia1-deficient T cells are impaired at the diapedesis step of TEM is consistent with our prior report that depletion of mDia1 in leukemia cells also impairs diapedesis¹³⁷. Given previous reports that mDia1 promotes T cell chemotaxis^{104,124,134,135}, it is unsurprising that mDia1-deficient T cells exhibited impaired TEM. However, given that mDia1 has been reported to be involved in integrin-mediated adhesion^{134,135}, it is striking that we observed no defects in attachment of mDia1-deficient T cells to the endothelium. While the previous studies looked at LFA-1-mediated adhesion to ICAM-1 in naive T cells^{134,135}, our TEM assay examined activated T cell binding to an endothelium that expresses both ICAM-1 and VCAM-1. Unlike naive T cells, which primarily express LFA-1, activated T cells also express the VCAM-1 binding partner VLA-4¹⁸³. Thus, it is possible that mDia1 is more involved in LFA-1 binding to ICAM-1, and that VLA-4 binding of VCAM-1 compensates in activated mDia1-deficient T cells binding to the endothelium. Furthermore, while the previous experiments examined cell adhesion in the absence of shear flow^{134,135}, our experiments were conducted under physiological shear forces. As shear forces affect integrin conformation and affinity⁴⁸, mDia1 may play different roles in integrin-mediated adhesion under shear and non-shear force conditions.

In Chapter V, we observed a similar impairment of diapedesis completion in activated FMNL1-deficient T cells. Despite the similarities between the diapedesis phenotypes, FMNL1

and mDia1 are likely serving different functions in T cell migration. In Chapter IV, we demonstrated that FMNL1-deficient T cells are selectively impaired in trafficking to non-lymphoid inflammatory sites. In contrast, mDia1-deficient T cells are impaired in trafficking to both lymphoid and non-lymphoid tissues. While prior reports indicate that loss of mDia1 impairs chemotaxis even through non-restrictive barriers^{124,137}, we showed in Chapter V that FMNL1 was selectively required for chemotaxis through narrow pores. Our observation that FMNL1 and MyoIIA co-inhibition entirely impaired T cell chemotaxis through narrow pores suggests that mDia1 alone is not sufficient to drive this process in T cells. Additionally, mDia1 has been reported to localize behind the lamellipodium in crawling T cells^{103,104} while we report a perinuclear enrichment localization of FMNL1 in transmigrating T cells. Furthermore, mDia1-deficient neutrophils are reported to be impaired in chemotaxis¹⁸⁴ while in Chapter V we observed that FMNL1-deficient neutrophils were not. Together, these findings suggest a distinct and specific role for FMNL1 in mediating nucleus transmigration through restrictive endothelial barriers compared to a more general role for mDia1 in cell motility. Future study of FMNL1 and mDia1 double-deficient T cells may further delineate the unique or overlapping roles for individual formins within T cells.

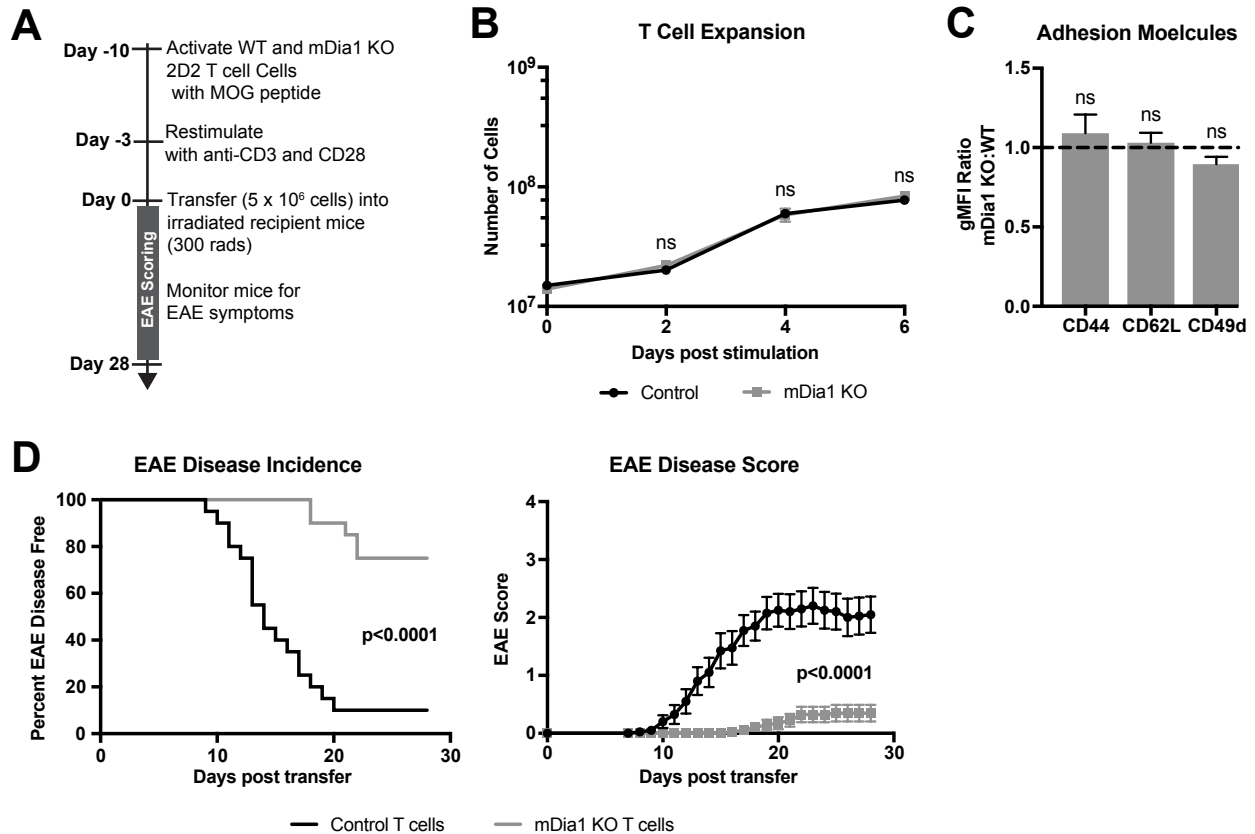


Figure 6.1: Self-reactive mDia1-deficient T cells are impaired in inducing EAE. **A)** Experimental set-up for induction of EAE via T cell transfer. Control or mDia1 KO MOG-specific 2D2 T cells were activated *ex vivo* and then transferred into WT recipient mice. EAE disease severity was scored daily for 28 days. **B)** Control and mDia1 KO T cells proliferate equivalently in response to MOG peptide stimulus. Total number of WT or KO T cells on days 0, 2, 4, and 6 days post-stimulus. **C)** Activated WT and mDia1 KO T cells express equivalent levels of adhesion molecules and activation markers. Ratio of geometric mean fluorescent intensity (gMFI) of antibody staining of indicated surface molecules mDia1 KO T cells compared to WT T cells after activation described in A, prior to transfer. A ratio above or below 1.0 (dashed line) indicates a respective increase or decrease in expression of the indicated marker on mDia1 KO T cells relative to WT. **D)** mDia1 deficiency in T cells delays EAE onset and partially protects from disease. EAE incidence (score ≥ 1.0) in mice receiving control or mDia1 KO 2D2 T cells (left). Mean EAE score \pm SEM over time in mice receiving control or mDia1 T cells 2D2 T cells (right). Data in B and C and D (right) are the mean \pm SEM from 4 independent experiments; data in D are pooled from 3 independent experiments with cohorts of 5 mice/group each. Statistics in B were calculated using repeated measures two-way ANOVA with Sidak's multiple comparisons test; statistics in C were calculated using a one-sample two-tailed t-test against a theoretical mDia1 KO:WT ratio of 1.0; statistics in D (left) were calculated by Log-rank test; statistical interaction of genotype with disease severity over time in D (right) was calculated by repeated measures two-way ANOVA. n.s. = not significant.

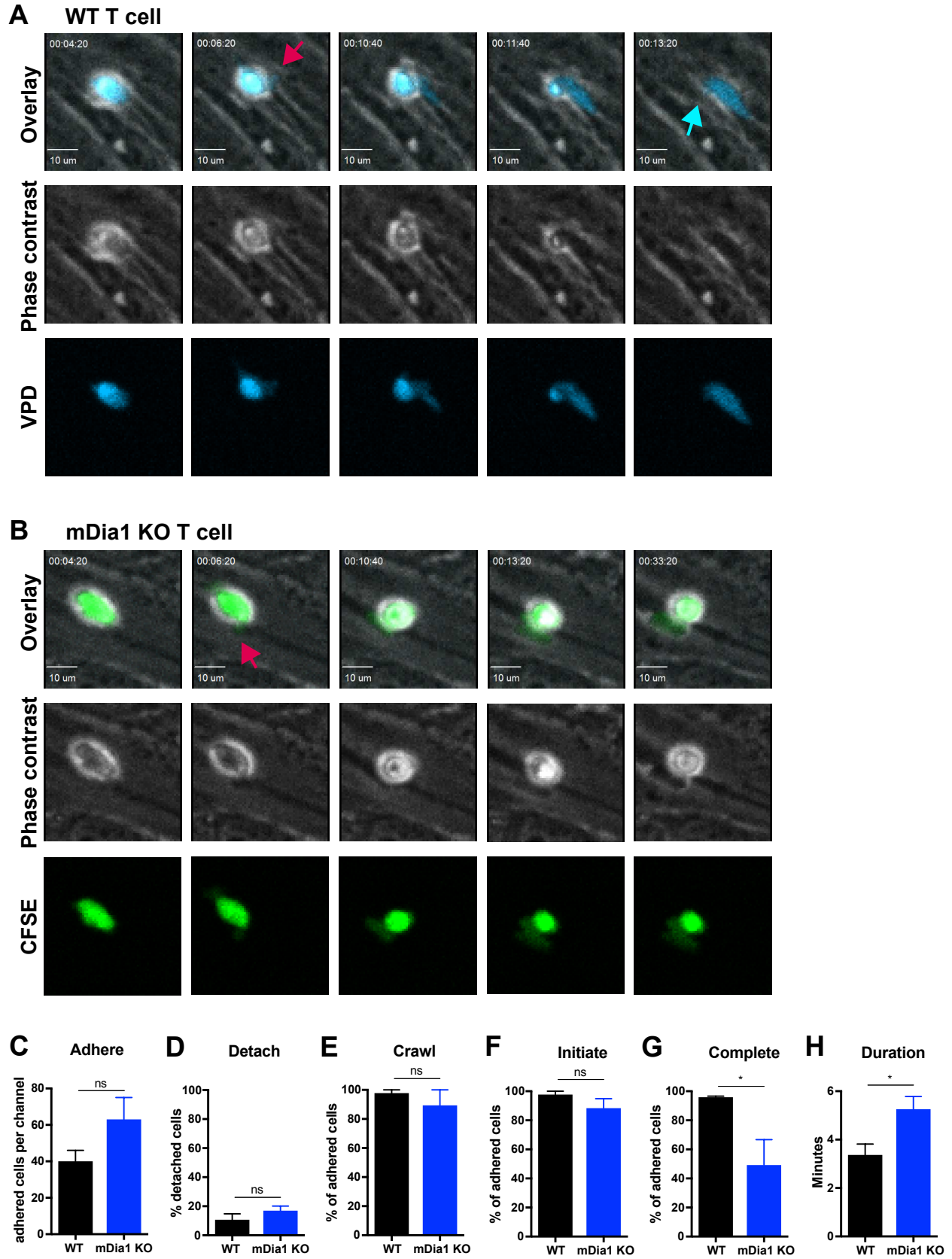


Figure 6.2: mDia1 deficiency impairs TEM at the diapedesis step.

Figure 6.2: mDia1 deficiency impairs TEM at the diapedesis step. *Ex vivo* activated CFSE or VPD dye-labeled T cells were perfused into flow chambers containing bEnd.3 brain endothelial cell monolayers and kept under shear flow (2 dyne/cm²) for up to 30 min. During this time, phase contrast and fluorescence images were acquired every 20 sec using a spinning-disk confocal microscope. **A)** Selected time-points of a representative WT T cell during transmigration. This transmigrating T cell undergoes trans-endothelial migration (TEM), evidenced by a stepwise darkening in the Phase contrast channel during the time-lapse. The red arrow points to the formation of membrane protrusions under the endothelial monolayer; the blue arrow points to the completion of TEM as shown by the disappearance of the phase halo. Time in min:s. **B)** Selected time-points of a representative mDia1 KO T cell attempting transmigration. The red arrow points to the formation of membrane protrusions under the endothelial monolayer. However, this mDia1 KO T cell never completes TEM, as evidenced by the preservation of the phase halo. Time in min:s. **C)** mDia1 deficiency does not alter the ability of T cells to adhere to the endothelial monolayer. Number of T cells adhered to the endothelial monolayer. **D)** mDia1 deficiency does not affect T cell detachment from the endothelial monolayer. Percentage of adhered T cells that detached from the endothelial monolayer. **E)** WT and mDia1 KO T cells have similar crawling behavior. Percentage of adhered T cells that crawled on the endothelial monolayer. **F)** mDia1 deficiency does not impair the ability of T cells to attempt TEM. Percentage of adhered cells that attempted TEM as evidenced by extension of membrane protrusions underneath the endothelial monolayer. **G)** mDia1 deficiency strongly impairs the ability of T cells to complete TEM. Percentage of adhered cells that completed TEM as evidenced by complete loss of the phase halo. **H)** mDia1 deficiency prolongs TEM duration. For cells able to complete TEM, the time in minutes from first attempt to completion was quantified. Statistics in C-H calculated using two-tailed paired t-tests. Data in C-H are the mean \pm SEM from 3 independent experiments with >80 cells analyzed per experiment. n.s. = not significant, * = $p < 0.05$.

CHAPTER VII

DISCUSSION

Summary of Major Findings

T cell trafficking is an essential component of proper immune function both in immune surveillance and in response to pathogens^{3,4}. However, in the context autoimmunity, T cell invasion of tissues can be a driver of disease^{28,29,32-34,36}. In order to carry out their functions, T cells must extravasate out of the bloodstream and into tissues. While many of the chemokines and adhesion molecules that guide T cell TEM have been well characterized^{3,4}, less is known about how downstream cytoskeletal effectors mediate morphological changes and force generation during the process of TEM. In particular, prior to this work, the function of FMNL1 in T cell migration and *in vivo* responses was unknown. While previous studies had identified mDia1 as key regulator of T cell trafficking^{124,134,135}, its role in T cell TEM and in autoimmune responses was unknown. Thus, the overall goal of this work was to characterize the role of formins in T cell TEM and induction of autoimmune disease.

In Chapter III, we described the development of a novel germline FMNL1 KO mouse as a tool for studying the *in vivo* functions of FMNL1. Using PCR and western blot, we confirmed deletion of FMNL1 at the both the genetic and protein level. In examining the blood, thymus, and secondary lymphoid organs of FMNL1 KO mice compared to WT mice, we found no differences in either developmental or mature T cell populations. Additionally, we found no differences in the populations of other lymphocytes and myeloid cells at steady state. These findings suggest that FMNL1 is not essential for hematopoiesis or maintenance of the major immune cell populations in the blood and secondary lymphoid organs. To further characterize the role of FMNL1 in T cell trafficking, we performed co-adoptive transfer studies of naive WT and FMNL1 KO T cells into WT recipient mice. We found that naive WT and FMNL1 KO T

cells trafficked equivalently to the spleen and lymph nodes of recipient mice. This finding suggests that FMNL1 is dispensable for homeostatic T cell trafficking. Additionally, we found that FMNL1 KO T cells and WT T cells could be activated equivalently *ex vivo*. Together, our data do not support a major role for FMNL1 in development, migratory function, or activation of naive T cells. However, it is possible that migratory patterns and lymphocyte behavior within tissues are affected. Additionally, immune populations in non-lymphoid tissues, not examined in this work, could have altered numbers or function. Future characterization of the FMNL1 KO mouse will further define the impacts of FMNL1-deficiency in immune populations at steady state.

The results in presented Chapter IV identified FMNL1 as a key regulator of activated T cell trafficking to sites of inflammation and induction of autoimmune disease. When we co-transferred *ex vivo* activated FMNL1 KO T cells into WT recipients with ongoing autoimmune inflammation in the pancreatic islets or CNS, we found they were impaired in trafficking to these sites. In contrast, trafficking of activated FMNL1KO cells to secondary lymphoid organs was not impaired. These findings suggest that FMNL1 has a selective role in mediating activated T cell trafficking to sites of inflammation. To examine whether these T cell trafficking defects would be of functional consequence, we tested the ability of activated self-reactive FMNL1 KO T cells to induce autoimmune disease in T cell transfer models of type 1 diabetes and EAE. In both cases, we found that FMNL1 KO T cells were substantially impaired in their ability to induce autoimmune disease. Together, our data in this chapter suggest that FMNL1 enables T cells to induce autoimmune disease by promoting activated T cell trafficking to non-lymphoid organs. However, in addition to impairing trafficking, it is also possible that FMNL1 deficiency impairs other aspects of T cell function within tissues, such as scanning for APCs and killing target cells.

Further study of FMNL1 KO T cell behavior and function within tissues will clarify whether FMNL1 has additional roles in T cells.

While we demonstrated a role for FMNL1 in promoting activated T cell trafficking *in vivo* in Chapter IV, the *in vitro* studies outlined in Chapter V investigated the potential causes of this selective trafficking defect. Our data determined FMNL1 promotes transmigration of the nucleus through restrictive endothelial barriers during T cell TEM. Using a model of TEM under shear flow, we found that activated FMNL1 KO T cells were impaired in completing diapedesis. Examining the cellular localization of FMNL1 during T cell TEM determined that it is enriched behind the nucleus. We further demonstrated that FMNL1 KO T cells are impaired in transmigrating the nucleus through the endothelium during TEM. This nucleus transmigration defect likely explains why FMNL1 KO T cells are impaired at completing TEM. Using transwell assays with differing membrane pore sizes, we determined that the requirement for FMNL1 in T cell chemotaxis is pore size dependent. However, FMNL1 KO neutrophils, with flexible nuclei, were unimpaired in migrating through narrow pores. Together, these data suggest that FMNL1 promotes transmigration of the rigid T cell nucleus through restrictive barriers. We also examined the contribution of another regulator of nucleus transmigration, the motor protein MyoIIA. We found that while single inhibition of MyoIIA or FMNL1 only partially impaired chemotaxis through narrow pores, co-inhibition completely abrogated chemotaxis. Additionally, we found that FMNL1 KO T cells were impaired in their ability to polymerize actin in response to chemokine stimulus. Combined, these data suggest T cells rely on both MyoIIA-mediated contraction or FMNL1-mediated actin polymerization to migrate through narrow pores with either process able to partially support migration through restrictive barriers. Finally, we demonstrated that re-expression of FMNL1 in FMNL1 KO T cells restores their ability to perform chemotaxis through restrictive barriers. We also found that the level of T cell migration

positively correlated with the level of FMNL1 expression. These findings further demonstrated that FMNL1 regulates T cell migration through narrow pores. Overall, the data presented in Chapter V are consistent with a model whereby actin polymerization by FMNL1 behind the nuclei of transmigrating T cells facilitates their passage through restrictive endothelial barriers during TEM. However, the specific actin structures that are being created by FMNL1 remains to be determined. The impaired ability of FMNL1-deficient T cells to transmigrate through narrow pores likely explains why they are impaired in trafficking to non-lymphoid organs with restrictive vascular beds but not secondary lymphoid organs with permissive vascular beds. The defects in nucleus transmigration observed in FMNL1 KO T cells may also hinder their interstitial migration within tissues with secondary barriers to entry or constrictive parenchyma, for example, due to the presence of dense extracellular matrix networks. Additionally, FMNL1 may have a similar role in the migration of other immune cells with rigid nuclei that must migrate through confined environments. Further studies of the motile properties of FMNL1-deficient immune cells to and within tissues will determine whether this mechanism is unique to T cell TEM.

While we established a role for FMNL1 in T cell migration and autoimmune disease in Chapters III-V, in Chapter VI, we performed similar studies with T cells deficient in mDia1. While previous reports indicated that mDia1 was involved in T cell activation and proliferation^{124,135}, we found that mDia1 KO 2D2 T cells activated equivalently to WT 2D2 cells *ex vivo*. However, similar to FMNL1 KO 2D2 T cells, when mDia1 KO 2D2 T cells were transferred into recipient mice they were impaired in their ability to induce EAE. This is consistent with a previous report that activated mDia1-deficient T cells are impaired in trafficking to inflamed skin¹³⁴. To further investigate why mDia1 KO T cells are impaired in trafficking, we performed *in vitro* TEM assays under shear flow. Though mDia1 has been shown

to localize to the lamellipodium in crawling T cells^{96,104}, we found no differences between mDia1 KO and WT T cells in the initial stages of TEM (i.e. adhesion and crawling). Instead, similar to FMNL1 KO T cells, mDia1 KO T cells were impaired in completion of diapedesis. This impairment in diapedesis may explain why mDia1 KO T cells display impaired trafficking, and, consequently, impaired ability to induce autoimmune disease. However, it is also possible that mDia1 KO T cells have other defects that impair their function in the context of autoimmunity. Further study of mDia1-deficient T cell behavior and function within inflamed tissues will clarify to what extent their impaired ability to induce autoimmune disease is due to trafficking. Additionally, the precise mechanism by which mDia1 promotes diapedesis remains undetermined. Further study of mDia1-deficient T cells will determine what specific actin networks or other cellular structures mDia1 mediates during TEM. Together, with the data from Chapters III-V, the data presented in Chapter VI suggests that formins are key regulators of both T cell TEM and ability to induce autoimmune disease.

Future Directions

Do Formins Regulate Interstitial T cell migration and Function?

While we examined the role of FMNL1 and mDia1 in T cell TEM herein, it is also possible they have roles in T cell interstitial migration. Tissues such as the CNS have secondary barriers to entry beyond the endothelium, and tissues such as the skin have dense extracellular matrix networks which can impede migration^{56,67,83}. The ability to manipulate the rigid structure of the nucleus has been demonstrated to be a determinant of tissue migratory ability^{66,67,179}. Given our data in Chapter V that FMNL1 promotes transmigration of the rigid nucleus through narrow pores, it is likely that FMNL1 may also facilitate T cell migration in restrictive tissue environments beyond the vascular endothelium. Additionally, a previous report has shown that mDia1-deficient T cells have impaired motility within the lymph node¹³⁴. Thus, mDia1 may also

regulate interstitial T cell motility. Using multi-photon imaging of either constitutively fluorescent or dye-labeled T cells within live mice or explanted tissues, we can determine the requirements for formins in regulating T cell migration within tissues. By employing established imaging systems for the inflamed brain¹⁸⁵, pancreas¹², or skin¹⁸⁶, we can examine both how activated FMNL1 or mDia1-deficient T cells migrate through secondary tissue barriers as well as migrate within the tissue parenchyma. Additionally, using established systems for imaging lymph nodes^{19,109}, we can determine the role for formins in T cell priming and restimulation. T cells have been reported to adopt different scanning patterns (i.e. Brownian walks vs Lévy Walks) between lymphoid and non-lymphoid tissues to optimize their ability to find their cognate APCs^{19,185}. Thus, altered migratory behavior in FMNL1-deficient or mDia1-deficient T cells could affect their ability to locate APCs and, consequently, their effector functions. The duration of interaction between a T cell and an APCs can determine whether a T-APC interaction is tolerogenic or activating^{13,187,188}. Therefore, multi-photon imaging of fluorescent formin-deficient T cells with fluorescent APCs could identify additional means by which formins contribute to T cell function in autoimmune responses. These *in vivo* imaging studies could be complemented by histological and immunofluorescence examination of tissues sections to determine if formins regulate T cell tissue localization and, consequently, their ability to mediate tissue damage.

In addition to potential effects on interstitial migration, FMNL1 and mDia1 deficiency could also alter other aspects of T cell effector function. Both mDia1 and FMNL1 have been implicated in actin organization and repositioning of the centrosome during immune synapse formation^{116,136}. Additionally, knockdown of mDia1 or FMNL1 in human CD8 T cells partially impaired their function in a redirected cytotoxicity assay¹¹⁶. Therefore, our observations of impaired induction of autoimmune disease by formin-deficient T cells in Chapters IV and VI

could be driven by defects in T cell effector function in addition to defects in migration. By examining the ability of antigen-specific FMNL1 KO or mDia1 KO T cells to mediate damage in brain tissue-slice cultures or in *in vitro* cytotoxicity assays, we can determine to what extent formins regulate T cell function independently of tissue entry. By comparing cytokine production and secretion capacity using intracellular cytokine staining assays and ELISAs with restimulated T cells, we can determine whether loss of FMNL1 or mDia1 specifically impacts the ability of effector T cells to secrete cytokines. Furthermore, *in vivo*, we can transfer increased numbers of self-reactive FMNL1 KO or mDia1 KO T cells to overcome the observed trafficking defects and ensure an equivalent number of T cells arrive at the disease site compared to WT, and then determine disease outcome. Alternatively, in the case of the EAE, it may be possible to directly inject KO T cells into the CNS. These studies would enable us to determine if there are additional defects in formin-deficient T cell effector function beyond impaired trafficking. While FMNL1 and mDia1-deficient T cell proliferation and activation appear to be normal *ex vivo*, longitudinal examination of transferred T cell viability and phenotype will determine whether formin-deficiency alters T cell persistence in our autoimmune models *in vivo*. Combined, these further investigations of formin-deficient T cells will delineate the extent to which FMNL1 and mDia1 regulate T cell behaviors beyond TEM.

How Do Formins Regulate Immune Responses To Pathogens?

While we have examined how formins regulate T cell trafficking in the context of autoimmune inflammation herein, T cell migration is also critical for clearance of pathogens. A common complication of immune cell migration-based therapies is immunosuppression and failure to control pathogens^{89,95,189,190}. Therefore, understanding to what extent formins regulate T cell trafficking and effector function in response to pathogenic challenge will be critical to determining their therapeutic viability. Our data on the trafficking and motility of FMNL1-

deficient T cells suggests that responses to pathogens in tissues permissive to lymphocyte entry, such as the spleen, would be less impaired compared to pathogen challenge in more entry-restricted non-lymphoid organs. Previous observations of more general defects in the trafficking of mDia1-deficient T cells^{124,134,135} would suggest that responses to pathogens in multiple types of tissues would be impaired in the absence of this formin. Using model pathogens with both systemic organ and mucosal modes of infection^{191–194}, we can delineate to what extent formins are required for effective pathogen clearance at different tissue sites. Using germline FMNL1 or mDia1 KO mice, T cell specific formin deletion models, or adoptive transfer of antigen-specific formin-deficient T cells, we can determine whether the potential requirements for formins in immune responses are T cell intrinsic. A number of specialized T cell and innate immune subsets reside in non-lymphoid tissues and can be important for pathogenic clearance at those sites^{162–165}. In addition to T cells, other immune cells such as, neutrophils, inflammatory monocytes, or NK cells infiltrate tissues and can be important for protective immune responses¹⁹⁵. Characterization of the immune cell populations in germline FMNL1 or mDia1 KO mice at mucosal and other tissue sites, both at steady state and longitudinally post-infection, will enable us to determine the respective contributions of formins to immune cell migration and protective function. While FMNL1 is largely restricted in expression to hematopoietic cells compared to mDia1, understanding its roles in other immune cell populations will be important in determining the viability of targeting FMNL1 therapeutically. Together, these experiments will determine the requirement for formins in immune responses to pathogens in different tissues.

How Do Formins Remodel Actin Cytoskeletal Networks During TEM?

While we identified that formins promote the completion of diapedesis during T cell TEM in Chapter V, the specific cytoskeleton changes they facilitate during this process remains unknown. As we have shown with FMNL1 and others have shown with mDia1¹²⁴, loss of either

of these formins partially impairs the ability of T cells to polymerize actin in response to chemokine stimulus. However, which actin structures are altered or missing during TEM is still unknown. Using T cells from mice which constitutively express fluorescently (GFP- or RFP-) tagged LifeAct, a small peptide that selectively binds polymerized actin, we can visualize actin dynamics in live cells in real-time¹⁹⁶. By comparing LifeAct-expressing WT and formin-deficient T cells in a TEM under shear flow assay we can determine how loss of a given formin affects actin polymerization at different stages of TEM. Being able to temporally link actin cytoskeletal changes to either the successful or unsuccessful completion of TEM will enable us to better define how actin polymerization by either mDia1 or FMNL1 facilitates diapedesis. Furthermore, by retrovirally expressing fluorescently tagged FMNL1 or mDia1 in these LifeAct T cells we can visualize the dynamic interaction between formins and specific actin networks within the cell during TEM.

It is possible that live imaging of LifeAct T cells may not have enough resolution to distinguish individual actin filaments and thus detect more subtle alterations to actin networks in formin-deficient T cells. Using super-resolution imaging techniques, such as photoactivation localization microscopy (PALM) with stochastic optical reconstruction microscopy (STORM) and stimulated emission depletion (STED) microscopy¹⁰³, we may be able to pinpoint the localization of individual FMNL1 or mDia1 dimers with precisely defined actin filaments. Additionally, such super-resolution techniques can enable the visualization and quantification of actin-rich micro-protrusions such as filopodia or podosomes¹⁰³ to determine the contribution of formins to these structures during T cell TEM. Together, these microscopy approaches will enable us to better define how actin polymerization by formins enables T cells to complete diapedesis.

How do Cytoskeletal Effectors Remodel the Actin Cytoskeleton to Facilitate Nucleus Passage Through Restrictive Barriers?

While our results from Chapter V indicate that FMNL1 promotes nucleus passage specifically through narrow pores, it remains to be determined how FMNL1 remodels the cytoskeleton to accomplish this task. Previous studies of how actin cytoskeletal remodeling contributes to nucleus deformation during migration through restrictive barriers have used imaging of immune cell migration within microchannels with defined constriction points^{179,197}. Due to the potential heterogeneity of barriers and diapedesis sites in a cultured endothelial monolayer, a microchannel system with restrictive sites of a known size can enable us to determine more precisely the contribution of actin remodeling at a defined moment of constriction. Using such microchannels in conjunction with WT or FMNL1 KO LifeAct T cells and fluorescent labeling of the nucleus, we can visualize how FMNL1-mediated actin remodeling facilitates nucleus passage through restrictive environments. Such experiments will better define the mechanism by which FMNL1 promotes nucleus transmigration through narrow pores. A similar microchannel system in which MyoIIA is inhibited in either WT or FMNL1 KO LifeAct T cells will enable us to further delineate the respective contributions made by these two cytoskeletal effectors to facilitating nucleus deformation and transmigration through restrictive barriers. We have previously used MyoIIA-GFP fusion proteins for the real-time imaging of MyoIIA during TEM⁶⁰. By expressing MyoIIA-GFP or FMNL1-GFP fusion proteins in LifeAct-RFP T cells with CFP-labeled nuclei and then imaging these cells migrating through microchannels, we can visualize the dynamic interplay between the localization of these cytoskeletal effectors, actin network changes, and nucleus deformation in real-time. Such experiments would enable us to visualize the respective contributions of MyoIIA-mediated contraction and FMNL1-mediated actin polymerization to nucleus transmigration. Our data on

FMNL1-deficient neutrophil migration in Chapter V and studies performed by others suggest that different cell types may employ different mechanisms to facilitate migration of the nucleus in constricting environments^{179,197}. For example, the Arp2/3 complex is critical in DCs for nucleus migration through restrictive environments¹⁷⁹. Performing similar microchannel experiments in other immune cells that migrate into and through restrictive environments, such as monocytes and neutrophils, will determine to what extent the FMNL1-mediated mechanism of nucleus transmigration is unique to T cells. Combined, these microchannel experiments will better define how cytoskeletal effectors remodel the actin cytoskeleton to facilitate migration through restrictive barriers.

Proposed Model of Cytoskeletal Effector Function in TEM

Studies of cytoskeletal effectors in T cell TEM both in this work and previously have identified that MyoIIA, Ena/VASP proteins, FMNL1, and mDia1 all contribute to the completion of the diapedesis step (Fig 7.1)^{60,119}. Though these effectors likely work through distinct mechanisms to promote diapedesis, their depletion leads to similar phenotypes during the completion of TEM. These findings highlight the morphological and physical challenge presented by the endothelium to extravasating cells and the importance of cytoskeletal remodeling to diapedesis. Based on the data presented in Chapter V, we propose, that in T cells, FMNL1 localizes behind the nucleus during TEM and, through actin polymerization downstream of chemokine stimulus, creates propulsive force to promote transmigration of the nucleus through the restrictive openings in the vascular cell wall (Figure 7.2). This propulsive force is complemented by contractile force mediated by MyoIIA^{51,60} to further enable squeezing of the nucleus through narrow openings (Figure 7.2). Based on our co-inhibition data, we proposed that loss of either one of these mechanisms can be partially compensated for by the other, but at least one is required for nucleus transmigration through narrow pores. In contrast to FMNL1, mDia1

localizes predominantly to the leading edge of the cell^{98,104}. Its upstream regulator RhoA localizes to both filopodia and lamellipodia and can be activated by both chemokine receptor and integrin ligation^{98,103}. Thus, we propose that mDia1 polymerizes actin to contribute to filopodia and lamellipodia formation and sensing function during TEM (Figure 7.2). During diapedesis, these protrusions may enable the migrating T cell to either detect and respond to chemokine gradients beneath the endothelium^{46,47,49}, as mDia1-deficient cells seem to be broadly impaired in chemotaxis^{124,135,137,184}. Additionally, mDia1 could mediate the sensing of permissive sites for diapedesis by promoting the formation of membrane protrusions that probe the endothelial monolayer. Ena/VASP proteins also localize to the leading edge of migrating cells and are associated with filopodia and lamellipodia protrusions^{116,119}. We have recently shown that Ena/VASP proteins mediate diapedesis through regulating $\alpha 4$ integrin expression and function¹¹⁹. Ligation of endothelial VCAM-1 by T cell $\alpha 4$ integrin can trigger the phosphorylation and internalization of VE-cadherin to enable loosening of endothelial cell-cell junctions^{58,59}. As we have proposed previously¹¹⁹, Ena/VASP proteins may facilitate the extension of $\alpha 4$ integrin-rich protrusions at the leading edge of the cell, which are able to signal to endothelial cells to make permissive sites for diapedesis (Figure 7.2). Alternatively, Ena/VASP-mediated $\alpha 4$ integrin adhesion may provide traction for the cell as it extrudes through the endothelial monolayer. Combined, we propose that mDia1 and Ena/VASP activity at the leading edge facilitate the creation and/or sensing of permissive sites for diapedesis while force generation by FMNL1 and MyoIIA at the rear of the T cell push the cell through these openings (Figure 7.2).

This model is consistent with the trafficking phenotypes we have observed herein and that have been described previously^{60,119,124,134,135}. FMNL1-mediated nucleus transmigration is only required in tissues with restrictive vascular barriers, and, consequently, FMNL1 deficiency

only impairs T cell trafficking to non-lymphoid tissues. Similarly, while MyoIIA has a role in uropod retraction during migration^{51,109}, loss of its function in contraction-mediated nucleus squeezing during TEM more substantially impairs trafficking to non-lymphoid organs⁶⁰. Since $\alpha 4$ integrins are upregulated by activated T cells and functionally regulated by EVL and VASP, we find that Ena/VASP proteins selectively mediate the trafficking of activated T cells¹¹⁹. In contrast, loss of mDia1, which is involved more generally in chemotaxis, impairs both naive and activated T cell trafficking to a diverse set of organs^{124,134,135}. Similar to how that chemokines and integrins are differentially involved in migration to different tissues^{3,4}, the requirement for cytoskeletal effectors in TEM also varies based on T cell type and anatomical site of extravasation. While FMNL1 and mDia1 may have other roles in T cell function during autoimmunity, we propose that their roles in promoting T cell TEM enable self-reactive T cells to access non-lymphoid tissue sites and drive autoimmunity.

Significance and Implications

To our knowledge, this work is the first examination of the role of FMNL1 in the migration and *in vivo* function of primary T cells. In this study, we describe and characterize a novel germline FMNL1 KO mouse. This mouse provides a new tool for investigating the function of FMNL1 in primary T cells and enables the future study of FMNL1 in other immune cell types. The data presented in this thesis identify a previously unknown role for FMNL1 in mediating transmigration of the rigid nucleus through restrictive endothelial barriers. Consequently, FMNL1 selectively promotes activated T cell trafficking to sites of inflammation and FMNL1 deficiency impairs the ability of self-reactive T cells to induce autoimmunity. Together, these findings characterize a new mechanism that enables T cells to migrate through restrictive barriers. Additionally, in this work, we demonstrate previously unknown roles for mDia1 in promoting the completion of diapedesis and T cell-mediated induction of

autoimmunity. In total, this thesis further delineates distinct mechanisms for formins and linear actin effectors in T cells, but also identifies similarities in TEM defects and disease phenotypes when these mechanisms are impaired.

Targeting T cell trafficking has proven to be an effective therapy against autoimmune and inflammatory diseases^{89,90,94,168,169,172}. However, some of these therapies such as Fingolimod, which blocks lymph node egress, and Natalizumab, which blocks $\alpha 4$ integrin-mediated trafficking, have broad effects on T cell trafficking^{90,198}. Consequently, such therapies can compromise immune function and lead to complications from infections, though whether this is a result of impaired peripheral or organ-specific immune function is still unresolved^{95,189,190}. Our observation that deficiency in mDia1 or FMNL1 in self-reactive T cells substantially impairs their ability to induce autoimmune disease suggests that targeting formins may be a possible alternative for autoimmune therapy. Given the broad expression of mDia1^{129,130} and its role in the migration of multiple cell types in multiple tissues^{124,134,135,184}, it is unlikely to be an improved target over current therapies. However, the restricted expression of FMNL1 to hematopoietic cells^{123,129,130}, its upregulation in T cells in autoimmune contexts^{88,146}, and its selective regulation of T cell trafficking to sites of inflammation, may make it a more viable therapeutic target. As we observed only a partial impairment in the trafficking FMNL1-deficient T cells to non-lymphoid organs, it is possible that sufficient T cell trafficking to provide pathogen control would persist. However, future studies are needed to establish to what degree loss of FMNL1 function compromises the protective immune function of T cells and other immune cell types. It is possible that targeting FMNL1 could be useful in the context of graft-versus-host disease where selective inhibition of activated T cell trafficking may be desirable¹⁶⁹. As FMNL1 is not a surface protein, any potential therapy would need to access the cytoplasm. The only currently available chemical inhibitor of FMNL1, SMIFH2 (small molecule inhibitor of

formin homology 2 domain), inhibits the actin polymerizing function of all formins¹⁹⁹. As the FH2 domain is the most conserved region across formins¹²², development of an inhibitor more specific to other regions of FMNL1 is necessary for specific chemical inhibition. Alternatively, an antibody-targeted RNAi approach could be used to achieve selective inhibition of FMNL1 function in T cells. While a significant amount of work remains to be done in order to create a viable FMNL1-based autoimmune therapy, our work here provides a proof-of-concept foundation and tools for studying FMNL1 as a modulator of immune responses.

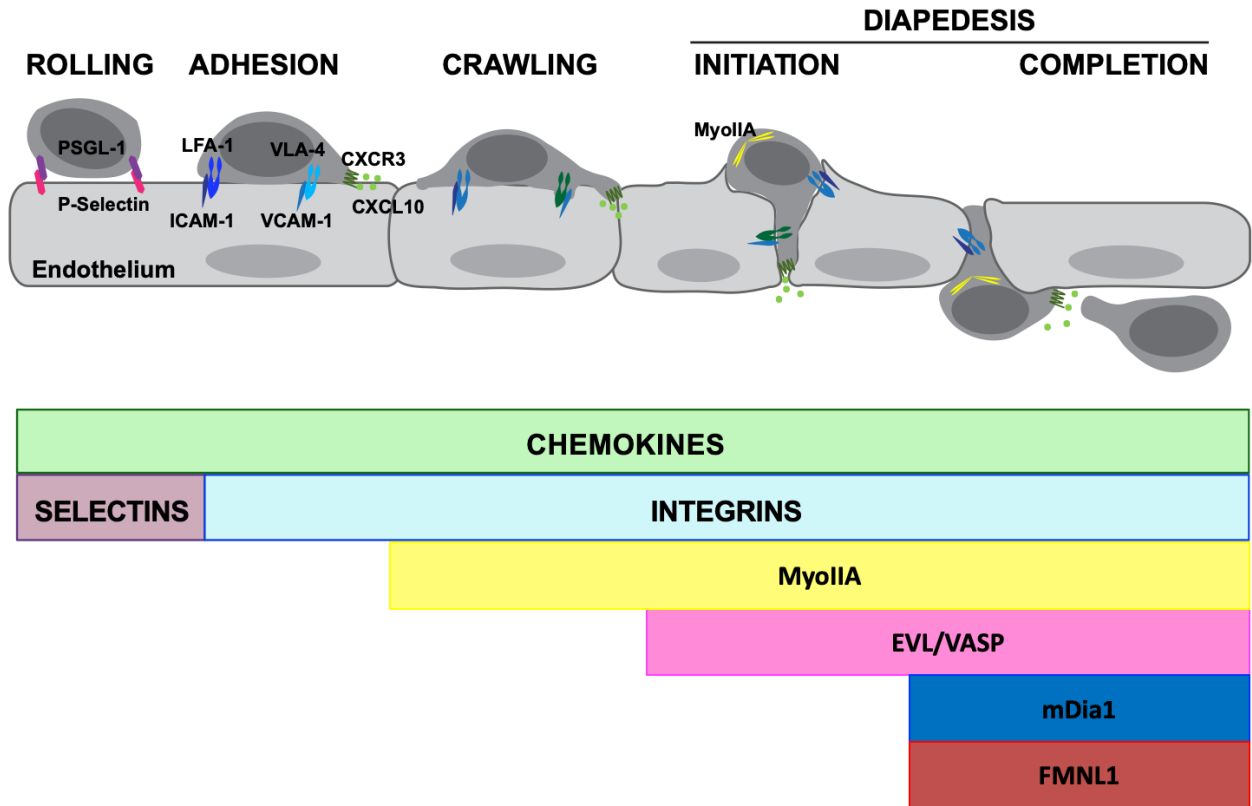


Figure 7.1: Proposed involvement of cytoskeletal effectors during the stages TEM. A model of the stages of TEM with the colored bars below depicting which stages the indicated molecules are likely important. Previous work by our lab and others has shown that depletion of MyoIIA can affect the both crawling, and diapedesis steps. Our work on EVL/VASP proteins suggests some involvement in both the initiation and completion of diapedesis. In this work deletion of FMNL1 or mDia1 did not substantially impact any stage of diapedesis except completion of diapedesis.

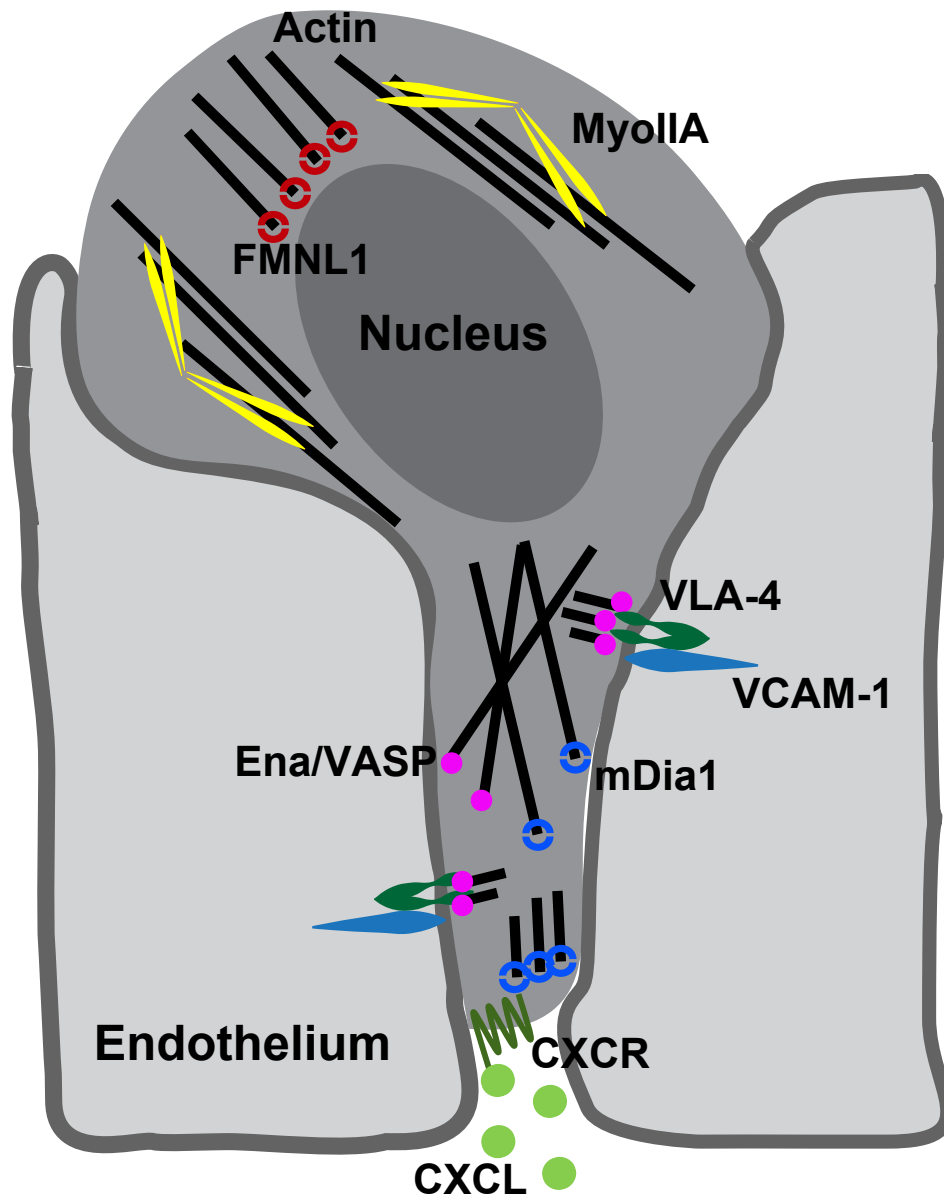


Figure 7.2: Proposed model of cytoskeletal effector function in TEM. Hypothesized model of the contribution of cytoskeletal effectors to the completion of TEM. Depicted is a T cell undergoing diapedesis through the vascular endothelium. We propose that mDia1 and Ena/VASP activity at the leading edge facilitate the creation and/or sensing of permissive sites for diapedesis while propulsion by FMNL1 and contraction by MyoIIA at the rear of the T cell push the cell through these openings.

REFERENCES

1. Gowans, J. L. & Knight, E. J. The Route of Re-Circulation of Lymphocytes in the Rat. *Proc. R. Soc. London. Ser. B, Biol. Sci.* **159**, 257–82 (1964).
2. Marchesi, V. T. & Gowans, J. L. The Migration of Lymphocytes Through the Endothelium of Venules in Lymph Nodes: an Electron Microscope Study. *Proc. R. Soc. London. Ser. B, Biol. Sci.* **159**, 283–90 (1964).
3. von Andrian, U. H. & Mackay, C. R. T-Cell Function and Migration — Two Sides of the Same Coin. *N. Engl. J. Med.* **343**, 1020–1034 (2000).
4. Masopust, D. & Schenkel, J. M. The integration of T cell migration, differentiation and function. *Nat. Rev. Immunol.* **13**, 309–20 (2013).
5. Bousso, P., Bhakta, N. R., Lewis, R. S. & Robey, E. Dynamics of thymocyte-stromal cell interactions visualized by two-photon microscopy. *Science* **296**, 1876–80 (2002).
6. Dupré, L., Houmadi, R., Tang, C. & Rey-Barroso, J. T lymphocyte migration: an action movie starring the actin and associated actors. *Front. Immunol.* **6**, (2015).
7. Cerwenka, A., Morgan, T. M., Harmsen, A. G. & Dutton, R. W. Migration kinetics and final destination of type 1 and type 2 CD8 effector cells predict protection against pulmonary virus infection. *J. Exp. Med.* **189**, 423–34 (1999).
8. Boissonnas, A., Fetler, L., Zeelenberg, I. S., Hugues, S. & Amigorena, S. In vivo imaging of cytotoxic T cell infiltration and elimination of a solid tumor. *J. Exp. Med.* **204**, 345–56 (2007).
9. Müller, A. J. *et al.* CD4⁺ T cells rely on a cytokine gradient to control intracellular pathogens beyond sites of antigen presentation. *Immunity* **37**, 147–57 (2012).
10. Reinhardt, R. L., Khoruts, A., Merica, R., Zell, T. & Jenkins, M. K. Visualizing the generation of memory CD4 T cells in the whole body. *Nature* **410**, 101–105 (2001).
11. Jacobelli, J., Chmura, S. A., Buxton, D. B., Davis, M. M. & Krummel, M. F. A single class II myosin modulates T cell motility and stopping, but not synapse formation. *Nat. Immunol.* **5**, 531–538 (2004).
12. Lindsay, R. S. *et al.* Antigen recognition in the islets changes with progression of autoimmune islet infiltration. *J. Immunol.* **194**, 522–30 (2015).
13. Jacobelli, J., Lindsay, R. S. & Friedman, R. S. Peripheral tolerance and autoimmunity: lessons from in vivo imaging. *Immunol. Res.* **55**, 146–154 (2013).
14. Scimone, M. L., Aifantis, I., Apostolou, I., von Boehmer, H. & von Andrian, U. H. A multistep adhesion cascade for lymphoid progenitor cell homing to the thymus. *Proc. Natl. Acad. Sci.* **103**, 7006–7011 (2006).

15. Klein, L. Dead man walking: How thymocytes scan the medulla. *Nat. Immunol.* **10**, 809–811 (2009).
16. Klein, L., Kyewski, B., Allen, P. M. & Hogquist, K. A. Positive and negative selection of the T cell repertoire: what thymocytes see (and don't see). *Nat. Rev. Immunol.* **14**, 377–91 (2014).
17. Zachariah, M. A. & Cyster, J. G. Neural crest-derived pericytes promote egress of mature thymocytes at the corticomedullary junction. *Science* **328**, 1129–35 (2010).
18. Weninger, W., Crowley, M. A., Manjunath, N. & von Andrian, U. H. Migratory properties of naive, effector, and memory CD8(+) T cells. *J. Exp. Med.* **194**, 953–66 (2001).
19. Miller, M. J., Wei, S. H., Parker, I. & Cahalan, M. D. Two-Photon Imaging of Lymphocyte Motility and Antigen Response in Intact Lymph Node. *Science (80-.)*. **296**, 1869–1873 (2002).
20. Miller, M. J., Wei, S. H., Cahalan, M. D. & Parker, I. Autonomous T cell trafficking examined in vivo with intravital two-photon microscopy. *Proc. Natl. Acad. Sci. U. S. A.* **100**, 2604–9 (2003).
21. Román, E. *et al.* CD4 effector T cell subsets in the response to influenza: heterogeneity, migration, and function. *J. Exp. Med.* **196**, 957–68 (2002).
22. Sallusto, F., Lenig, D., Förster, R., Lipp, M. & Lanzavecchia, A. Two subsets of memory T lymphocytes with distinct homing potentials and effector functions. *Nature* **401**, 708–712 (1999).
23. Ariotti, S. *et al.* Tissue-resident memory CD8+ T cells continuously patrol skin epithelia to quickly recognize local antigen. *Proc. Natl. Acad. Sci. U. S. A.* **109**, 19739–44 (2012).
24. Mueller, S. N., Gebhardt, T., Carbone, F. R. & Heath, W. R. Memory T cell subsets, migration patterns, and tissue residence. *Annu. Rev. Immunol.* **31**, 137–61 (2013).
25. Glennie, N. D. *et al.* Skin-resident memory CD4+ T cells enhance protection against *Leishmania major* infection. *J. Exp. Med.* jem.20142101- (2015). doi:10.1084/jem.20142101
26. Schneider-Hohendorf, T. *et al.* Regulatory T cells exhibit enhanced migratory characteristics, a feature impaired in patients with multiple sclerosis. *Eur. J. Immunol.* **40**, 3581–3590 (2010).
27. Campbell, D. J. Control of Regulatory T Cell Migration, Function, and Homeostasis. *J. Immunol.* **195**, 2507–13 (2015).
28. Norman, M. U. & Hickey, M. J. Mechanisms of lymphocyte migration in autoimmune disease. *Tissue Antigens* **66**, 163–172 (2005).
29. Engelhardt, B. & Ransohoff, R. M. The ins and outs of T-lymphocyte trafficking to the CNS: anatomical sites and molecular mechanisms. *Trends Immunol.* **26**, 485–495 (2005).

30. Vajkoczy, P., Laschinger, M. & Engelhardt, B. Alpha4-integrin-VCAM-1 binding mediates G protein-independent capture of encephalitogenic T cell blasts to CNS white matter microvessels. *J. Clin. Invest.* **108**, 557–65 (2001).
31. Laschinger, M., Vajkoczy, P. & Engelhardt, B. Encephalitogenic T cells use LFA-1 for transendothelial migration but not during capture and initial adhesion strengthening in healthy spinal cord microvessels in vivo. *Eur. J. Immunol.* **32**, 3598–3606 (2002).
32. Jäger, A., Dardalhon, V., Sobel, R. A., Bettelli, E. & Kuchroo, V. K. Th1, Th17, and Th9 effector cells induce experimental autoimmune encephalomyelitis with different pathological phenotypes. *J. Immunol.* **183**, 7169–77 (2009).
33. Flier, J. S., Underhill, L. H. & Eisenbarth, G. S. Type I Diabetes Mellitus. *N. Engl. J. Med.* **314**, 1360–1368 (1986).
34. Magnuson, A. M. *et al.* Population dynamics of islet-infiltrating cells in autoimmune diabetes. *Proc. Natl. Acad. Sci. U. S. A.* **112**, 1511–6 (2015).
35. Friedman, R. S. *et al.* An evolving autoimmune microenvironment regulates the quality of effector T cell restimulation and function. *Proc. Natl. Acad. Sci. U. S. A.* **111**, 9223–8 (2014).
36. Mellado, M. *et al.* T cell migration in rheumatoid arthritis. *Front. Immunol.* **6**, 384 (2015).
37. Pène, J. *et al.* Chronically inflamed human tissues are infiltrated by highly differentiated Th17 lymphocytes. *J. Immunol.* **180**, 7423–30 (2008).
38. Nourshargh, S. & Alon, R. Leukocyte Migration into Inflamed Tissues. *Immunity* **41**, 694–707 (2014).
39. Abadier, M. *et al.* Effector and Regulatory T Cells Roll at High Shear Stress by Inducible Tether and Sling Formation. *Cell Rep.* **21**, 3885–3899 (2017).
40. Pickard, J. E. & Ley, K. Micro-PTV Measurement of the Fluid Shear Stress Acting on Adherent Leukocytes In Vivo. *Biophys. J.* **96**, 4249–4259 (2009).
41. Ley, K. & Gaetgens, P. Endothelial, not hemodynamic, differences are responsible for preferential leukocyte rolling in rat mesenteric venules. *Circ. Res.* **69**, 1034–1041 (1991).
42. Gallatin, W. M., Weissman, I. L. & Butcher, E. C. A cell-surface molecule involved in organ-specific homing of lymphocytes. *Nature* **304**, 30–4
43. Ley, K. The role of selectins in inflammation and disease. *Trends Mol. Med.* **9**, 263–8 (2003).
44. Zarbock, A. *et al.* PSGL-1 engagement by E-selectin signals through Src kinase Fgr and ITAM adapters DAP12 and FcR γ to induce slow leukocyte rolling. *J. Exp. Med.* **205**, 2339–2347 (2008).

45. Bao, X. *et al.* Endothelial heparan sulfate controls chemokine presentation in recruitment of lymphocytes and dendritic cells to lymph nodes. *Immunity* **33**, 817–29 (2010).
46. Shulman, Z. *et al.* Lymphocyte Crawling and Transendothelial Migration Require Chemokine Triggering of High-Affinity LFA-1 Integrin. *Immunity* **30**, 384–396 (2009).
47. Alon, R. & Shulman, Z. Chemokine triggered integrin activation and actin remodeling events guiding lymphocyte migration across vascular barriers. *Exp. Cell Res.* **317**, 632–641 (2011).
48. Alon, R. & Ley, K. Cells on the run: shear-regulated integrin activation in leukocyte rolling and arrest on endothelial cells. *Curr. Opin. Cell Biol.* **20**, 525–532 (2008).
49. Shulman, Z. *et al.* Transendothelial migration of lymphocytes mediated by intraendothelial vesicle stores rather than by extracellular chemokine depots. *Nat. Immunol.* **13**, 67–76 (2012).
50. Krummel, M. F., Friedman, R. S. & Jacobelli, J. Modes and mechanisms of T cell motility: roles for confinement and Myosin-IIA. *Curr. Opin. Cell Biol.* **30C**, 9–16 (2014).
51. Soriano, S. F. *et al.* In vivo analysis of uropod function during physiological T cell trafficking. *J. Immunol.* **187**, 2356–64 (2011).
52. Carman, C. V. *et al.* Transcellular Diapedesis Is Initiated by Invasive Podosomes. *Immunity* **26**, 784–797 (2007).
53. Schoefl, G. I. & Miles, W. an A. by R. E. The migration of lymphocytes across the vascular endothelium in lymphoid tissue. A reexamination. *J. Exp. Med.* **136**, 568–88 (1972).
54. Feng, D., Nagy, J. A., Pyne, K., Dvorak, H. F. & Dvorak, A. M. Neutrophils emigrate from venules by a transendothelial cell pathway in response to FMLP. *J. Exp. Med.* **187**, 903–15 (1998).
55. Woodfin, A. *et al.* The junctional adhesion molecule JAM-C regulates polarized transendothelial migration of neutrophils in vivo. *Nat. Immunol.* **12**, 761–769 (2011).
56. Nourshargh, S., Hordijk, P. L. & Sixt, M. Breaching multiple barriers: leukocyte motility through venular walls and the interstitium. *Nat. Rev. Mol. Cell Biol.* **11**, 366–378 (2010).
57. Vestweber, D. How leukocytes cross the vascular endothelium. *Nat. Rev. Immunol.* **15**, 692–704 (2015).
58. Vockel, M. & Vestweber, D. How T cells trigger the dissociation of the endothelial receptor phosphatase VE-PTP from VE-cadherin. *Blood* **122**, 2512–22 (2013).
59. Wessel, F. *et al.* Leukocyte extravasation and vascular permeability are each controlled in vivo by different tyrosine residues of VE-cadherin. *Nat. Immunol.* **15**, 223–30 (2014).

60. Jacobelli, J., Estin Matthews, M., Chen, S. & Krummel, M. F. Activated T Cell Trans-Endothelial Migration Relies on Myosin-IIA Contractility for Squeezing the Cell Nucleus through Endothelial Cell Barriers. *PLoS One* **8**, (2013).
61. Barzilai, S. *et al.* Leukocytes Breach Endothelial Barriers by Insertion of Nuclear Lobes and Disassembly of Endothelial Actin Filaments. *Cell Rep.* **18**, 685–699 (2017).
62. Friedl, P., Wolf, K. & Lammerding, J. Nuclear mechanics during cell migration. *Curr. Opin. Cell Biol.* **23**, 55–64 (2011).
63. Gupta, S. *et al.* Developmental Heterogeneity in DNA Packaging Patterns Influences T-Cell Activation and Transmigration. *PLoS One* **7**, e43718 (2012).
64. Yadav, S. K. *et al.* Frontline Science: Elevated nuclear lamin A is permissive for granulocyte transendothelial migration but not for motility through collagen I barriers. *J. Leukoc. Biol.* **104**, 239–251 (2018).
65. Jill Mackarel, A., Cottell, D. C., Russell, K. J., FitzGerald, M. X. & O'Connor, C. M. Migration of Neutrophils across Human Pulmonary Endothelial Cells Is Not Blocked by Matrix Metalloproteinase or Serine Protease Inhibitors. *Am. J. Respir. Cell Mol. Biol.* **20**, 1209–1219 (1999).
66. Wolf, K. *et al.* Amoeboid shape change and contact guidance: T-lymphocyte crawling through fibrillar collagen is independent of matrix remodeling by MMPs and other proteases. *Blood* **102**, 3262–9 (2003).
67. Wolf, K. *et al.* Physical limits of cell migration: Control by ECM space and nuclear deformation and tuning by proteolysis and traction force. *J. Cell Biol.* **201**, 1069–1084 (2013).
68. Miyasaka, M. & Tanaka, T. Lymphocyte trafficking across high endothelial venules: Dogmas and enigmas. *Nat. Rev. Immunol.* **4**, 360–370 (2004).
69. Bajénoff, M., Glaichenhaus, N. & Germain, R. N. Fibroblastic reticular cells guide T lymphocyte entry into and migration within the splenic T cell zone. *J. Immunol.* **181**, 3947–54 (2008).
70. Bradley, L. M., Watson, S. R. & Swain, S. L. Entry of naive CD4 T cells into peripheral lymph nodes requires L-selectin. *J. Exp. Med.* **180**, 2401–6 (1994).
71. Xie, H., Lim, Y. C., Luscinskas, F. W. & Lichtman, A. H. Acquisition of selectin binding and peripheral homing properties by CD4(+) and CD8(+) T cells. *J. Exp. Med.* **189**, 1765–76 (1999).
72. Vachino, G. *et al.* P-selectin glycoprotein ligand-1 is the major counter-receptor for P-selectin on stimulated T cells and is widely distributed in non-functional form on many lymphocytic cells. *J. Biol. Chem.* **270**, 21966–74 (1995).

73. Luscinikas, F. W., Ding, H. & Lichtman, A. H. P-selectin and vascular cell adhesion molecule 1 mediate rolling and arrest, respectively, of CD4⁺ T lymphocytes on tumor necrosis factor alpha-activated vascular endothelium under flow. *J. Exp. Med.* **181**, 1179–86 (1995).
74. Austrup, F. *et al.* P- and E-selectin mediate recruitment of T-helper-1 but not T-helper-2 cells into inflamed tissues. *Nature* **385**, 81–83 (1997).
75. Sundd, P. *et al.* ‘Slings’ enable neutrophil rolling at high shear. *Nature* **488**, 399–403 (2012).
76. Oppenheimer-Marks, N., Davis, L. S., Bogue, D. T., Ramberg, J. & Lipsky, P. E. Differential utilization of ICAM-1 and VCAM-1 during the adhesion and transendothelial migration of human T lymphocytes. *J. Immunol.* **147**, 2913–21 (1991).
77. Groom, J. R. & Luster, A. D. CXCR3 in T cell function. *Exp. Cell Res.* **317**, 620–31 (2011).
78. Piali, L. *et al.* The chemokine receptor CXCR3 mediates rapid and shear-resistant adhesion-induction of effector T lymphocytes by the chemokines IP10 and Mig. *Eur. J. Immunol.* **28**, 961–972 (1998).
79. Sallusto, F., Lenig, D., Mackay, C. R. & Lanzavecchia, A. Flexible programs of chemokine receptor expression on human polarized T helper 1 and 2 lymphocytes. *J. Exp. Med.* **187**, 875–83 (1998).
80. Lim, H. W., Lee, J., Hillsamer, P. & Kim, C. H. Human Th17 cells share major trafficking receptors with both polarized effector T cells and FOXP3⁺ regulatory T cells. *J. Immunol.* **180**, 122–9 (2008).
81. Yamamoto, J. *et al.* Differential expression of the chemokine receptors by the Th1- and Th2-type effector populations within circulating CD4⁺ T cells. *J. Leukoc. Biol.* **68**, 568–74 (2000).
82. Qin, S. *et al.* The chemokine receptors CXCR3 and CCR5 mark subsets of T cells associated with certain inflammatory reactions. *J. Clin. Invest.* **101**, 746–54 (1998).
83. Shechter, R., London, A. & Schwartz, M. Orchestrated leukocyte recruitment to immune-privileged sites: absolute barriers versus educational gates. *Nat. Rev. Immunol.* **13**, 206–218 (2013).
84. Mehta, D. & Malik, A. B. Signaling Mechanisms Regulating Endothelial Permeability. *Physiol. Rev.* **86**, 279–367 (2006).
85. Iwata, M. *et al.* Retinoic acid imprints gut-homing specificity on T cells. *Immunity* **21**, 527–38 (2004).
86. Sigmundsdottir, H. *et al.* DCs metabolize sunlight-induced vitamin D3 to ‘program’ T cell attraction to the epidermal chemokine CCL27. *Nat. Immunol.* **8**, 285–293 (2007).

87. Mikhak, Z., Strassner, J. P. & Luster, A. D. Lung dendritic cells imprint T cell lung homing and promote lung immunity through the chemokine receptor CCR4. *J. Exp. Med.* **210**, 1855–69 (2013).
88. Odoardi, F. *et al.* T cells become licensed in the lung to enter the central nervous system. *Nature* **488**, 675–9 (2012).
89. Luster, A. D., Alon, R. & von Andrian, U. H. Immune cell migration in inflammation: Present and future therapeutic targets. *Nat. Immunol.* **6**, 1182–1190 (2005).
90. Engelhardt, B. & Kappos, L. Natalizumab: targeting alpha4-integrins in multiple sclerosis. *Neurodegener. Dis.* **5**, 16–22 (2008).
91. Ghosh, S. *et al.* Natalizumab for Active Crohn's Disease. *N. Engl. J. Med.* **348**, 24–32 (2003).
92. Feagan, B. G. *et al.* Vedolizumab as Induction and Maintenance Therapy for Ulcerative Colitis. *N. Engl. J. Med.* **369**, 699–710 (2013).
93. Sandborn, W. J. *et al.* Vedolizumab as Induction and Maintenance Therapy for Crohn's Disease. *N. Engl. J. Med.* **369**, 711–721 (2013).
94. Reshef, R. *et al.* Blockade of Lymphocyte Chemotaxis in Visceral Graft-versus-Host Disease. *N. Engl. J. Med.* **367**, 135–145 (2012).
95. Weber, T. Progressive Multifocal Leukoencephalopathy. *Neurol. Clin.* **26**, 833–854 (2008).
96. Ridley, A. J. Life at the leading edge. *Cell* **145**, 1012–1022 (2011).
97. Rougerie, P. & Delon, J. Rho GTPases: Masters of T lymphocyte migration and activation. *Immunol. Lett.* **142**, 1–13 (2012).
98. Heasman, S. J. & Ridley, A. J. Multiple roles for RhoA during T cell transendothelial migration. *Small GTPases* **1**, 174–179 (2010).
99. Tybulewicz, V. L. J. & Henderson, R. B. Rho family GTPases and their regulators in lymphocytes. *Nat. Rev. Immunol.* **9**, 630–644 (2009).
100. Tybulewicz, V. L. J. Vav-family proteins in T-cell signalling. *Curr. Opin. Immunol.* **17**, 267–274 (2005).
101. Nishikimi, A. *et al.* Sequential regulation of DOCK2 dynamics by two phospholipids during neutrophil chemotaxis. *Science* **324**, 384–7 (2009).
102. Gérard, A., Mertens, A. E. E., van der Kammen, R. A. & Collard, J. G. The Par polarity complex regulates Rap1- and chemokine-induced T cell polarization. *J. Cell Biol.* **176**, 863–75 (2007).

103. Heasman, S. J., Carlin, L. M., Cox, S., Ng, T. & Ridley, A. J. Coordinated RhoA signaling at the leading edge and uropod is required for T cell transendothelial migration. *J. Cell Biol.* **190**, 553–63 (2010).
104. Vicente-Manzanares, M. *et al.* The RhoA effector mDia is induced during T cell activation and regulates actin polymerization and cell migration in T lymphocytes. *J. Immunol.* **171**, 1023–34 (2003).
105. Nobes, C. D. & Hall, A. Rho, rac, and cdc42 GTPases regulate the assembly of multimolecular focal complexes associated with actin stress fibers, lamellipodia, and filopodia. *Cell* **81**, 53–62 (1995).
106. Zhang, Q. *et al.* DOCK8 regulates lymphocyte shape integrity for skin antiviral immunity. *J. Exp. Med.* **211**, 2549–66 (2014).
107. Blanchoin, L., Boujemaa-Paterski, R., Sykes, C. & Plastino, J. Actin Dynamics, Architecture, and Mechanics in Cell Motility. *Physiol. Rev.* **94**, 235–263 (2014).
108. Morin, N. A. *et al.* Nonmuscle myosin heavy chain IIA mediates integrin LFA-1 de-adhesion during T lymphocyte migration. *J. Exp. Med.* **205**, 195–205 (2008).
109. Jacobelli, J. *et al.* Confinement-optimized three-dimensional T cell amoeboid motility is modulated via myosin IIA-regulated adhesions. *Nat. Immunol.* **11**, 953–961 (2010).
110. Johnston, S. A., Bramble, J. P., Yeung, C. L., Mendes, P. M. & Machesky, L. M. Arp2/3 complex activity in filopodia of spreading cells. *BMC Cell Biol.* **9**, 65 (2008).
111. Snapper, S. B. *et al.* WASP deficiency leads to global defects of directed leukocyte migration in vitro and in vivo. *J. Leukoc. Biol.* **77**, 993–998 (2005).
112. Lanzi, G. *et al.* A novel primary human immunodeficiency due to deficiency in the WASP-interacting protein WIP. *J. Exp. Med.* **209**, 29–34 (2012).
113. Shioy, L. R. *et al.* The actin regulator coronin 1A is mutant in a thymic egress-deficient mouse strain and in a patient with severe combined immunodeficiency. *Nat. Immunol.* **9**, 1307–1315 (2008).
114. Sims, T. N. *et al.* Opposing effects of PKC θ and WASp on symmetry breaking and relocation of the immunological synapse. *Cell* **129**, 773–85 (2007).
115. Calvez, R. *et al.* The Wiskott-Aldrich syndrome protein permits assembly of a focused immunological synapse enabling sustained T-cell receptor signaling. *Haematologica* **96**, 1415–23 (2011).
116. Gomez, T. S. *et al.* Formins regulate the actin-related protein 2/3 complex-independent polarization of the centrosome to the immunological synapse. *Immunity* **26**, 177–90 (2007).
117. Hansen, S. D. & Mullins, R. D. VASP is a processive actin polymerase that requires monomeric actin for barbed end association. *J. Cell Biol.* **191**, 571–584 (2010).

118. Bear, J. E. *et al.* Ena/VASP: towards resolving a pointed controversy at the barbed end. *J. Cell Sci.* **122**, 1947–53 (2009).
119. Estin, M. L. *et al.* Ena/VASP proteins regulate activated T-cell trafficking by promoting diapedesis during transendothelial migration. *Proc. Natl. Acad. Sci. U. S. A.* **114**, E2901–E2910 (2017).
120. Krause, M. *et al.* Fyn-binding protein (Fyb)/SLP-76-associated protein (SLAP), Ena/vasodilator-stimulated phosphoprotein (VASP) proteins and the Arp2/3 complex link T cell receptor (TCR) signaling to the actin cytoskeleton. *J. Cell Biol.* **149**, 181–94 (2000).
121. Kühn, S. & Geyer, M. Formins as effector proteins of Rho GTPases. *Small GTPases* **5**, 1–16 (2014).
122. Schönichen, A. & Geyer, M. Fifteen formins for an actin filament: A molecular view on the regulation of human formins. *Biochim. Biophys. Acta - Mol. Cell Res.* **1803**, 152–163 (2010).
123. Yayoshi-Yamamoto, S., Taniuchi, I. & Watanabe, T. FRL, a Novel Formin-Related Protein, Binds to Rac and Regulates Cell Motility and Survival of Macrophages. *Mol. Cell. Biol.* **20**, 6872–6881 (2000).
124. Sakata, D. *et al.* Impaired T lymphocyte trafficking in mice deficient in an actin-nucleating protein, mDia1. *J. Exp. Med.* **204**, 2031–8 (2007).
125. Painter, M. W. *et al.* Transcriptomes of the B and T lineages compared by multiplatform microarray profiling. *J. Immunol.* **186**, 3047–57 (2011).
126. Seth, A., Otomo, C. & Rosen, M. K. Autoinhibition regulates cellular localization and actin assembly activity of the diaphanous-related formins FRLalpha and mDia1. *J. Cell Biol.* **174**, 701–13 (2006).
127. Watanabe, N. *et al.* p140mDia, a mammalian homolog of *Drosophila* diaphanous, is a target protein for Rho small GTPase and is a ligand for profilin. *EMBO J.* **16**, 3044–56 (1997).
128. Watanabe, N., Kato, T., Fujita, A., Ishizaki, T. & Narumiya, S. Cooperation between mDia1 and ROCK in Rho-induced actin reorganization. *Nat. Cell Biol.* **1**, 136–143 (1999).
129. Yue, F. *et al.* A comparative encyclopedia of DNA elements in the mouse genome. *Nature* **515**, 355–364 (2014).
130. Fagerberg, L. *et al.* Analysis of the human tissue-specific expression by genome-wide integration of transcriptomics and antibody-based proteomics. *Mol. Cell. Proteomics* **13**, 397–406 (2014).
131. Lammers, M., Meyer, S., Kühmann, D. & Wittinghofer, A. Specificity of interactions between mDia isoforms and Rho proteins. *J. Biol. Chem.* **283**, 35236–46 (2008).

132. Sarmiento, C. *et al.* WASP family members and formin proteins coordinate regulation of cell protrusions in carcinoma cells. *J. Cell Biol.* **180**, 1245–60 (2008).
133. Ishizaki, T. *et al.* Coordination of microtubules and the actin cytoskeleton by the Rho effector mDia1. *Nat. Cell Biol.* **3**, 8–14 (2001).
134. Dong, B. *et al.* Mammalian diaphanous-related formin 1 regulates GSK3 β -dependent microtubule dynamics required for T cell migratory polarization. *PLoS One* **8**, (2013).
135. Eisenmann, K. M. *et al.* T cell responses in mammalian diaphanous-related formin mDia1 knock-out mice. *J. Biol. Chem.* **282**, 25152–25158 (2007).
136. Murugesan, S. *et al.* Formin-generated actomyosin arcs propel T cell receptor microcluster movement at the immune synapse. *J. Cell Biol.* **215**, 383–399 (2016).
137. Thompson, S. B. *et al.* The Formin mDia1 Regulates Acute Lymphoblastic Leukemia Engraftment, Migration, and Progression in vivo. *Front. Oncol.* **8**, 389 (2018).
138. Gardberg, M. *et al.* Characterization of Leukocyte Formin FMNL1 Expression in Human Tissues. *J. Histochem. Cytochem.* **62**, 460–470 (2014).
139. Favaro, P. *et al.* FMNL1 promotes proliferation and migration of leukemia cells. *J. Leukoc. Biol.* **94**, 503–12 (2013).
140. Harris, E. S., Li, F. & Higgs, H. N. The mouse formin, FRLalpha, slows actin filament barbed end elongation, competes with capping protein, accelerates polymerization from monomers, and severs filaments. *J. Biol. Chem.* **279**, 20076–87 (2004).
141. Miller, M. R., Miller, E. W. & Blystone, S. D. Non-canonical activity of the podosomal formin FMNL1 γ supports immune cell migration. *J. Cell Sci.* **130**, 1730–1739 (2017).
142. Naj, X., Hoffmann, A.-K., Himmel, M. & Linder, S. The formins FMNL1 and mDia1 regulate coiling phagocytosis of *Borrelia burgdorferi* by primary human macrophages. *Infect. Immun.* **81**, 1683–95 (2013).
143. Han, Y. *et al.* Formin-like 1 (FMNL1) is regulated by N-terminal myristoylation and induces polarized membrane blebbing. *J. Biol. Chem.* **284**, 33409–17 (2009).
144. Han, Y. *et al.* Proteomic investigation of the interactome of FMNL1 in hematopoietic cells unveils a role in calcium-dependent membrane plasticity. *J. Proteomics* **78**, 72–82 (2013).
145. Colón-Franco, J. M., Gomez, T. S. & Billadeau, D. D. Dynamic remodeling of the actin cytoskeleton by FMNL1 γ is required for structural maintenance of the Golgi complex. *J. Cell Sci.* **124**, 3118–26 (2011).
146. Degroote, R. L. *et al.* Formin like 1 expression is increased on CD4 + T lymphocytes in spontaneous autoimmune uveitis. *J. Proteomics* **154**, 102–108 (2017).
147. Hogquist, K. A. *et al.* T cell receptor antagonist peptides induce positive selection. *Cell* **76**, 17–27 (1994).

148. Barnden, M. J., Allison, J., Heath, W. R. & Carbone, F. R. Defective TCR expression in transgenic mice constructed using cDNA-based α - and β -chain genes under the control of heterologous regulatory elements. *Immunol. Cell Biol.* **76**, 34–40 (1998).
149. Bettelli, E. *et al.* Myelin oligodendrocyte glycoprotein-specific T cell receptor transgenic mice develop spontaneous autoimmune optic neuritis. *J. Exp. Med.* **197**, 1073–81 (2003).
150. Shen, F. W. *et al.* Cloning of Ly-5 cDNA. *Proc. Natl. Acad. Sci. U. S. A.* **82**, 7360–3 (1985).
151. Kurts, C. *et al.* Constitutive class I-restricted exogenous presentation of self antigens in vivo. *J. Exp. Med.* **184**, 923–30 (1996).
152. Sikorski, E. E., Hallmann, R., Berg, E. L. & Butcher, E. C. The Peyer's patch high endothelial receptor for lymphocytes, the mucosal vascular addressin, is induced on a murine endothelial cell line by tumor necrosis factor-alpha and IL-1. *J. Immunol.* **151**, 5239–50 (1993).
153. Muppidi, J. R. *et al.* Cannabinoid receptor 2 positions and retains marginal zone B cells within the splenic marginal zone. *J. Exp. Med.* **208**, (2011).
154. Anderson, K. G. *et al.* Intravascular staining for discrimination of vascular and tissue leukocytes. *Nat. Protoc.* **9**, 209–22 (2014).
155. Wigton, E. J., Thompson, S. B., Long, R. A. & Jacobelli, J. Myosin-IIA regulates leukemia engraftment and brain infiltration in a mouse model of acute lymphoblastic leukemia. *J. Leukoc. Biol.* **100**, 1–11 (2016).
156. Weinreich, M. A. & Hogquist, K. A. Thymic emigration: when and how T cells leave home. *J. Immunol.* **181**, 2265–70 (2008).
157. Grakoui, A. *et al.* The immunological synapse: a molecular machine controlling T cell activation. *Science* **285**, 221–7 (1999).
158. Kumari, S., Curado, S., Mayya, V. & Dustin, M. L. T cell antigen receptor activation and actin cytoskeleton remodeling. *Biochim. Biophys. Acta - Biomembr.* **1838**, 546–556 (2014).
159. Friedman, R. S., Beemiller, P., Sorensen, C. M., Jacobelli, J. & Krummel, M. F. Real-time analysis of T cell receptors in naive cells in vitro and in vivo reveals flexibility in synapse and signaling dynamics. *J. Exp. Med.* **207**, 2733–2749 (2010).
160. Keerthivasan, G. *et al.* Aberrant overexpression of CD14 on granulocytes sensitizes the innate immune response in mDial heterozygous del(5q) MDS. *Blood* **124**, 780–90 (2014).
161. Ebert, P. J. R., Ehrlich, L. I. R. & Davis, M. M. Low ligand requirement for deletion and lack of synapses in positive selection enforce the gauntlet of thymic T cell maturation. *Immunity* **29**, 734–45 (2008).

162. Olivares-Villagómez, D. & Van Kaer, L. Intestinal Intraepithelial Lymphocytes: Sentinels of the Mucosal Barrier. *Trends Immunol.* **39**, 264–275 (2018).
163. Heath, W. R. & Carbone, F. R. The skin-resident and migratory immune system in steady state and memory: innate lymphocytes, dendritic cells and T cells. *Nat. Immunol.* **14**, 978–985 (2013).
164. Jenne, C. N. & Kubes, P. Immune surveillance by the liver. *Nat. Immunol.* **14**, 996–1006 (2013).
165. Davies, L. C., Jenkins, S. J., Allen, J. E. & Taylor, P. R. Tissue-resident macrophages. *Nat. Immunol.* **14**, 986–995 (2013).
166. Miller, M. R. & Blystone, S. D. Human Macrophages Utilize the Podosome Formin FMNL1 for Adhesion and Migration. *CellBio* **4**, 1–11 (2015).
167. Sallusto, F. *et al.* T-cell trafficking in the central nervous system. *Immunol. Rev.* **248**, 216–227 (2012).
168. Cohen, J. A. *et al.* Oral fingolimod or intramuscular interferon for relapsing multiple sclerosis. *N. Engl. J. Med.* **362**, 402–15 (2010).
169. Huang, Y. *et al.* CRK proteins selectively regulate T cell migration into inflamed tissues. *J. Clin. Invest.* **125**, 1019–1032 (2015).
170. Lo, C. G., Lu, T. T. & Cyster, J. G. Integrin-dependence of lymphocyte entry into the splenic white pulp. *J. Exp. Med.* **197**, 353–61 (2003).
171. Mempel, T. R., Scimone, M. L., Mora, J. R. & Von Andrian, U. H. In vivo imaging of leukocyte trafficking in blood vessels and tissues. *Curr. Opin. Immunol.* **16**, 406–417 (2004).
172. Lobatón, T., Vermeire, S., Van Assche, G. & Rutgeerts, P. Review article: anti-adhesion therapies for inflammatory bowel disease. *Aliment. Pharmacol. Ther.* **39**, 579–594 (2014).
173. Manevich, E., Grabovsky, V., Feigelson, S. W. & Alon, R. Talin 1 and paxillin facilitate distinct steps in rapid VLA-4-mediated adhesion strengthening to vascular cell adhesion molecule 1. *J. Biol. Chem.* **282**, 25338–48 (2007).
174. Smith, A. *et al.* A talin-dependent LFA-1 focal zone is formed by rapidly migrating T lymphocytes. *J. Cell Biol.* **170**, 141–51 (2005).
175. Mellor, H. The role of formins in filopodia formation. *Biochimica et Biophysica Acta - Molecular Cell Research* **1803**, 191–200 (2010).
176. Han, Y.-H. *et al.* Requirement of a vasodilator-stimulated phosphoprotein family member for cell adhesion, the formation of filopodia, and chemotaxis in dictyostelium. *J. Biol. Chem.* **277**, 49877–87 (2002).

177. Ericson, J. A. *et al.* Gene expression during the generation and activation of mouse neutrophils: Implication of novel functional and regulatory pathways. *PLoS One* **9**, (2014).
178. Issekutz, T. B. Inhibition of in vivo lymphocyte migration to inflammation and homing to lymphoid tissues by the TA-2 monoclonal antibody. A likely role for VLA-4 in vivo. *J. Immunol.* **147**, 4178–84 (1991).
179. Thiam, H.-R. *et al.* Perinuclear Arp2/3-driven actin polymerization enables nuclear deformation to facilitate cell migration through complex environments. *Nat. Commun.* **7**, 10997 (2016).
180. Stroka, K. M., Hayenga, H. N. & Aranda-Espinoza, H. Human Neutrophil Cytoskeletal Dynamics and Contractility Actively Contribute to Trans-Endothelial Migration. *PLoS One* **8**, e61377 (2013).
181. Hoffmann, K., Sperling, K., Olins, A. L. & Olins, D. E. The granulocyte nucleus and lamin B receptor: avoiding the ovoid. *Chromosoma* **116**, 227–235 (2007).
182. Tanizaki, H. *et al.* Rho-mDial pathway is required for adhesion, migration, and T-cell stimulation in dendritic cells. *Blood* **116**, 5875–5884 (2010).
183. Ferguson, T. A. & Kupper, T. S. Antigen-independent processes in antigen-specific immunity. A role for alpha 4 integrin. *J. Immunol.* **150**, 1172–82 (1993).
184. Shi, Y. *et al.* The mDial formin is required for neutrophil polarization, migration, and activation of the LARG/RhoA/ROCK signaling axis during chemotaxis. *J. Immunol.* **182**, 3837–45 (2009).
185. Harris, T. H. *et al.* Generalized Lévy walks and the role of chemokines in migration of effector CD8⁺ T cells. *Nature* **486**, 545–548 (2012).
186. Overstreet, M. G. *et al.* Inflammation-induced interstitial migration of effector CD4⁺ T cells is dependent on integrin α V. *Nat. Immunol.* **14**, 949–958 (2013).
187. Hugues, S. *et al.* Distinct T cell dynamics in lymph nodes during the induction of tolerance and immunity. *Nat. Immunol.* **5**, 1235–1242 (2004).
188. Shakhar, G. *et al.* Stable T cell-dendritic cell interactions precede the development of both tolerance and immunity in vivo. *Nat. Immunol.* **6**, 707–14 (2005).
189. Sabath, B. F. & Major, E. O. Traffic of JC Virus from Sites of Initial Infection to the Brain: The Path to Progressive Multifocal Leukoencephalopathy. *J. Infect. Dis.* **186**, S180–S186 (2002).
190. Fontoura, P. Monoclonal antibody therapy in multiple sclerosis: Paradigm shifts and emerging challenges. *MAbs* **2**, 670–81 (2010).
191. Schuppler, M. & Loessner, M. J. The Opportunistic Pathogen *Listeria monocytogenes*: Pathogenicity and Interaction with the Mucosal Immune System. *Int. J. Inflam.* **2010**, 704321 (2010).

192. Kollias, C. M., Huneke, R. B., Wigdahl, B. & Jennings, S. R. Animal models of herpes simplex virus immunity and pathogenesis. *J. Neurovirol.* **21**, 8–23 (2015).
193. Mohammed, R. N. *et al.* L-selectin Is Essential for Delivery of Activated CD8⁺T Cells to Virus-Infected Organs for Protective Immunity. *Cell Rep.* **14**, 760–771 (2016).
194. Beura, L. K. *et al.* Lymphocytic choriomeningitis virus persistence promotes effector-like memory differentiation and enhances mucosal T cell distribution. *J. Leukoc. Biol.* **97**, 217–25 (2015).
195. Haist, K. C., Burrack, K. S., Davenport, B. J. & Morrison, T. E. Inflammatory monocytes mediate control of acute alphavirus infection in mice. *PLOS Pathog.* **13**, e1006748 (2017).
196. Riedl, J. *et al.* Lifeact: a versatile marker to visualize F-actin. *Nat. Methods* **5**, 605–7 (2008).
197. Salvermoser, M. *et al.* Myosin 1f is specifically required for neutrophil migration in 3D environments during acute inflammation. *Blood* **131**, 1887–1898 (2018).
198. Chun, J. & Hartung, H.-P. Mechanism of action of oral fingolimod (FTY720) in multiple sclerosis. *Clin. Neuropharmacol.* **33**, 91–101
199. Rizvi, S. A. *et al.* Identification and characterization of a small molecule inhibitor of formin-mediated actin assembly. *Chem. Biol.* **16**, 1158–68 (2009).